AN EM STUDY OF IMMUNOGOLD-LABELLED BASIC FGF IN DYSTROPHIC MDX AND NORMAL MOUSE DIAPHRAGM

by

KAREN ANITA HAHN PENNER

A Thesis
Submitted to the Faculty of Graduate Studies
in Partial Fulfilment of the Requirements
for the degree of

MASTER OF SCIENCE

Department of Anatomy
Faculty of Medicine
University of Manitoba
Winnipeg, Canada

July, 1993

ISBN 0-315-98963-7

Name _____

Dissertation Abstracts International is arranged by broad, general subject categories. Please select the one subject which most nearly describes the content of your dissertation. Enter the corresponding four-digit code in the spaces provided.

ANATOMY
SUBJECT TERM

SUBJECT CODE

U·M·I

Subject Categories

THE HUMANITIES AND SOCIAL SCIENCES

COMMUNICATIONS AND THE ARTS
Architecture 0729
Art History 0377
Cinema 0900
Dance 0378
Fine Arts 0357
Information Science 0723
Journalism 0391
Library Science 0399
Mass Communications 0708
Music 0413
Speech Communication 0459
Theater 0465

EDUCATION
General 0515
Administration 0514
Adult and Continuing 0516
Agricultural 0517
Art 0273
Bilingual and Multicultural 0282
Business 0688
Community College 0275
Curriculum and Instruction 0727
Early Childhood 0518
Elementary 0524
Finance 0277
Guidance and Counseling 0519
Health 0680
Higher 0745
History of 0520
Home Economics 0278
Industrial 0521
Language and Literature 0279
Mathematics 0280
Music 0522
Philosophy of 0998
Physical 0523
Psychology 0525
Reading 0535
Religious 0527
Sciences 0714
Secondary 0533
Social Sciences 0534
Sociology of 0340
Special 0529
Teacher Training 0530
Technology 0710
Tests and Measurements 0288
Vocational 0747

LANGUAGE, LITERATURE AND LINGUISTICS
Language
- General 0679
- Ancient 0289
- Linguistics 0290
- Modern 0291

Literature
- General 0401
- Classical 0294
- Comparative 0295
- Medieval 0297
- Modern 0298
- African 0316
- American 0591
- Asian 0305
- Canadian (English) 0352
- Canadian (French) 0355
- English 0593
- Germanic 0311
- Latin American 0312
- Middle Eastern 0315
- Romance 0313
- Slavic and East European 0314

PHILOSOPHY, RELIGION AND THEOLOGY
Philosophy 0422
Religion
- General 0318
- Biblical Studies 0321
- Clergy 0319
- History of 0320
- Philosophy of 0322

Theology 0469

SOCIAL SCIENCES
American Studies 0323
Anthropology
- Archaeology 0324
- Cultural 0326
- Physical 0327

Business Administration
- General 0310
- Accounting 0272
- Banking 0770
- Management 0454
- Marketing 0338

Canadian Studies 0385
Economics
- General 0501
- Agricultural 0503
- Commerce-Business 0505
- Finance 0508
- History 0509
- Labor 0510
- Theory 0511

Folklore 0358
Geography 0366
Gerontology 0351
History
- General 0578
- Ancient 0579
- Medieval 0581
- Modern 0582
- Black 0328
- African 0331
- Asia, Australia and Oceania 0332
- Canadian 0334
- European 0335
- Latin American 0336
- Middle Eastern 0333
- United States 0337

History of Science 0585
Law 0398
Political Science
- General 0615
- International Law and Relations 0616
- Public Administration 0617

Recreation 0814
Social Work 0452
Sociology
- General 0626
- Criminology and Penology ... 0627
- Demography 0938
- Ethnic and Racial Studies 0631
- Individual and Family Studies 0628
- Industrial and Labor Relations 0629
- Public and Social Welfare 0630
- Social Structure and Development 0700
- Theory and Methods 0344

Transportation 0709
Urban and Regional Planning 0999
Women's Studies 0453

THE SCIENCES AND ENGINEERING

BIOLOGICAL SCIENCES
Agriculture
- General 0473
- Agronomy 0285
- Animal Culture and Nutrition 0475
- Animal Pathology 0476
- Food Science and Technology 0359
- Forestry and Wildlife 0478
- Plant Culture 0479
- Plant Pathology 0480
- Plant Physiology 0817
- Range Management 0777
- Wood Technology 0746

Biology
- General 0306
- Anatomy 0287
- Biostatistics 0308
- Botany 0309
- Cell 0379
- Ecology 0329
- Entomology 0353
- Genetics 0369
- Limnology 0793
- Microbiology 0410
- Molecular 0307
- Neuroscience 0317
- Oceanography 0416
- Physiology 0433
- Radiation 0821
- Veterinary Science 0778
- Zoology 0472

Biophysics
- General 0786
- Medical 0760

EARTH SCIENCES
Biogeochemistry 0425
Geochemistry 0996
Geodesy 0370
Geology 0372
Geophysics 0373
Hydrology 0388
Mineralogy 0411
Paleobotany 0345
Paleoecology 0426
Paleontology 0418
Paleozoology 0985
Palynology 0427
Physical Geography 0368
Physical Oceanography 0415

HEALTH AND ENVIRONMENTAL SCIENCES
Environmental Sciences 0768
Health Sciences
- General 0566
- Audiology 0300
- Chemotherapy 0992
- Dentistry 0567
- Education 0350
- Hospital Management 0769
- Human Development 0758
- Immunology 0982
- Medicine and Surgery 0564
- Mental Health 0347
- Nursing 0569
- Nutrition 0570
- Obstetrics and Gynecology .. 0380
- Occupational Health and Therapy 0354
- Ophthalmology 0381
- Pathology 0571
- Pharmacology 0419
- Pharmacy 0572
- Physical Therapy 0382
- Public Health 0573
- Radiology 0574
- Recreation 0575
- Speech Pathology 0460
- Toxicology 0383

Home Economics 0386

PHYSICAL SCIENCES
Pure Sciences
Chemistry
- General 0485
- Agricultural 0749
- Analytical 0486
- Biochemistry 0487
- Inorganic 0488
- Nuclear 0738
- Organic 0490
- Pharmaceutical 0491
- Physical 0494
- Polymer 0495
- Radiation 0754

Mathematics 0405
Physics
- General 0605
- Acoustics 0986
- Astronomy and Astrophysics 0606
- Atmospheric Science 0608
- Atomic 0748
- Electronics and Electricity 0607
- Elementary Particles and High Energy 0798
- Fluid and Plasma 0759
- Molecular 0609
- Nuclear 0610
- Optics 0752
- Radiation 0756
- Solid State 0611

Statistics 0463

Applied Sciences
Applied Mechanics 0346
Computer Science 0984
Engineering
- General 0537
- Aerospace 0538
- Agricultural 0539
- Automotive 0540
- Biomedical 0541
- Chemical 0542
- Civil 0543
- Electronics and Electrical 0544
- Heat and Thermodynamics ... 0348
- Hydraulic 0545
- Industrial 0546
- Marine 0547
- Materials Science 0794
- Mechanical 0548
- Metallurgy 0743
- Mining 0551
- Nuclear 0552
- Packaging 0549
- Petroleum 0765
- Sanitary and Municipal 0554
- System Science 0790

Geotechnology 0428
Operations Research 0796
Plastics Technology 0795
Textile Technology 0994

PSYCHOLOGY
General 0621
Behavioral 0384
Clinical 0622
Developmental 0620
Experimental 0623
Industrial 0624
Personality 0625
Physiological 0989
Psychobiology 0349
Psychometrics 0632
Social 0451

AN EM STUDY OF IMMUNOGOLD-LABELLED BASIC FGF IN DYSTROPHIC MDX AND NORMAL MOUSE DIAPHRAGM

BY

KAREN ANITA HAHN PENNER

A Thesis submitted to the Faculty of Graduate Studies of the University of Manitoba in partial fulfillment of the requirements for the degree of

MASTER OF SCIENCE

TABLE OF CONTENTS

ABSTRACT:

Duchenne muscular dystrophy (DMD) is a progressive, X-linked neuromuscular disease affecting 1 in 4000 boys. It is characterized by the absence of dystrophin, a protein known to play a vital role in the maintenance of sarcolemmal integrity. Progressive and rampant muscle degeneration, concurrent with extensive fibrotic and fatty infiltration compromise the structure and function of axial and limb muscles within the first decade of life. Medical, rehabilitative, and psychosocial concerns of those with DMD are extensive due to the prolonged degenerative nature of the disease, and ultimately cardio-respiratory insufficiency and failure prove fatal.

The mdx mouse is a valued and intriguing animal model for DMD, with a well documented and remarkable capacity for myofibre regeneration following dystrophic insult in its hindlimb muscles. In contrast, little is known about the mdx diaphragm (DIA) muscle, which reportedly demonstrates the progressive myofibre degeneration characteristic of DMD. Considering the importance of targeting future therapies such as myoblast transfer therapy and gene therapy to the DMD diaphragm, it is important to ascertain the role of specific myogenic and mitogenic agents in this process in diaphragm tissue.

Basic fibroblast growth factor (bFGF) is a pervasive and potent mitogenic, angiogenic, neurotropic, and chemotactic agent vital to myogenesis and muscle tissue integrity. This study represents the first known attempt to localize and quantify the distribution of bFGF at the ultrastructural (EM) level in mdx skeletal muscle, and in the diaphragm in particular. In this investigation, an immunocytochemistry protocol was developed, following extensive experimentation, to link electron dense collodial gold particles to bFGF epitopes in resin-embedded muscle sections which had been tagged with specific anti-bFGF antibodies. Omission of primary antibody and presorbtion with the bFGF antigen were used as controls for the gold labelling procedure. Gold-labelled bFGF in

myogenic cells (myoblasts, fusing myoblasts, central nuclei, satellite cells, peripheral nuclei), non-myogenic cells (endothelial cells and fibroblasts), sarcoplasm and extracellular matrix (ECM) was identified on micrographs of high resolution (x18,000 to x25,000), quantified, and compared statistically by means of a labelling index (LI) derived as the number of gold particles/μm^2 area.

Ultrastructural study of mdx diaphragm confirmed that there was significant histopathology, consistent with that of DMD limb muscles, and also markedly more severe than dystrophic changes in the hindlimb skeletal muscle. In addition, secondary dystrophic damage was observed in many fibres previously regenerated from an initial insult, suggesting early and repetitive damage. Statistically lower LIs were evident in most cell types and compartments in the dystrophic (mdx) diaphragm than in the control. Control muscle endothelial cells had the highest bFGF LI, followed in descending order by myoblasts and the ECM. A gradual and persistent decline in bFGF LIs was evident and statistically significant between the phases of myogenesis (fusion to differentiation and quiescence) in both control and mdx muscle, with the largest bFGF LI evident following the commitment of muscle precursor cells (myoblasts) to the myogenic lineage and expression of muscle specific filament proteins. In comparison, the hindlimb muscle of mdx mice, which demonstrated successful repair following dystrophic insult, exhibited much greater bFGF LIs than control hindlimb muscles, and the dystrophic mdx diaphragm. These findings suggest that there is a correlation between the amount of bFGF sequestered in the muscle tissue (both myogenic and non-myogenic cells, as well as in the ECM) and the ability of those muscles to respond adaptively to normal strain and to dystrophic insult. This may have implications for promoting the ability of dystrophic tissue to respond favourably to future cell and molecular therapies for DMD.

ACKNOWLEDGEMENTS:

Well, the thesis has been corrected, the oral defense passed and I'm still sitting at the computer trying to figure out how to begin the long list of thank-yous that are in order. This is not going to be easy...

To Dr. Judy Anderson: for being a remarkable advisor, provocative mentor, exemplary scientist, and 150% down-right super person and friend. Thanks for looking for the "potential" in this would-be researcher and then helping me to grow and develop (in the right directions!) to finally get there.

To the Manitoba Health Research Council: for the two year studentship that enabled the completion of this study on a full-time basis.

To my Examining Committee members Drs. Cheryl Greenberg, Jean Patterson, and Jim Thliveris: for their thoughtful critiques, questions, and interest shown in this project. Happy "trails" to you all!

To the Faculty and staff of the Anatomy Department at the University of Manitoba: for providing technical assistance and instruction in the "how tos" and "whys" of science, and helping me find my way around this place.

To Roy Simpson: who overcame tremendous adversity (ie. terrible negatives and a deadline of yesterday) to produce quality photographic plates and slides that brought my data "to life".

To my fellow Graduate students in the Anatomy Department: it's always nice to know you're not alone in your trials and in your achievements. The comradely chats in the hall and in class were great.

To the members of our lab: the people who made coming to work actually a pleasure (especially when there was a food offence on deck). Special thanks to Laura (Hey Cous with the cute cat!), Andrea (whose muscles have better regenerative capacities than those of my mice!), Kerryn (our Doc from down-under with the fuzzy friend), Annu (who "stuck" with me at poster time), and Chris (the original, through now token and phantom male). Thanks also to our fellow labbies now departed... Michael (the Co-founder of the Anderson Lead Pants Society), Steven (who knew where things belonged and actually put them back in place), and especially Marianne (Hey-Doc! Does life have meaning without mouse muscles?).

To Archie Cooper, Annie Strock, and Mary Pfleuger: for convincing me the persuit of a graduate degree was a (generally) good idea.

To the Faculty of the Division of Occupational Therapy, School of Medical Rehabilitation: for your encouragement, support, and interest as I journeyed through the realms of "graduate school".

To my parents-in-law, Erwin and Anna Penner: who were always there at the right time with practical help at home, support, and words of wisdom. You made a BIG difference!

To my parents, Paul and Margaret Hahn: though far away, you encouraged me to keep growing (not just in height). Your excitement and interest in my work has been a real boost and motivator thoughout my carreer. Thanks++.

And last but not least- to my husband Meredith and children: This is dedicated to you with thanks and appreciation for your tolerance, patience, TLC, and curiosity about what I was trying to do. You five were always there at the end of the day for me, making everyday (not just the good ones) seem worthwhile.

DEDICATION:

To my husband, Meredith

and our children

Zarah, Rebekkah,

Katherine, and Daniel

1.0 INTRODUCTION:

Striated skeletal muscle is a dynamic tissue which has the ability to successfully repair and regenerate following many forms of insult or injury. Myogenic repair is governed by a complex interplay of many factors, including the presence of muscle precursor cells (myoblasts) and appropriate levels of localized growth factors (Florini et al.,1991). When damaged skeletal tissue is unable to repair itself successfully or functionally, as in the case of Duchenne Muscular Dystrophy (DMD) (Rojas & Hoffman 1991; Emery 1989; Carpenter & Karpati 1984), the consequences may ultimately prove lethal. For those diagnosed with DMD and their families, a traumatic and lifelong process of attempting to adjust to acute, chronic, progressive, and finally terminal disease sequelae ensues (Miller, 1991). It is hoped, therefore, by gaining a better understanding of specific factors which promote successful muscle regeneration, we may in turn shed some light on future therapies appropriate for those afflicted with progressive deteriorating muscular disease such as DMD.

In this study immunocytochemisty techniques and electron microscopy (EM) were used to localize and compare the presence and distribution of basic fibroblast growth factor (bFGF), a potent mitogen implicated in muscle repair in normal and dystrophic skeletal muscle tissue (Florini 1990; Schweigerer 1990; Gospodarowicz 1986), particularly in myoblasts, the pool of muscle precursor cells in mature muscle (Stockdale 1989; Stockdale 1990; Johnson 1989; Emery 1989). An interesting animal model which demonstrates an X-linked muscular dystrophy, the mdx mouse (Bulfield et al 1984), was selected for use in the study. Mdx mouse muscle, while lacking the same dystrophin gene product as is absent in DMD (Partridge 1991), survives the dystrophic insult and ultimately is able to compensate through myoblast proliferation and regeneration to maintain a successful, functional outcome (Anderson et al., 1990; Anderson et al., 1988; Rojas & Hoffman 1991; Carnwath & Shotton 1987). This is in marked contrast to the boy with DMD, in which successful muscle repair ultimately fails and the

resulting disease sequelae prove fatal (Swash & Schwartz 1984).

Recent reports have identified a specific muscle in the mdx mouse, the diaphragm, which undergoes progressive fibrosis and deterioration rather than the characteristic repair and regeneration of the skeletal limb muscles in this model (Stedman et al., 1991; Dupont-Versteegden & McCarter, 1992). This observation raises the interesting and perplexing question "what mitogenic or repair factor(s) found in mdx skeletal hindlimb muscle are compromised or absent in the diaphragm, making the latter tissue susceptible to rampant fibrosis and degeneration?" This study addresses the question through a comparison of immunogold localization of bFGF in normal and dystrophic (mdx) diaphragm skeletal muscle tissue at the EM level. During the first phase of this project an effective immunogold labelling protocol was developed to visualize bFGF in C57Bl ScSn control and mdx (dystrophic) muscle. In the second phase, a bFGF labelling index (LI) was derived from observations and morphometric data (gold particles per micrometer^2) and the populations of muscle precursor cells (myoblasts, satellite cells) and mononuclear non-myogenic cells (fibroblasts, endothelial cells) were compared both within and between the two muscle strains. Significant differences in the bFGF labelling index (LI) might suggest a role for bFGF in promoting successful myogenic repair following dystrophic insult.

2.0 NORMAL SKELETAL STRIATED MUSCLE:

Normal skeletal muscle is composed of muscle cells (myocytes or myofibres) organized by connective tissue elements into groups of cells which act in a coordinated fashion to generate mechanical force. Muscle represents the active component of the musculoskeletal system, translating electrical and chemical signals into mechanical energy essential for movement, respiration, and the maintenance of body homeostasis. Muscle tissue compromises roughly 45% of the total human adult body weight, and can be further identified as over 350 distinctly named muscles, often occurring in pairs. Muscle tissue may be further classified according to structure as smooth, striated cardiac, or striated skeletal muscle, and according to metabolic profile as fast glycolytic, slow oxidative or mixed fast and slow.

2.1 Development of Muscle:

2.11 Origin of Muscle:

Beginning at week three in human embryonic development, the paraxial mesoderm differentiates in the longitudinal region adjacent to the developing notochord and neural groove (Moore, 1989). By 5 weeks gestation, the paraxial mesoderm has become segmented into 42 - 44 characteristic and distinct elevated blocks known as somites which ultimately give rise to the dermis, skeleton, and skeletal muscle (Johnson, 1989). Embryonic somites contain myotomal muscle primordia which proliferate, differentiate, and migrate to ultimately form the majority of trunk and limb musculature. Mesoderm from the branchial arches (head and neck primordia) differentiates into the muscles of mastication (branchial arch I), facial expression (branchial arch II), and pharynx/larynx (branchial arches III, IV, and V). In situ condensation of local mesenchyme involves aggregation and differentiation of the myoblast stem cell populations adjacent to the developing skeleton and was previously thought to account for the origin of some distal extremity

skeletal musculature (Moore, 1989). More recent evidence suggests, however, that the myoblast precursor cells migrate distally from the somites, and differentiate in a progressive lateral wave as the limb elongates (Olson et al., 1992). Nearly all myocytes therefore arise from intraembryonic mesoderm, the exception being the ectodermally-derived muscles of the iris.

2.12 **Development of Muscle Fibres:**

Four principal stages of myogenesis occur as an animal matures, beginning with commitment of undifferentiated presumptive myoblast-mesenchymal cells to definitive myoblasts. Upon commitment to distinct myogenic cell lineages, specific muscle contractile proteins are expressed in either slow or fast isoforms, depending on the muscle, innervation, hormonal status, location, species, and functional demands. This protein expression continues throughout myogenesis within existing fibres and results in the diversity of fibre type profiles evident between different muscles.

The four distinct stages of myogenesis include: i) formation of myotomal myoblasts, myotubes, and fibres from myogenic precursor cells in the somites, ii) formation of primary fibres in embryonic muscle prior to the completion of morphogenesis, iii) formation of secondary fibres in the embryonic and neonatal periods associated with rapid muscle growth, and iv) formation of regenerating or replacement fibres originating from satellite myoblast cells during adult life. (Stockdale et al., 1989). The following paragraphs expand on these stages and define parameters which are involved in defining muscle tissue at each stage.

The premyoblast cell originates as an undifferentiated mesenchymal cell with a ruffled border and containing typical cellular organelles such as ER, ribosomes, Golgi, mitochondria, and nucleus. This "presumptive myoblast" retracts its cellular processes to become spindle shaped, migrates out from the myotome region of the somites, and divides. It

and/or its daughter cells are somitic and differentiate into the striated muscle cell lineage (Boettiger et al., 1989). The definitive myoblast, arising postmitotically, is characterized by the synthesis and intracellular accumulation of actin and muscle specific proteins including myosin, troponin, tropomyosin, and alpha-actinin (Stockdale, 1989; Johnson, 1989). Ultrastructurally the myoblast is characterized by a prominent, central, oval nucleus with an enlarged nucleolus, many free-floating ribosomes and Golgi, glycogen granules, a well-developed rough endoplasmic reticulum, and a few globular mitochondria (Johnson, 1989). The myoblast develops muscle-specific membranous channels and compartments including the sarcoplasmic reticulum (SR) and T-tubules which form the muscle triad (Jorgenson, personal communication). Myoblasts express muscle-specific intermediate filament proteins desmin and H36+ just prior to the onset of terminal differentiation, suggesting or indicating that a specific myoblast phenotype exists even prior to the onset of terminal differentiation (Kaufman, 1989).

The myoblasts, having withdrawn from the cell-cycle under signals from muscle regulatory genes including MyoD and myogenin (Beilharz et al., 1992; Olson et al., 1991), aggregate and initiate synthesis of the contractile proteins actin and myosin. Actin and myosin myofilaments initially accumulate in an apparently random fashion within the myoblast cytoplasm and become distributed loosely in sheets beneath the plasma membrane. Eventually these myofilaments are assembled as parallel aggregates of thin and thick filaments, during which time, the myocyte becomes bipolar and elongated. The myocyte represents a mono-nucleated intermediate stage in myogenesis: although Z-line formation has begun to anchor the actin filaments no clearly discernable sarcomere patterns are yet visible.

The fusion of the juxtaposed plasma membranes of several adjacent myocytes results in the formation of the definitive syncytial primary myotube. As the primary myotubes mature, they undergo a reversible change

in cellular phenotype known as modulation in which a series of changes occur within the myoblast cytoarchitecture (Johnson, 1989). However, some myoblasts continue to proliferate into a second population. As the skeletal muscle anlage forms, the primary myotubes mature, and then the secondary population of myoblasts collect at the muscle to form secondary myotubes (Cox & Buckingham, 1992).

Initially the myofilament proteins of the contractile apparatus are localized to the periphery of the myotubes, and a core region is evident, comprised of central nuclei, mitochondria, and many glycogen granules. T-tubules develop as the myotube plasma membrane invaginates and concurrently the sarcoplasmic reticulum cisterns differentiate from the endoplasmic reticulum. The central myotube nuclei begin to migrate to subsarcolemmal positions as the ribosomes arrange into multiple long chains. With polymerization, the actin and myosin myofilaments orient longitudinally within the existing myotube and become organized into a regular array (sarcomere) that increases the myotube's functional efficiency in generating a contraction (Johnson, 1989). Mitochondria become elongated and also orient parallel to the long axis of the developing sarcomeres. New sarcomeres are added resulting in lengthening of individual myofibrils. Differentiation continues and an external lamina appears around each fibre, later to become associated with the appearance of collagen fibres.

A variety of fibre phenotypes may ultimately be manifest, depending upon the activation of specific genes that encode for unique isoforms of myofibrillar proteins, ATP-generating enzymes and acetylcholine receptors (Stockdale et al, 1989, Kaufman & Foster, 1989). Cox and Buckingham (1992), in their study on mouse skeletal muscle development, concluded that there are complex changes in the pattern of contractile protein gene expression at both the RNA and protein levels that transcriptionally regulate actin and myosin production.

The sarcolemma is the limiting membrane of an individual fibre and

is covered by an amorphous external lamina. Between the plasma membrane and the external lamina of myotubes, skeletal muscle myoblasts identified as satellite cells are evident (Moss & Leblond, 1971). These cells are committed to the muscle lineage, and become dormant in normal intact muscle once growth has ceased. Satellite cells appear as spindle-shaped mononuclear cells with an ovoid nucleus, highly condensed peripheral heterochromatin, a thin rim of cytoplasm containing few and rudimentary cell organelles, and usually have no myofilaments. The prevalence of satellite cells evident in mature healthy striated muscle typically declines with increasing age as a percentage of total muscle nuclei on a per fibre basis, and although they retain the ability to divide and differentiate into muscle, a decreased proliferative potential has been demonstrated with age(reviewed in Caplan et al., 1988). Satellite cell proliferation and fusion into myotubes plays a vital role in skeletal muscle repair and regeneration (Schmalbruch 1976; reviewed by Ontell, 1974). By comparison, mature striated cardiac muscle has no satellite cells and cannot proliferate in response to injury.

Intrinsic myonuclei of mature skeletal muscle fibres cannot divide since only satellite cells have that potential. Growth results instead from an increase in the number and/or size of individual myofibres depending upon the stage of development of the particular muscle, processes which are completed with the proliferation and fusion of satellite cells into new muscle. Most skeletal muscle fibres are in place at birth (Moore, 1989). Prenatal growth to the muscles or to older fibres occurs primarily as an increase in the number of myofibres present in a given muscle, although not all embryonic muscle fibres persist until birth (Moore, 1989). From birth through the first year of life the size and to a smaller extent, the number of the myofibers increases to accompany rapid skeletal growth. From this point on the actual numbers of myofibers remain very nearly constant. Normal muscle fibres increase in size with maturation from 16 microns diameter at 1 year-of-age to 40 microns in

diameter at 10 years-of-age. Adult muscle fibre size is achieved by 12 to 15 years-of-age and ranges in men from 40-80 microns and in women from 30-70 microns in diameter (Swash & Schwartz, 1984).

Muscle hypertrophy, or an increase in the size of fibres, results when increasing numbers of myofilaments are formed and the overall fibre diameter increases (Moore, 1989). Hypertrophy may also occur when nuclei generated from satellite cell division, fuse with parent fibres, The interplay of the two processes (myofilament expansion and nuclear expansion) during hypertrophy is limited by the size of local nuclear domains along the length of a fibre, within which nuclei are able to regulate protein synthesis. Skeletal muscle will differentiate and develop in the absence of innervation but innervation is critical to the final maturation of normal skeletal muscle activity and strength or force generation.

2.2 **Mature Skeletal Muscle Structure:**

Mature muscle fibres (myofibers) are elongated, cylindrical, multinucleated "giant" cells. In healthy tissue myofibers appear unbranched with conical or semiconical ends. Muscle fibres average 1 to 40 millimetres in length (up to 30 cm),and 10 to 100 micrometers in width (Junqueira et al, 1989). Factors including age, sex, nutritional and hormonal status, and physical training account for the variation in diameter evident between specific muscle fibres. Individual muscles typically consist of a muscle belly, the contractile portion, which tapers to ends attached by connective tissue tendons via Sharpey's fibres to bone. Fibre branching is rare and normal only at sites of tendon insertion or as a response to work-induced hypertrophy following training. In healthy mature skeletal muscle tissue regenerating and necrotic fibres are also rare.

Muscle fibres are enclosed in a fine connective tissue layer known

as the endomysium, composed of mainly external lamina and reticular fibres. Muscle fibres are regularly arranged in small, variable sized groupings known as fascicles. Each fascicle in turn is surrounded by a fibrous connective tissue perimysium, which originates as thin septa extending inward from the external epimysium. Multiple fascicles make up an individual muscle which is covered by the thick external dense connective tissue layer of epimysium or fascia. The ensheathing connective tissue layers play a vital role in the alignment of the mechanical transmission of forces generated by contracting muscle cells. As well, the internal layers provide a route between and parallel to the muscle fibres for the dense capillary and lymphatic network to run (Junqueira et al, 1989). Myofibers are each supported in a stroma consisting of collagen, reticular and elastic fibres, fibroblasts, mast cells, and histiocytes which populates the interstitium between fibres.

Transverse sections of healthy, intact, mature human skeletal muscle tissue are characteristically polygonal with multiple peripheral nuclei. Fat and fibrous tissue may be evident interfasicularly in small amounts with thicker fibrous planes expected near sites of fibre insertion on internal tendons. Fatty tissue is uncommon within fascicles but may occur in greater amounts in the larger interfasicular boundaries. Within fascicles, fatty tissue should not infiltrate or replace individual muscle fibres. With aging, the endomysium thickens slightly but this causes only a slight separation between adjacent muscle fibres.

Myonuclei are ovoid, typically elongated along the same axis as the myofibre. They are bound by a double membrane, demonstrate prominent nucleoli, contain heterochromatin and euchromatin, and are peripheral in location in the fibre, between the sarcolemma and the contractile myofibrils. In healthy mature skeletal muscle, up to 3 to 5% of myonuclei are centrally placed, due to the previous repair of muscle injured by normal use and exercise. Multiple central myonuclei, a hallmark of regenerated muscle tissue in mouse and man, are most evident in damaged

or pathological tissue such as DMD (Karpati et al., 1988).

The muscle cell cytoplasm or sarcoplasm contains numerous mitochondria, glycogen granules, myoglobulin, and myofibrillar inclusions. Most organelles and much of the non-contractile sarcoplasm lies adjacent to the nuclear poles along the sarcolemma. The sarcoplasm also contains long, cylindrical protein myofilaments organized into bundles known as myofibrils. The exact number of myofibrils in each muscle fibre varies. The contractile myofilaments are in turn composed of two major types: a thin (6nm diameter) actin myofilament and a thick (16nm diameter) myosin myofilament. Actin and myosin filaments lie parallel to the long axis of the myofibrils and account for 55% of the total protein of striated muscle: the remaining 35% includes alpha-actinin, tropomyosin, troponin polypeptide complexes, and many cytoskeletal proteins including dystrophin (see section 3.3) and dystrophin-associated glycoprotein (DAP) (Ervasti et al., 1990).

Myosin filaments are 1.6 micrometers long and occupy the central portion of the sarcomere. Myosin is a complex protein made up of six different polypeptides; two identical heavy chains which twist together and 2 pairs of light chains (Ganong, 1989). Myosin molecules are asymmetrical rods with tiny projections or "heads" found at one end of each heavy chain. Each myosin filament seen by EM is composed of several hundred myosin molecules arranged by an overlapping of the rod-like portions of the individual myosin molecules, and demonstrating six rows of heads. The heads are arranged in pairs at intervals of 14.3 nm along the length of the filament with each pair precisely rotated in relation to the previous. The myosin heads are globular and contain a site which binds and hydrolyses ATP. The head of the myosin molecule and a portion of its rod-like base form cross-bridges between the thin and thick filaments in the regions where the two filaments overlap in the sarcomere. During isotonic contraction, the cross bridges are the force producing element, and their "rowing" acts to slide actin filaments attached along myosin

rods to shorten the muscle.

Actin is composed of two strands of globular actin molecules polymerized and twisted into a double helix which form filamentous actin. Each globular actin monomer contains a binding site for myosin. In cross section at the ultrastructure level, 6 actin filaments may be found in a hexagonal array surrounding each myosin filament in the sarcomere region of actin- myosin overlap.

Tropomyosin molecules are about 40 nm in length and contain two polypeptide chains twisted in an alpha helix form (Junqueria, 1989). The molecules bind head-to-tail to form tropomyosin filaments that run along the outer grooves of the actin filaments. Troponin is in fact a complex of three distinct proteins: TnT, which binds firmly to tropomyosin; TnC, which binds to calcium ions; and TnI which inhibits the interaction between actin and myosin. Each troponin complex is bound to one specific site on the tropomyosin molecule, which in turn spans seven globular-actin molecules. The unit formed by this combination of actin, tropomyosin, and troponin is known as a "thin" filament.

Longitudinally myofilaments are arranged into a linear unit of contraction known as a sarcomere, visible at the light microscopic (LM) level. Sarcomeres may vary in length depending upon the state of contraction (1.8 nm maximally contracted to 3.8 nm fully relaxed) in width from .5 to 1.0 nm. (*1) Perpendicular to the long axis of the myofibril, distinct bands or lines are evident within the sarcomere resulting from the specific arrangement of actin and myosin filaments. The chain-like arrangement of individual sarcomeres in series with each other and in register with adjacent myofibrils results in distinct continuous bands, evident at the LM level, which serve as useful reference points and give rise to the term striated muscle.

An individual sarcomere is demarcated by the Z-line or Z-disk at either end. The Z-line contains the protein alpha- actinin which anchors one end of each thin filament perpendicular to the Z-line. Alpha actinin

serves to maintain the specific spatial distribution of each thin filament as it projects into the middle of the sarcomere and is thought to play an important role with desmin (an intermediate filament protein) in binding adjacent sarcomeres together. Actin filaments exhibit reverse polarity on opposing sides of the Z-line.

The I-Bands (isotropic), contain thin filaments and connectin anchoring proteins, and are found on each side of the Z-line. The overall length of the I-band is determined by the phase of contraction: with muscle shortening it becomes reduced as the thin filaments are drawn towards the central M-line in the myosin filament. The A-band (anisotropic) is found in the mid-sarcomere region and has a fixed length of approximately 1.6 nm. The A-band denotes the position of the thick myosin filaments and lies between I-bands where thin filaments do not overlap thick filaments. At higher magnification, a paler central region of the A-band known as the H-band and darker peripheral portion, where the thick and thin filaments overlap become evident. The H-band contains only the myosin molecule shafts and is in turn bisected by a thin M-line. The M-line marks the centre of the sarcomere and demarcates the region where lateral connections are made between adjacent thick filaments (Junqueria, 1989).

Muscle cells contain specialized smooth endoplasmic reticulum. In striated muscle this sarcoplasmic reticulum (SR) consists of a network of anastomosing membrane-limited tubules and cisternae which surround each myofibril and regulate calcium ion flow. Calcium ions, sequestered in the SR cisternae are released following neurally mediated cell depolarization. Calcium binds to troponin (TnC) and allows bridging between actin and myosin. When membrane depolarization ends, the calcium ions are actively transported back into the SR cisternae and contraction ceases.

From the periphery of the muscle fibre, the sarcolemma invaginates and penetrates to encircle the A/I junctions of each sarcomere in every myofibril (Junqueria, 1989). This invagination, known as the transverse

tubule or T-tubule system allows for rapid transmission of the surface-initiated depolarization signal to all myofibrils, essential for uniform skeletal muscle contraction. Adjacent to each T-tubule at the A/I junctions are the expanded terminal cisternae of the SR. The combination of 2 terminal cisternae and one intervening T-tubule is know as a triad. The muscle triad transmits the neurally-derived depolarization signal at the sarcolemma via the T-tubule system to the SR cisternae to stimulate the release of calcium from the SR and the initiation of muscle contraction. The triad also regulates the subsequent calcium sequestering by the SR to relax the contractile apparatus.

Specialized connections or synapses known as a myoneural or neuromuscular junction occur between the sarcolemma of skeletal muscle fibres and the terminal boutons of a motor neuron. Contraction is initiated through a complex chain of events in which the axon terminal transmits chemical signals in synaptic vesicles of acetylcholine across the junction, resulting sequentially in depolarization of the muscle motor end plate, sarcolemma and T-tubules, resulting in calcium release. Ultimately depolarization triggers the binding of myosin filament heads to actin, resulting in the movement of actin filaments towards the centre of each sarcomere. This movement generates the production of energy and results in the shortening of the I band, the sarcomere, the myofibrils in the fibre, and the entire muscle in turn. When calcium is resequestered by the SR, binding of myosin heads to actin filaments is once again inhibited and the sarcomere returns to its longer resting length.

All human striated muscle contains encapsulated sensory receptors known as muscle spindles which act to relay information on dynamic and static proprioception. Muscle spindles are typically 1.5 nm long and are comprised of 2 to 20 specialized myofibers (intrafusal fibres) contained within a fluid-filled connective tissue capsule. The intrafusal fibres have accumulated nuclei in their equatorial regions. One or two longer, thicker Nuclear Bag intrafusal fibres may be distinguished by their

distinct nuclear swellings from the shorter, thinner nuclear chain intrafusal fibres. Both types of intrafusal fibres detect changes in the length of the extrafusal muscle fibres and have distinct roles to play in the adjustment of muscle length and tension.

Muscle spindles occur typically close to neurovascular bundles in an interfasicular plane. Neurovascular bundles contain small arteries and veins in addition to myelinated and non-myelinated nerve fibres. The diameter of the neurovascular bundles varies, but each nerve innervates a specific number of muscle fibres call a motor unit. Small arterioles, venules, and perimysial capillaries (typically 2 to 5) surround each muscle fibre.

Motor endplates or myoneural junctions are found on each mature muscle fibre within the perimysial connective tissue. The neural and muscle components of the neuromuscular junction are separated by a specialized synaptic cleft. The dilated neural axon terminal bouton consists of short axonal expansions overlain by Schwann cell cytoplasm. The axonal expansions contain numerous mitochondria and clear synaptic vesicles, the latter containing the neurotransmitter acetylcholine. Acetylcholine (ACH) is liberated from the synaptic vesicles following the arrival of an action potential at the motor end-plate, and diffuses across the synaptic cleft. It then binds to ACH receptors in the sarcolemma of the post-synaptic junctional folds. Through a series of interactions, the binding of the ACH transmitter causes a membrane depolarization which is ultimately propagated along the surface of the muscle cell and deep into the fibres by the T-tubule system. This in turn results in the release of calcium ions and initiates the muscle contraction cycle. Motor endplates are not often seen in routine muscle biopsies as they are typically localized to specific regions along the length of the fibres in a muscle.

In summary, normal, mature skeletal muscle is characterized histologically by the following features: homogeneous, polygonal fibres in fasicles on cross section, striated fibres on longitudinal section,

multiple peripheral nuclei, little intrafasicular connective or fatty tissue infiltration, substantial vascularization, and minimal numbers of inflammatory cells.

2.3 Size and Fibre Typing of Skeletal Muscle:

Skeletal muscle fibres may be typed according to myoglobin content, the number of mitochondria, and contraction speed. Different fibre types are found in a mosaic distribution pattern across a given muscle, and in human muscle fibres the types are intermingled. Type I fibres, also known as "red" or "slow-twitch" fibres, are fatigue resistant and capable of prolonged, vigorous activity (Junqueria, 1989). They predominate in muscles in which sustained contraction is important and demonstrate a slow steady response to stimulation and then slow relaxation. Significant quantities of myoglobin, cytochrome and mitochondria are evident in Type I muscles, which predominate in postural and lower limb muscles. An example of a Type I muscle referred to in this study is the hindlimb soleus muscle of the mouse.

Type II or "white", "fast twitch" fibres are larger, glycolytic and exert a brief , rapid, phasic contraction and show rapid fatigue. They cannot support continuous heavy work but produce more force than slow-twitch fibres (Junqueriq, 1989). Type II fibres can be further subtyped into 4 classifications: Type II-A, II-B, II-C, II-M, and II-X depending upon the type of myosin heavy chain present usually by staining with immunohistochemical techniques. Type II fibres predominate in extraocular and in upper limb and hand muscles. The extensor digitorum longus (EDL) hindlimb muscle in the mouse is an example of a muscle which has predominately Type II fibres.

The majority of human striated skeletal muscle is composed of mixtures of Type I, Type II and intermediate fibre types, its differentiation into a particular muscle type being influenced in part by its innervation (Junqueria, 1989). The relative proportions of different

fibre types are under genetic influences, the effects of training and exercise, and hormone status (Swash & Schwartz, 1984).

3. DUCHENNE MUSCULAR DYSTROPHY:

Duchenne Muscular Dystrophy (DMD) is the most common form of muscular dystrophy in humans, a class of genetic disorders of muscle characterized by progressive degenerative changes in skeletal muscle fibres. Segmental myofibre necrosis occurs, and is followed by fibre loss and consequent "attempts" at regeneration which fail to supply enough new fibres to prevent the advancing course of the disease. Concomitant with the loss of muscle fibres is the progressive proliferation and infiltration of fibrotic and adipose tissue into muscle fasicles (Rojas & Hoffman 1991). Ultimately DMD proves lethal.

DMD was first formally described in the mid 1800's by Duchenne de Bologne who noted a progressive disease of muscle weakness that led to death by age 20 in affected males. Others believe that pictorial representations of boys afflicted with muscular dystrophy date back to early Egyptian and the Middle Age periods in history. It was only recently that abnormalities of the dystrophin gene (see section 3.3) were implicated in the etiology of DMD (Hoffman et al., 1987).

3.1 Clinical Manifestations of DMD:

Considerable variability in the clinical manifestation of DMD exists. This arises as the disease affects primarily or possibly secondarily a variety of tissues including skeletal muscle, cardiac and smooth muscle, brain tissue, and some visceral organs (Emery, 1989). Progressive symptomatology experienced by the DMD population is multisystemic involving respiratory, cardiac, musculoskeletal, and gastrointestinal systems.

Skeletal muscle involvement is pronounced in DMD and rampant muscle fibre degeneration, connective tissue infiltration, and proliferation of fatty tissue are hallmarks of the disease process. Skeletal muscle weakness usually is evident in the large proximal muscles of the lower limbs. Involvement of the hip and knee extensors is soon accompanied by

weakness of the pelvic girdle. By 3 to 5 years of age the boy with DMD demonstrates difficulty in climbing stairs, running, and in rising from the floor (Carpenter & Karpati, 1984). Delayed motor milestones become progressively prominent, and the DMD boy demonstrates frequent falls and eventually difficulty walking, maintaining a broad-based waddling gait. Gower's manoeuvre, a characteristic clinical sign in the DMD population, becomes evident as DMD boys must raise themselves from the floor to standing by compensatory upper limb pushing, climbing up their legs due to proximal leg muscle weakness (Korenyi-Both, 1983). As the disease progresses, the feet and shoulder girdle also become involved, but typically to a lesser extent. Pseudohypertrophy of the calves, deltoids, and serratus anterior results, as increased connective and fatty tissue replace muscle bulk. Often severe myofibre atrophy in muscle biopsies and clinical muscle weakness are evident despite the external appearance of well-developed, robust musculature. Contractures in the Achilles tendon, force the boys into a compensatory and less stable tiptoe gait which in turn, reinforces an excessively lordotic lumbar posture and marked postural distortions result (Carpenter & Karpati, 1984).

Between 9 and 12 years of age, the DMD child faces the "wheelchair crisis stage". Walking ceases to be a functional and safe method of ambulation and the child begins to become dependent upon a wheelchair. This results in a cascade of further complications, brought on in part by physical inactivity. The development of contractures accelerates, notably involving the tensor fascia lata and calf muscles (Carpenter & Karpati, 1984). Scoliosis and significant back pain become a major concern, and rapid progression in the degree of musculoskeletal weakness, deformity and discomfort experienced is common following confinement to a wheelchair. Spinal fusion done prophylactically and customized seating and positioning units often prove necessary for the support and comfort of many mid-to-late stage DMD patients (Colbert & Curran, 1991).

Abnormalities in the vascular and skeletal systems such as decreased

peripheral circulation and reduced bone density have been noted, likely as a result of both the disease itself and secondary to the decreased muscle strain important in maintenance of bone strength. The extraocular and majority of the craniofacial muscles demonstrate no functional impairment (Carpenter & Karpati, 1984) although progressive weakness and contractures of the masseter and pharyngeal muscles may be evident during the late-stage of the disease process.

Involvement of the cardiac muscle has been noted by several authors. Korenyi-Both (1983) noted the presence of ECG abnormalities both with and without cardiac symptoms in the DMD population. Emery (1989) reported frequent persistent sinus tachycardia and arrhythmias in DMD boys and the tendency of the postero-basal part of the outer-free wall of the left ventricle to be particularly affected by fibrosis. Chamberlain et al. (1989) reported that death may result from the cardiac arrhythmias evident, although Carpenter & Karpati (1984) report that cardiac symptomology usually occurs in the late stages of the disease process when significant compromise is evident in many tissues, most noteably those involved with respiration. Colbert & Curran (1991) in a study of 30 late-stage, ventilator-dependent young men with DMD cited primary or secondary cardiac complications as the most common cause of patient death. They also noted that 70 to 80% of this population experienced significant and distressing chronic respiratory insufficiency in addition to severe gastrointestinal symptoms.

Studies of the gastrointestinal tract in DMD patients demonstrated marked variation in muscle fibre size, atrophy and loss of smooth muscle fibres, and regions of pronounced fibrosis (Emery, 1989). Difficulties chewing and/or swallowing, gastrointestinal malabsorption, constipation, abdominal discomfort, halitosis and obesity are frequently reported as secondary but not inconsequential problems for this population (Colbert & Curran, 1991).

CNS involvement has been suggested, due to a 30% incidence of non-

progressive mental retardation and learning disabilities evident in boys with DMD (Hoffman, Bertelson, & Kunkel, 1989), where scores of intelligence rank one deviation below the normal mean (Emery, 1989). Although the intellectual impairment is slight, a normal distribution with a mean 20 points lower than unaffected siblings was noted by Korenyi-Both (1983), suggesting an organic basis to the retardation. Leibowitz & Dubowitz (1981) reported that the reduction in intelligence score affected verbal more than performance scores, and was not related to either the extent of physical disability or a lack of educational opportunities. No significant pathology has been determined at autopsy to date which could account for this intellectual impairment (Emery, 1989), although known dystrophin deficiencies within the CNS are likely implicated.

Ultimately the disease sequelae prove fatal, and 75% of the DMD population dies before 21 years-of-age, usually from cardio-respiratory complications (Swash & Schwartz, 1984). Survival beyond 30 years-of-age is unusual, and then only since the advent of life support systems.

3.2 **Inheritance of DMD:**

Duchenne Muscular Dystrophy is an X-linked recessive disorder, with the trait carried on the short arm of the X chromosome at band Xp21. DMD affects 1 in 4000 male births, making it the second most common single gene disorder affecting man after cystic fibrosis (Emery 1989). It is estimated that 1/3 of the boys affected represent new mutations (Swash & Schwartz, 1984), the remainder affected by transmission from carrier mothers. Both the very large size of the DMD gene and non-equal crossing over during meiosis, caused by specific homologous sequences in the dystrophin gene, have been given as possible explanations for this high mutation rate (van Essen et al., 1992). Half of the male offspring of carrier mothers develop the full clinical DMD syndrome; half the female offspring will be carriers. Female carriers themselves typically show no overt clinical signs of DMD, although a few carriers with X-autosome

translocations manifest the disease and demonstrate hypertrophied calves, slight-to-severe proximal weakness, raised CK levels, and a mosaic pattern of dystrophin positive and negative fibres (Carpenter & Karpati, 1984, Rojas & Hoffman 1991).

3.3 **The DMD Gene:**

The DMD gene, first identified by Hoffman et al. (1987), spans approximately 2.5 million base pairs of the X chromosome (Rojas & Hoffman, 1991) and is ten times larger than any other gene characterized to date (Hoffman, Bertelson, & Kunkel, 1989). This unusually large target size for possible mutagenic agents is hypothesized to explain the high spontaneous mutation rate (30%) evident in the DMD population (Monaco & Kunkel 1987; Rojas & Hoffman, 1991). DNA probes around the site of the breakpoint have been generated and to identify the DMD gene as having approximately 70 exons (Rojas & Hoffman, 1991) and a mean size for introns of 35 kb (Koenig et al 1987; Emery, 1989).

At least sixty-five percent of affected boys demonstrate submicroscopic gene deletions of DMD cDNA with a high degree of heterogeneity of the specific exons deleted (Bartlett et al.,1988; Emery,1989; Hoffman et al.,1989). Duplication mutations have been found in 5 to 6 % of Duchenne patients (Hu et al., 1990) and the remaining 30% are presumed to have point mutations (Rojas & Hoffman, 1991). Hoffman further identified "hot spots" for the initiation of the DMD mutation. Monaco et al. (1988) noted, however, that the size of the actual gene deletion does not appear to correlate with the clinical phenotype. What is important is important whether the deletion causes a reading frame shift, to result in truncated, non-functional dystrophin (DMD) or not (Becker Muscular Dystrophy, BMD) (Hoffman et al., 1989). Partial gene duplications and point mutations have been identified in both Duchenne and Becker type muscular dystrophies. Arahata et al. (1991), while supporting

the reading frame hypothesis, provided evidence that the carboxy-terminal domain plays a key role in correct dystrophin function in the cytoskeleton.

3.4 Dystrophin- The Missing Gene Product:

The characteristic protein product of the DMD gene has been called dystrophin. Dystrophin was originally presented as an "intracellular, plasma-membrane-associated, large molecular weight, low abundance, cytoskeletal protein present in nearly equal levels in all types of terminally differentiated myogenic cells" (Hoffman et al., 1987). Dystrophin is a very large protein with a molecular mass of 420 kD subdivided into four domains which have similarities with other muscle cytoskeletal proteins such as spectrin and alpha-actinin. Dystrophin is present in very small amounts in normal skeletal muscle. It is thought to account for less than 0.002% of the total striated muscle protein or 2% of the plasma membrane fraction protein (Hoffman et al., 1987) and to play primarily a structural rather than enzymatic role (Rojas & Hoffman, 1991; Kelly et al., 1992).

Subcellular localization studies have confirmed the distribution of dystrophin along the intracellular face of the plasma membrane in striated and smooth skeletal muscle (Hoffman, 1987; Sugita et al., 1988; Emery, 1989), synaptic regions of neurons (Miikw et al., 1989; Miyatake et al., 1990), neuromuscular junctions especially in the postjunctional folds (Huard et al., 1992), and myotendon junctions (Shimizu et al., 1989). Dystrophin has also been detected in cardiac and smooth muscle though to a lesser extent, and in renal, cerebral cortical, lung tissue (Chelly et al., 1988) and the spinal cord (Chamberlain et al., 1989). Yaffe et al. (1989) localized DMD mRNA in small quantities in the spleen, brain, lung, and testis of the rat, suggesting different mRNAs in the brain and in muscle may result from alternative initiation of transcription. There are now approximately 11 isoforms of dystrophin described which confirm the

alternative splicing during transcription. In skeletal muscle, expression of the DMD gene is thought to occur following myoblast stem cell fusing and differentiation into myotubes (Miranda et al., 1990). Hoffman (1988) also reported DMD gene expression in a neuron population in cell culture, though not by any cell type found in the peripheral circulation.

Initial studies of muscle tissue localized dystrophin in close association with muscle triads and the T-tubule system in particular (Hoffman et al. 1989). Later however, Zubrzycka-Gaarn et al. (1989, 1991) proposed a role for dystrophin associated with the sarcolemma rather than with triads. They propose that dystrophin anchors internal cytoskeletal elements to the surface membrane, thereby strengthening the sarcolemma itself. Subsequent ultrastructural studies (Cullen et al., 1990; Petrof et al., in press) confirmed the subsarcolemmal rather than the triad localization, and proposed that the primary function of dystrophin is to provide mechanical reinforcement and protection to the sarcolemma during stresses induced by muscle contraction. Dystrophin is bound to the plasma membrane by strong interactions with other intrinsic membrane proteins, acting as a member of a larger family of cytoskeletal proteins, including DAP, alpha- actinin and spectrin with which it displays structural and sequence similarities (Rojas & Hoffman, 1991). Dystrophin accumulations have also been correlated with accumulations of desmin in striated and smooth muscle cells and neuromuscular junctions in various species (Huard et al., 1992). Petrof et al (in press) propose two distinct mechanisms whereby dystrophin impacts sarcolemmal stability during muscle contraction. In the first instance he proposes that the interaction of dystrophin with structural elements known to exert tension upon the sarcolemma, helps to distribute the mechanical forces associated with contraction over a broader membrane area. Alternately or additionally, the presence of a dystrophin-associated glycoprotein (DAP) complex which spans the sarcolemma, may protect the sarcolemma by transmitting mechanical forces across and beyond the membrane to the extracellular

matrix as well.

Immunoblot, immunoflourescent and immunohistochemical techniques found dystrophin to be absent in DMD skeletal muscle even in preclinical cases (Emery 1989, Hoffman et al. 1989), which was confirmed in the mdx mouse model of DMD (Anderson et al., 1990). Together these studies conclusively demonstrate that classic DMD is caused by a marked deficiency of the carboxy terminal of dystrophin in skeletal muscle (reviewed by Rojas & Hoffman, 1991).

3.5 **Effects of Dystrophin Deficiency:**

The exact mechanism by which dystrophin deficiency causes DMD remains uncertain. Hoffman (1989) speculated that dystrophin, being involved in maintaining sarcolemmal integrity, regulates intra-cellular levels of calcium. The total calcium content of dystrophic muscle fibres appears elevated (reviewed in Hollingworth et al., 1990) with the large influxes of calcium ions potentially resulting in striated myofibre hypercontraction and necrosis, visceral and vascular defects (secondary to smooth muscle fibre involvement), and possible neuronal defects (Hoffman, 1989). Haws and Lansman (1991) found the normal developmental down-regulation of mechanosensitive calcium channels lacking in dystrophin-deficient (mdx) murine skeletal muscle, and support the notion that alteration of mechanisms which regulate the expression of functional channels may be an early step in the dystrophic process. These observations have not been supported by more recent work which contends that mechanical instability of the membrane due to dystrophin deficiency is the etiology of mdx and likely DMD dystrophy (Kelly et al., 1992).

Both the quantity and the quality of the dystrophin present are felt to determine the clinical severity of the dystrophy that results from its absence: the total absence of dystrophin results in the severe Duchenne form of muscular dystrophy, while the presence of a truncated form of dystrophin accounts for the milder clinical presentation of Becker

Muscular Dystrophy (Hoffman, 1988). A physiological or biochemical threshold may exist which must be crossed before a dystrophin deficient myofibre is subject to necrosis (Hoffman et al., 1989).

Emery (1989) proposed that dystrophin deficiency in skeletal muscle tissue results in altered cell surface membrane stability and altered cell surface antigens. This in turn might render the muscle susceptible to T-cell attack resulting in damage to the muscle membrane and an influx of calcium ions. If calcium-activated proteases were then enhanced, muscle fibre necrosis and mitochondrial overload would follow, leading to reductions in oxidative phosphorylation and cell death.

Three current working hypotheses reviewed by Rojas and Hoffman (1991) attempt to explain the effects of dystrophin dysfunction in DMD. The first "leaky membrane" hypothesis proposes that the dystrophin deficiency results in a non-specific instability of the plasma membrane, leading to localized, transient rifts in the sarcolemma which allow for unregulated passage of materials into and out of the cell (Hoffman, 1991). This position has been supported by findings which localize large quantities of large molecules (creatine kinase and aldolase) outside the cell and significant accumulations of serum albumin and calcium ions intracellularly. The model further proposes that many variables, in addition to dystrophin-deficiency induced plasma membrane instability, are involved and lead to calcium induced myofibre necrosis (Hoffman, 1991).

The second hypothesis proposes that the dystrophin deficiency causes a specific biochemical dysfunction of the associated integral membrane proteins known to be anchored, localized, or regulated by dystrophin (Rojas & Hoffman, 1991). Dystrophin forms a complex with several glycoproteins of different molecular weights (35 kD, 43 kD, 50 kD, and 156 kD) in the membrane (Ervasti et al., 1990). When absent, dysfunction of the integral proteins results, which could allow abnormal calcium ion homeostasis to play a central role in DMD pathogenesis. Specific dystrophin-associated glycoproteins become deficient when

dystrophin (which keeps them in a non-random distribution) is lacking (Ervasti et al., 1990).

Keller (1992) refutes the involvement of calcium-activated proteases and proposes instead that the lack of membrane stability results in a susceptibility to work-induced injury and may be a key event leading to cell death. This position, supported by Campbell et al. (1989), Hutter et al. (1991), and Anderson et al., (1993 in press), notes that dystrophin, by stabilizing the plasma membrane and maintaining normal membrane folding and flexibility, gives increased resistance to muscle contractile stresses and protects against mechanical damage.

In reviewing a series of patch-clamp studies of dystrophic skeletal muscle, Rojas & Hoffman (1991) conclude that the observed increased sensitivity of the membrane to the mechanical stresses (generated by the patch-clamp) results from the dystrophin deficiency which affects normal plasma membrane-cytoskeletal interactions. They also note that the progressive fibrosis evident in DMD may be in turn stimulated by leaking myofibre cytoplasm and misdirected wound repair. Menke et al. (1991) observed a reduced resistance to osmotic stress in mdx myotubes and muscle fibres. More recent work (Petrof et al., 1992) in which dystrophin deficient mice demonstrated increased susceptibility to contraction-induced sarcolemmal rupture, correlated to the magnitude of the mechanical stress placed on the membrane during contraction, have supported the proposition that a primary function of dystrophin is to provide mechanical reinforcement to the sarcolemma.

McArdle et al. (1991) while refuting the notion that dystrophin-deficient muscle is more susceptible to work induced damage, noted that the release of intracellular CK in vitro was greater in control than mdx muscle following excessive contractile activity. They proposed that dystrophin-deficiency influences instead, the activity of muscle membrane phospholipase enzymes such as prostaglandin E_2.

3.6 Muscle pathology and regeneration in DMD:

Muscle biopsies were routinely employed for diagnostic purposes prior to the development of appropriate DNA used in PCR detection of DMD gene deletions from lymphocyte DNA. Characteristic changes, though not specific to DMD, are evident in dystrophic muscle depending upon the stage of the disease. The work of Swash & Schwartz (1984) and Carpenter & Karpati (1984) outlined these changes in detail:

1) Early in the disease process, typically between years one to five when the child is still ambulatory, hyaline fibres appear in transverse sections as darker, larger, and rounder than the normal polygonal fibres evident in striated muscle. Hyaline fibres, thought to result from segmental myofibril hypercontraction secondary to the absence of dystrophin, have a glassy, homogeneous sarcoplasm and often show tears in their cytoplasm. Longitudinal sections of hyaline fibres demonstrate the absence of cross-striations in the hypercontracted segments.

2) Fibre necrosis appears during the early and middle stages of the disease, spreading in a variable, longitudinal fashion to adjacent components of the affected fibre. The transition zone between necrotic and intact segments occurs at different levels, creating a staggered appearance histologically. Necrotic fibres, found typically in small clusters of 3 to 10 fibres, are especially prevalent during the preclinical stage of the disease. The fibres undergo a series of characteristic changes, summarized below, and demonstrate peripheral precipitations of calcium and a "ground glass" matrix appearance.

3) Significant macrophage infiltration of necrotic fibre segments occurs and the fibre segments attract abundant numbers of macrophages by an unknown chemotactic signal, possibly fibroblast growth factor (FGF). Phagocytosis of debris by macrophages both within the necrotic segment and between muscle cells is marked.

4) Regenerating fibres appear in small, basophilic clusters within a fascicle in the early disease stage. They have a small cross-sectional

area, vesicular cytoplasm, (cytochemically reacting with ribonucleic acid) and large central or nonperipheral nuclei. Regenerating fibres are often closely associated with endomysial inflammatory cell infiltrates, and fibres may demonstrate branching if regeneration results from incomplete or aberrant fusion of myoblasts. Split fibres occur when segments of multiple daughter fibres fuse, each with a distinct sarcolemma, within one endomysial sheath. During the midstage of the disease process, fibre splitting is most prominent, declining as the disease progresses. This also would suggest that a once regenerated myofibre is still subject to damage.

5) Hypertrophied fibres with tremendous variation in size appear in the middle stage of DMD (years 6 - 10), as marked muscle weakness and pseudohypertrophy become evident. This means that "pseudohypertrophy" must at one stage not be "pseudo" but real. Hypertrophic, rounded fibres may range from the normal 10-40 to 235-250 micrometers in diameter, and are distinct from hypercontracted fibres by the preservation of their cross striations. Marked interfasicular and endomysial fibrosis may be evident, independent from the integrity of any local muscle fibres. Type I and Type II myofibres are both affected, although there is a larger susceptibility of fast-twitch (than slow twitch) fibres to dystrophic insult, perhaps related to the greater contraction speed and force generation producing larger strain and perturbations of an unstable fibre membrane (Webster et al., 1988).

Central nuclei are prominent in the majority of myofibers during the middle stage of DMD. Central nuclei appear large and pale staining, and demonstrate prominent nucleoli, thought to indicate increased protein production (Korenyi-Both, 1983). The accentric persistence of myonuclei within the centre of regenerated myotubes in human and mouse skeletal muscle enables their use as an effective index of muscle regeneration in dystrophic tissues (Karpati and Carpenter, 1984). As central nuclei demonstrate the potential to ultimately migrate back to the periphery

(Anderson, 1990), this index must be interpreted with some care. Indeed different counts of nuclear members rather than an index of fibre centronucleation reveal different aspects of muscle regeneration (Zacharias & Anderson, 1991).

From the mid to the later stages of DMD, muscle fibre hypertrophy, though less obvious, continues. Blood vessels continue to demonstrate a normal distribution pattern and, like muscle spindle fibres and intramuscular nerve bundles, appear preserved through end stages in the disease process. Thickening of the spindle capsule and enlargement of the periaxial space may be evident.

Significant collagen and adipose tissue infiltration occurs concurrent to the progressive muscle cell loss. Eventually fat replaces much of the muscle bulk and the interstitium of muscles becomes heavily fibrotic. Prominent inflammatory cell infiltration, characteristic of the earlier disease process, diminishes although macrophage clustering in and around newly necrotic fibres persists. Actively dystrophic striated skeletal muscle thus contains a combination of hypertrophic, atrophic, necrotic and regenerating myofibres within a fatty and fibrous connective tissue matrix that contains numerous inflammatory cells.

Limited fibre-type differentiation in DMD muscle has been demonstrated through myofibrillar ATPase histochemistry. Type 2C fibres occur commonly in DMD muscle, typically in small groupings, and may represent a transitional myosin heavy chain (MHC) in undifferentiated form. Adult maturation of fibre types is generally incomplete during the mid to late clinical stages of DMD.

Discrete muscle pathology has been demonstrated in some carriers of DMD. Muscle fibre hypertrophy, increased central nucleation, variability in fibre size, fibre splitting, and occasional basophilic fibres are the most common findings in this group (Dubowitz & Brooke, 1973). Other carriers have presented clinically with features similar to severe DMD although the onset is usually delayed. This variation in clinical

phenotype may relate to the Lyonization of different alleles on the two X chromosomes of the female carrier.

Following cell injury or death, serum creatine kinase (CK) and pyruvate kinase (PK) levels escalate after their release from damaged myocytes. In DMD males, significantly elevated CK and PK levels, which precede apparent clinical manifestations, have proven useful as diagnostic tools though not specific to DMD (Swash & Schwartz, 1984). In later stages of the disease process however, the CK level does not correlate with the severity of muscle damage as little intact muscle tissue remains to release the enzymes.

Muscle regeneration subsequent to necrotic insult follows a series of steps similar in nature to those described during embryonic and fetal muscle development. As focal fibre necrosis spreads longitudinally along individual myofibers, characteristic changes in the mitochondria, myofibrils, and T-tubules ensue, resulting in the disrupted morphology described previously. Pronounced macrophage infiltration and phagocytosis of necrotic debris occurs within old external lamina tubes, which eventually become relined by regenerative myoblasts. Caplan et al. (1988) noted macrophage infiltration precedes in vivo activation of these myogenic cells in damaged fibres. He speculated that the macrophagic infiltration either removed a negative feedback influence on myogenic cells during phagocytosis of damaged myofibre cytoplasm, or alternately, provided an intrinsic positive stimulus triggering myogenic cellular activation.

Myofibre regeneration is mediated by the proliferation of mononuclear myoblasts (precursor or satellite cells), which form a sparse population (4 %) of the total peripherally located nuclei evident by light microscopy. Peripheral myonuclei (inside myofibres) are not thought to divide (Moss & Leblond, 1971; Stockdale, 1990) although there is one supposed report of myonuclei activating for division (Naidoo, 1992). Satellite cell populations, evident between the external lamina and the

sarcolemma of a myofibre in normal muscle tissues (Mauro, 1961), appear to be in a state of dynamic change. Following necrotic insult and macrophage invasion, satellite cells develop pseudopodia and demonstrate mass migration to the outside of fibres within the external lamina. In some instances, cells are thought to migrate between muscles, their number peaking at 18 to 24 hours post insult (reviewed in Macro et al., 1988). This satellite stem cell migration, evident during and/or preceding a myogenic regenerative response, is an integral component of the total process (Schultz et al., 1988). The actual chemotactic signal employed to guide the movement of satellite cells is however unknown, though growth factors released from dying myofibers or the extracellular matrix have been suggested to play a significant role (Kardami et al., 1985; Bischoff, 1986). Satellite cells from dystrophic (mdx) mouse muscle, which develops genetically induced myofibre lesions, are thought to be particularly activated by fibroblast growth factor (DiMario et al., 1988), although that study was not careful with controlling experimental variables in tissue culture studies.

Following proliferation and migration of satellite/ myoblast stem cells, fusion occurs longitudinally and transversely amongst those cells, and with the surviving myofibre stump, to reestablish muscle fibre continuity and generate new myotubes. Cytologic features of regenerating myotubes, characteristic for cells producing large amounts of intracellular protein, include: enlarged nuclei with prominent nucleoli, abundant polyribosomes, and an intensely basophilic cytoplasm resulting from high cellular RNA content. Contractile proteins assemble initially at the myotube periphery with later myofibrils added in succession towards the myotube core. The definitive transition from myotube to muscle fibre is a gradual process in development: chains of fusing myonuclei break up and individual nuclei migrate peripherally. The presence of peripheral myonuclei marks a mature myofibre rather than a myotube in the regeneration process, and for the most part complete fibre differentiation

in regenerating muscle remains innervation dependent and may never be attained (Hasley & Anderson, submitted; Beilharz et al., 1992). The percentage of proliferating vs. quiescent satellite cells evident in regenerating fast and slow muscle tissue returns to normal levels following the usual sequence of myofibre differentiation in normal muscle(reviewed in Caplan et al. 1988).

In DMD muscle tissues, repetitive cycles of necrosis and regeneration are apparent. Interestingly, subsequent rounds of necrosis do not appear to affect regenerated fibre segments until they reach maturity and a more normal size (Anderson et al., 1987). One report (DiMario et al.,1991) supposedly detailed that fibre regeneration is not persistent, that cells do not undergo more than one round of degeneration, although their data were based on tissue level expession of neonatal MHC not an examination of whether centronucleated fibres could be damaged as seen by Anderson et al., 1987 and Anderson et al., 1991. Duplication of the external lamina or absence of that layer apposed to the plasma membrane may occur (Anderson et al., 1987). Dystrophic skeletal fibres may branch due to incomplete lateral fusion, end blindly, or fail to regenerate (Anderson, 1991; Caplan et al., 1988), as ultimately evident in mdx diaphragm tissue (Stedman et al.,1991). Wakayama (1976) reported that although an increased number of satellite cells exist in DMD skeletal muscle, the repetitive, cyclical, necrotic insults inherent in the disease process render satellite cells unable to successfully compensate for fibre loss by making sufficient new fibres.

Interestingly, myoblast fusion is not species restricted. The potential therefore exists to inject normal myoblasts into host and DMD tissue. This procedure, known as myoblast transfer therapy, has been shown to partially rescue dystrophic muscle fibres from their biochemical defect (Partridge et al., 1989; Karpati et al., 1989; Karpati, 1990). As well foreign genes can be cloned and transfected in harvested muscle precursor cells, and the altered cells reinjected into host tissue.

Injected myoblasts fuse during myogenesis and form fibres of specific properties at discrete developmental periods (Stockdale, 1990; Partridge et al., 1989), although preliminary studies (Merrifield, 1993 personal communication) show that fusion into homotypic (all injected cells) or heterotypic (injected cells fused to host) fibres cannot be predicted. Preliminary investigations of myoblast transfer therapy, and gene transcription as a therapeutic approach in the management of DMD are interesting, though success to date has been limited in producing dystrophin-positive fibres(Partridge et al., 1989; Karpati et al., 1989; Karpati, 1990; Huard et al., 1991).

Distinct histological pathology has also been demonstrated in fetal tissue, presumed by family history and raised placental CK levels to be DMD. Pathological findings evident in fetal skeletal muscle biopsies taken at 18 to 20 weeks gestation included increased variation in muscle fibre diameter, increased connective tissue, and the presence of hyaline fibres (Emery & Burt 1980; Emery, 1989). The significance of these findings is interesting but unclear. Most puzzling is the knowledge that although individuals with DMD lack dystrophin from fetal life onwards, overt clinical signs of dysfunction do not become apparent until approximately four years of age (Hoffman, 1991). The presence of DAP and dystrophin-related proteins (DRP) may provide initial protection to the sarcolemma despite the genetic absence of dystrophin itself.

3.7 **Ultrastructure of DMD Skeletal Muscle:**

Four stages in the disease progression have been identified in ultrastructural studies of DMD. The first stage is evident as a membrane defect, secondary to the dystrophin deficiency, results in discontinuities in the plasma membrane of muscle fibres secondary to the dystrophin deficiency. This is followed by a "decompensated enzyme stage" in which widespread dilation of the SR becomes evident. During the third stage of active dystrophy myofibre hypertrophy, increased numbers of small

myofibrils, and hyaline necrosis are apparent (Korenyi-Both, 1983). EM abnormalities described are many and include: invaginated and indented subsarcolemmal nuclei and prominent central nuclei; focal disruptions of the myofilaments evident as Z-line streaming; a honeycomb appearance to the now vesicular T-tubule system ("pentads" arrangement) accompanied by significant dilation of SR terminal cisternae; and a increasing number of swollen mitochondria lacking their usual cristae become grouped at the myofibre periphery.

During the final atrophic stage, fibre contractile elements aggregate with mitochondria and cell organelles along the central axis of the fibre. An empty 'halo' appears separating cellular organelles and the sarcolemma, possibly reflecting a swelling of the cell and/or atrophy of contractile material. The number of satellite cells continues to increase (Wakayama, 1976), as does significant fibroblast infiltration accompanied by increased interstitial collagen deposition. Ultimately cellular infiltration results in a "sclerotic mass of dense connective tissue" (Karpati 1984) containing phagocytes and monocytes surrounding severely disrupted fibres. Myotubes with new fibrils, myoblasts, and myocytes may all be present together in one muscle. Satellite cells continue to display active mitosis throughout the disease process however attempts at regeneration become unsuccessful.

4.0 **ANIMAL MODELS FOR DMD:**

Dystrophin has been detected in the muscle of all vertebrates studied to date. This includes human, rat, dog, cat, guinea pig, rabbit, frog, and chicken (Hoffman et al., 1987, 1988). Three unique dystrophin deficient models which emerged spontaneously in otherwise normal populations, include the mdx mouse (Bulfield et al., 1984), the CXMD canine (Cooper, 1989; Kornegay, 1988), and the dystrophin deficient feline (Carpenter et al., 1989). All show significantly elevated serum creatine kinase (CK) from birth and a similar muscle histopathology early in the

disease process (Rojas & Hoffman, 1991). These animal models demonstrate minimal pathology during the neonatal period despite having significantly high serum CK levels. High CK is used as an indicator of the extent of muscle damage, however samples taken after muscle damage secondary to manipulation or surgery (eg. thoracotomy) may be artificially elevated, which could impact this finding. Most interestingly, the clinical outcomes of dystrophin deficiency among the animal models are notably divergent as the disease progresses. Not all animal models demonstrate the end-stage histopathology characteristic of DMD. The mechanism by which an identical genetic and biochemical abnormality results in significant variations of the expressed clinical phenotype among different dystrophin-deficient species is as yet unknown, but may relate to many processes including proliferative capacity, muscle fibre types, animal activity, the exact gene defect, Lyonization differences between species, etc.

4.1 **The dystrophin deficient canine:**

The CXMD canine demonstrates a progressive histopathology which resembles DMD. Histologic lesions, apparent even in preclinical stages (Valentine & Cooper, 1991), continue and attempts at myoregeneration following necrosis ultimately fail. Muscle degeneration persists, accompanied by progressive fibrous and fatty infiltration and diffuse calcification (Partridge, 1991). Clinical weakness is evident in the CXMD model by 2 months of age, followed by the development of muscle contractures, hypertrophy of select muscle groups, and deterioration to an early death in a manner similar to that of the DMD patient. Unlike man, however the X-linked dystrophic dog demonstrates an earlier onset, a more rapid progression of dystrophy followed by a phase of relative clinical stability, and a highly variable clinical phenotype (Valentine et al., 1990). Valentine & Cooper (1991) noted the muscles first displaying signs of myofibre necrosis are those experiencing the greatest activity in the

newborn state (tongue, diaphragm, pectoral girdle) and also show an early maturation to the adult fibre type pattern. A high frequency of neonatal death is evident in the dystrophin-deficient dogs, linked to significant pathological lesions evident at the time of birth in the CXMD diaphragm. The authors propose that, with severe myofibre necrosis also evident in neonatal CXMD limb muscle tissue, myofibre maturation may not be a critical antecedent to dystrophic necrotic insult. They furthur propose that small diameter fibres may not be protected from the ensuing necrotic episodes as previously speculated (Karpati et al., 1988).

4.2 **The dystrophin-deficient feline:**

The X-linked dystrophic cat model, discovered spontaneously in a non-breeding colony, demonstrated "stiff muscles", selective muscle hypertrophy, striking variation in fibre size, and widespread fibre necrosis and regeneration with limited fibrotic infiltration (Carpenter et al., 1989). The limited descriptive data available on this animal model suggests a chronic but mild myopathy similar to that of the mdx mouse (see below). A second litter of fertile dystrophin-deficient cats has been identified more recently and attempts are underway to establish breeding colony for further research purposes (Hoffman, 1991).

4.3 **The dystrophin-deficient mouse:**

The first widely used animal models of DMD were dy and dy^{2j} mice. Both demonstrated progressive muscle weakness, carried as an autosomal-recessive disease, and compromised health and lifespan, but were abandoned as true animal models for DMD following a report by Hoffman et al., (1987) which demonstrated the presence of dystrophin positive muscles fibres in these animals. This was later confirmed by Anderson et al. (1990) who noted the presence of dystrophin positive bands in both fast- and slow-twitch hindlimb muscles in the $D4^{25}$ strain.

The mdx strain of dystrophic mouse arose as a spontaneous mutation

in a colony of ScSn Bl57 mice, characterized by Bulfield et al. (1984), and accepted a genetic model for human Duchenne muscular dystrophy (Chamberlain et al., 1989; Partridge, 1991). Mdx mice persistently lack dystrophin (Hoffman et al., 1987; Anderson et al., 1990) secondary to a point specific single base substitution on the X-chromosome that results in premature termination of the polypeptide chain (Sicinski et al., 1989). There are greatly reduced DMD gene mRNA levels in both mdx muscle and brain (Chamberlain et al., 1989) and significantly reduced (80-90%) dystrophin-associated muscle membrane glycoproteins (DAP) (Ohlendieck et al., 1991). Matsumura et al. (1992) however, found DAPs preserved in small skeletal muscles (lumbricals, extraoccular) and cardiac muscle of mdx mouse and noted a simultaneous increase of dystrophin-related proteins (DRP) in these tissues (a four fold increase in mdx cardiac tissue and 1.3 fold increase in the quadriceps muscles). DRP is an autosomal homologue of dystrophin, expressed in fetal and regenerating tissue (Tinsley et al., 1992). Matsumura et al (1992) proposed that altered levels of DRP somehow compensate for dystrophin deficiency in mdx mice by helping to retain DAPs in extrajunctional regions of the sarcolemma. Altered DRP expression therefore could result in preservation of small skeletal and cardiac muscles evident in mdx mice.

Although mdx mice share the same biochemical and genetic defect as DMD boys, they do not develop clinically overt weakness, the histologically rampant fibrosis, or failure of myoproliferation characteristic of DMD (Carnwath & Shotton, 1987; Anderson et al., 1987; Dangain & Vrbova, 1986; Hudecki and Pollina, 1990). Rather, these mice demonstrate successful cycles of myofibre degeneration and regeneration accompanied by progressive muscle hypertrophy, indicated by muscle fibres up to two or more fold larger than the norm (Anderson et al., 1988; Rojas & Hoffman 1991). The mechanism of the fibre hypertrophy may relate to an increased accumulation of contractile material in dystrophic muscle (Sacco et al., 1992) though the cause of this is not yet known (Valentine & Cooper,

1991).

Histologically, X-linked dystrophic mice demonstrate a sudden onset of massive, segmental muscle fibre necrosis 2 1/2 to 3 weeks after birth in skeletal muscles of the limb and trunk, accompanied by active compensatory myofibre regeneration (Carnwath & Shotton, 1987; Coulton et al., 1987; Anderson et al., 1987). Satellite cells and immature myotubes appear adjacent to degenerating muscle fibres, with clusters of neutrophils and macrophages visible between apparently intact myofibres. Z-line streaming, evident very early in the disease process, spreads progressively until much of the contractile apparatus of the fibre becomes disorganized (Torres & Duchen, 1987). By three weeks of age widespread loss of sarcoplasmic structure accompanied by vacuolation is visible alongside newly regenerating myofibers in hindlimb muscles (Carnwath & Shotton, 1987; Anderson et al., 1987). Satellite cells demonstrate rapid proliferation during this period (Anderson et al., 1987; McGeachie et al., 1992) and the expression of skeletal myogenic regulatory genes MyoD and myogenin is most pronounced (Beilharz et al., 1992). Significantly reduced force production, fatiguability in fast muscle, and prolonged half relaxation times become apparent by 3 - 4 weeks of age in mdx mice, attributed to extensive muscle damage (Anderson et al., 1988), disorganization of the contractile apparatus, reduced muscle strength, and/or the immature state of regenerating fibres (Dangain & Vrbova, 1984). Foci of acute segmental necrosis and myofibre regeneration, most prominent at one to two months of age, persist though gradually declining throughout adulthood (Torres & Duchen, 1987; Anderson et al., 1987).

By two to three months of age mdx skeletal muscle fibre necrosis decreases in intensity (Tanabe, Esaki & Nomura, 1986) and whole muscle contraction speed, tension, and relaxation appear equal to or greater than those of control populations (Anderson et al., 1988), although individual fibres are likely weaker than normal since muscle weights are large. Adult mdx skeletal limb muscle demonstrates central nucleation in

70 - 80% of fibres (Karpati et al., 1988), marked variability of fibre diameter (Anderson et al., 1988), and sporadic fibre splitting (Anderson et al., 1987; Partridge, 1991). Following the phase of active dystrophy the serum PK and CK levels diminish (Coulton et al., 1988). The total number of muscle fibres appears maintained (Anderson et al., 1987; Carnwath & Shotton, 1987), however muscle hypertrophy is evident (Anderson et al., 1988). Hypertrophied mdx muscles appear stronger than controls; however, their force when estimated per unit of cross-sectional area is significantly lower than normal (Sacco et al., 1992; Dupont-Versteegden et al., 1992; Anderson et al., 1988).

By six months of age virtually all skeletal muscle fibres in the mdx mouse appear centrally nucleated, indicative of a muscle that has regenerated, with limited fibrosis and interstitial adipose tissue replacement (Tanabe et al., 1986; Anderson et al., 1987). Foci of single, peripherally nucleated original, myofibers persist (Anderson et al., 1987).

Mature regenerated mdx fibres appear generally resistant to furthur significant degeneration (Karpati et al., 1990), although pockets of localized myofibre damage continue to be observed in regenerating fibres (Anderson et al., 1987). Regenerated mdx myofibers demonstrate increased endomysial and perimysial collagen (Marshall et al., 1989), and a major and concurrent transition from Type 2 to Type 1 fibres (Carnwath & Shotton,1987), and from Type IIB (fast glycolytic) to IIA (fast oxidative glycolytic) (Anderson et al., 1988). Mdx hindlimb muscles appear differentially affected by dystrophic insult, the slow-twitch soleus demonstrating relatively stable fibre typing and earlier and more successful regeneration than the fast-twitch extensor digitorum longus (EDL) (Anderson et al., 1988). A similar disproportional increase in the proportion of Type 1 fibres has been noted in DMD populations (reviewed in Carnwath & Shotton, 1987).

Clinically, adult mdx mice do not demonstrate overt signs of muscle

weakness or of functional compromise. They are heavier (Anderson et al., 1987; Coulton et al., 1988) and muscles, such as the tibialis anterior, may weigh up to 80% more than controls (Anderson et al., 1987; Sacco et al., 1992). Muscle weight to body weight ratios however are unchanged (Anderson et al., 1987). The spontaneous physical behaviour and endurance of adult mdx mice decreases with age, but is not significantly different from age-, sex-, and body-weight matched controls (Hudecki & Pollina, 1990). Their longevity appears unaffected by dystrophin deficiency, in stark contrast to those with DMD (Carnwath & Shotton, 1987).

One mechanism linked to the successful myogenic response of mdx mice to dystrophy is the maintenance of intact blood and nerve supplies and basal lamina (Dangain & Vrbova, 1984). Studies of the neuromuscular junction(NMJ) in mdx mice, however identified a reduction of at least 50% in the complexity, number and depth of postsynaptic folds (Torres & Duchen, 1987), although intact fibres appear to have normal NMJ . Lyons and Slater (1991) demonstrated both redistribution of postsynaptic molecules and reduction in synaptic foldings exclusive to neuromuscular junctions in regenerated young adult (8 week) mdx muscle fibres. They concluded the repeated cycles of myofibre necrosis and regeneration, not dystrophin deficiency at the neuromuscular junction, accounted for the evident remodelling of pre- and postsynaptic components. Focal degeneration at the junctional folds, widening of the synaptic cleft and simplification of the postsynaptic region were found also in DMD neuromuscular junctions, resulting in altered but not impaired neuromuscular transmission (reviewed in Nagel et al., 1990).

Grounds and McGeachie (1992) proposed that ultimately the myogenic responses of mdx mice and non-dystrophic strains to injury are similar in terms of the timing and the pattern of myogenic cell replication. This conclusion following experimental crush injury however, was based on a very small sample population. Others view the ability of mdx muscle to initiate and maintain regenerative capacities and recover after imposed

injury as unique, citing regeneration to be greater in young than old mdx muscle (Zacharias & Anderson (1991), and greater in mdx than their control strain populations (Anderson, 1991; Zacharias & Anderson, 1991; McIntosh, Pernitsky, & Anderson, submitted). Mdx skeletal muscle appears to demonstrates prolonged or greater levels of satellite cell proliferation relative to control muscle following crush injury (McIntosh, Pernistky, Anderson personal communication) which in combination with factors such as the presence of greater levels of endogenous bFGF (Anderson et al., 1991; DiMario et al., 1989), may account in part for its remarkable regenerative capacities.

Differences in muscle fibre typing have also been linked with varying degrees of successful muscle regeneration. Following denervation and devascularization of the EDL at four weeks of age, mdx fast-twitch hindlimb muscle demonstrated significantly greater recovery of contractile characteristics (isometric twitch and tetanus tensions) than controls (Mechalchuk et al., 1992). Anderson et al. (1987) reported an earlier onset of necrosis in mdx s low-twitch (soleus) than fast-twitch (EDL) myofibers, although conversely at later stages fast-twitch muscles ultimately demonstrated greater pathology, a factor in common with DMD muscle (Webster et al., 1988). Cooper and Valentine (1991) found distinct patterns of necrotic insult in the CXMD model, first evident in muscle groups essential for survival, and required by the neonatal dog to breathe, suckle, and crawl. Antigravity muscles required to stand and walk, activated later between 2-4 weeks of age, showed a delayed onset of dystrophy. These studies suggest mechanical stress may in part determine the degree of necrosis evident in actively contracting dystrophin-deficient muscle. Whether dystrophin deficiency itself renders skeletal muscle more susceptible to mechanical damage remains controversial (reviewed in Sacco et al., 1992), although it is known to render the sarcolemma more susceptible to focal breaks (Weller et al., 1990; Petrof et al., in press 1993).

4.31 Mdx diaphragm tissue:

The histopathology of the mdx diaphragm appears to be distinct from hindlimb skeletal muscle, in that the mdx mouse diaphragm reproduces the degenerative changes characteristic in DMD than do most of the limb muscles (Stedman et al., 1991). Distinct patterns of degeneration, fibrosis, and severe functional deficit are evident in mdx diaphragm muscle (Dupont-Versteegden et al., 1992). Adult mdx mice do not appear to demonstrate overt clinical signs of respiratory compromise, however (Kelly et al., 1991), despite significantly reduced force generation, and a gradual shift to slower, though less fatiguable, fibre types (Dupont-Versteegden & McCarter, 1992). Petrof et al. (1992a) found the maximal twitch and tetanic tension of mdx diaphragm reduced to 15% and 20% respectively of control values. This was accompanied by a concurrent increase in expression of type I myosin heavy chain and substantially increased muscle endurance. This response to the dystrophic insult contrasts markedly with that of the DMD population in which histological and functional respiratory compromise is significant (Carpenter et al., 1984).

Stedman et al. (1991) first documented the dystrophic changes evident in mdx diaphragmatic tissue. He noted the presence of limited foci of myofibre degeneration, necrosis, mineralization, and regeneration in coexistence by 30 days of life. From this point on, progressive myofibre deterioration occurred without the corresponding regeneration evident in mdx skeletal hindlimb muscle. By six months of age, the adult mdx diaphragm demonstrates a wide variation in myofibre size and architecture, continued necrosis, marked fibrosis, and adipose infiltration. Collagen density increases to seven times that of control diaphragm tissue and 10 times that of mdx hind limb muscle (Stedman et al., 1991).

By two years of age, limited signs of attempted regeneration persist in mdx diaphragm, however significant physiological changes now accompany

the histopathology. These include severe loss of tissue strength (to 13.5% of control) and elasticity, reduced twitch speed, a 35% net loss in sarcomere and fibre resting length, a four fold reduction is isometric force generation, and a two fold increase in the proportion of slow fibres relative to control populations. Stedman et al. (1991) proposed that dystrophin deficiency alters the threshold for work-induced injury in the diaphragm, thereby perturbing the normal balance between injury and repair in muscle fibres bearing the greatest workload. In the case of cage-reared mice, they speculate that the obligatory respiratory work of the diaphragm significantly out measures that of the limb muscles, resulting in degenerative changes despite the large pool of regenerative satellite cells evident. Studies in which cage reared mdx mice underwent strenuous physical exercise, however, failed to demonstrate significantly increased degeneration in skeletal limb muscles following work-induced stress, which did impact on diaphragmatic muscle injury (Hudecki & Pollina, 1990).

4.32 **Selection of the mdx model:**

Mdx mice have been described as excellent therapeutic models for DMD because, though they fully manifest dystrophin deficiency, they lack the progressive secondary effects of the disease process, thereby proving valuable to monitor the effects of treatment, such as myoblast transfer, in an uncompromised manner (Hoffman, 1991). Mdx mice are an excellent mammalian model to study the process of fibre degeneration and regeneration (Carnwath & Shotton, 1987; Anderson et al., 1987, 1988), and are an important model for understanding the disease processes involved in DMD (McGeachie et al., in press 1993). The mdx animal model is unique in that although mdx hindlimb skeletal muscle overcomes the initial effects of dystrophic insult and demonstrates successful myoproliferation, the diaphragm muscle conversely demonstrates the progressive myopathy and fibrosis characteristic of DMD. Though a transient increase in the

development of active tension is evident in mdx diaphgram during the first 100 days of life, it is followed by progressive deterioration of muscle strength and endurance, alterations of fibre type, and a decrease in protein content (Dupont-Veersteegden and McCarter, 1992). This replicates the dystrophic changes evident in DMD muscle. These attributes, in combination with the relative ease in care, handling, and breeding, short gestation period, rapid onset of dystrophy, and natural longevity of the mdx mouse model of DMD, make it a valuable model for many research projects. The strikingly divergent responses to dystrophin deficiency in the mdx diaphragm vs. skeletal limb muscle make it also a most interesting and perplexing animal model for DMD.

5.0 FIBROBLAST GROWTH FACTORS

Growth factors (GF) are relatively small polypeptides, produced and secreted by a variety of cells and tissue types (Florini et al., 1991; Logan, 1990). Growth factors, like endocrine system hormones, regulate cellular functions through distinct cell membrane receptor-mediated mechanisms in a manner not yet fully comprehended (Logan, 1990). Though some propose that the "distinction between protein hormones and growth factors is arbitrary and has little biological difference" (Florini et al., 1991), current research clearly differentiates the two entities (Logan, 1990; Yayon & Klagsbrun, 1990; Baird & Bohlen, 1991).

Peptide growth factors are signalling molecules which promote growth, control differentiation, and act in a multifunctional nature, depending upon the other effectors and receptors present (Sporn et al., 1991). Peptide growth factors provide an essential means for cellular communication with its immediate environment, promote local cellular homeostasis, and control gene transcription.

Problems inherent in the early identification of growth factors, including divergent naming of common entities by the discipline or by the function(s) first assigned, resulted in confusion over the classification

of specific GFs. Fibroblast growth factor (FGF), for example, comprises a family of structurally related proteins and a number of oncogene products known by at least 23 synonyms (Florini et al., 1991) but thought to derive from one ancestral gene (Gospodarowicz et al., 1986). The FGF family includes acidic FGF (aFGF), basic FGF (bFGF), int-2, hst/K-fgf, FGF-5, FGF-6, and FGF-7 (Gospodarowicz et al., 1987a; Baird & Bohlen, 1991; Rifkin & Moscatelli, 1989; Gospodarowicz et al., 1987b; Mignatti & Rifkin, 1991) and is characterized by a high affinity to heparin (Vlodavsky et al., 1991), heat and acid lability (Gospodarowicz et al., 1987b), and known pleiotropic, multifunctional effects that vary depending on cell type (Baird & Bohlen, 1991). FGFs regulate cell growth and differentiation (Florini et al., 1991) and have perhaps the widest range of tissue distribution and broadest spectrum of biological activities of all known growth factors (Mignatti & Rifkin, 1991). They exert potent mitogenic and angiogenic effects on mesodermal- and neuroectodermal-derived tissues (Baird & Bohlen, 1991; Vlodavsky et al., 1991; Gospodarowicz et al., 1987b), and are inducers of mesenchymal formation (Vlodavsky et al., 1991).

Different FGF pools use paracrine, autocrine and/or intracrine mechanisms to effect cellular responses (Logan, 1990). Paracrine secretion, in which trophic factors travel to the target cells by diffusion, and autocrine secretion, in which the target cells produce and "secrete" the trophic factor which in turn interacts with receptors on the same cell surface, are known to regulate FGF-cellular interactions (Logan, 1990; Mignatti et al., 1991). Research continues to focus on the intracrine action of FGF, which can remain within the cell of origin and act directly as an intracellular messenger to regulate nuclear gene expression and therefore affect cell function (Baird & Bohlen, 1991).

Immunoflourescence studies which localized nuclear and cytoplasmic bFGF found only nonspecific associations of bFGF in secretory vesicles, mitochondria, or membrane fractions, suggesting a distribution pattern

inconsistent with that of an autocrine or paracrine protein (Renko et al., 1990). Yayon and Klagsbrun (1990) proposed a comigration and continuous interaction of growth factors and growth factor receptors along the length of a cell's secretory pathway, an "internal autocrine transformation" loop. Following "secretion", bFGF binds to high affinity cell surface receptors and generates a mitogenic signal which results in rapid internalization and degradation of the receptor-ligand complex. Subsequently non-lysosomal transport pathways translocate the intact bFGF into the nuclei of target cells (Bouche, 1987).

The concept of intracrine regulation of FGF is supported by its intracellular localization, its lack of a peptide signal sequence required for translocation across rough endoplasmic reticulum membranes, and its known effects at modulating gene transcription within the nucleus (Logan, 1990).

5.1 **Identification of Basic FGF**

Fibroblast stimulating factors were known to exist in tissue extracts since the 1940's. Initial identification and characterization of FGF occurred in 1974 by Gospodarowicz, who purified from bovine brain and pituitary extracts, a 12kD mitogen capable of causing the proliferation and phenotypic transformation of BALB-C 3T3 mouse fibroblast cells (Gospodarowicz, Neufled, & Schweigerer, 1987b; Rifkin & Moscatelli, 1989; Schweigerer, 1990). The FGF mitogen has since been purified to homogeneity, its amino acid sequences determined, and its cDNA cloned and sequenced (Baird & Walicke, 1989). This led to the identification of two distinct though structurally related FGF peptide chains; acidic and basic FGF (Baird & Bohlen, 1991). Characterization also led to the discovery of a plurality of 16 names previously assigned to the single bFGF mitogen by researchers who identified and labelled it in a variety of ways based upon observed angiogenic-, fibroblast- and endothelial- stimulating properties, and its marked affinity for heparin (Gospodarowicz et al.,

1987a; Baird & Bohlen, 1991).

The two main prototypes of the FGF family, acidic (aFGF) and basic (bFGF) mediate their effects through binding to common cell surface receptors. Basic FGF, however, is more widely distributed than aFGF, and is 50 to 100 fold more potent (Schweigerer, 1990). Acidic FGF and bFGF are unique polypeptides in that both lack a signal sequence to govern secretion along typical pathways (D'Amore, 1990). The acquisition of a signal peptide has been documented to convert bFGF into a transforming protein, analogous to FGF-related oncogenes, resulting in uncontrolled cell growth and tumorigenicity (Yayon & Klagsbrun, 1990).

Acidic FGF shares 55% total sequence homology to bFGF (Gospodarowicz et al., 1986; 1987b), is a 140 amino acid protein with an acidic isoelectric point and may exist in a truncated form, lacking the first 6 amino acids (Gospodarowicz et al., 1987b). Acidic FGF is an agonist of bFGF (Gospodarowicz et al., 1987a) and contributes only a small portion of the total mitogenic activity present in crude brain (8%) or retinal (0.15%) extracts relative to bFGF (Gospodarowicz et al., 1987a).

The human genome contains one copy of the bFGF gene located on chromosome 4 (Baird & Bohlen, 1991; Rifkin & Moscatelli, 1989). The bFGF gene spans over 40 base pairs (Rifkin & Moscatelli, 1989) of genomic DNA and appears highly conserved through evolution. It is present in all vertebrates studied to date including avian, mammalian, fish, and amphibian species (Baird & Bohlen, 1991). Basic FGF is known to alter protein synthesis, motility and migration in differentiated cells, and to affect the cell's survival, and onset of senescence (Baird & Bohlen, 1991).

Restriction enzyme mapping has characterized 3 exon coding sequences in the bFGF gene (1-60, 61-94, 95-155) (Schweigerer, 1990) widely separated by two large noncoding introns (between 60/61, 94/95) (Schweigerer, 1990). The nucleotide sequence for cDNA of bFGF reveals a primary translation product of 155 amino acids which lack a hydrophobic

signal peptide sequence (Baird & Bohlen, 1991). The bFGF precursor molecules undergo proteolytic cleavage of the first nine residues to generate the mature bFGF protein, which may be cleaved further (Gospodarowicz et al., 1987b; Rifkin & Moscatelli, 1989). Variants of the bFGF amino acid sequence have been identified, including truncated forms which lack the amino (NH_2) terminal in the kidney and corpus luteum (Rifkin & Moscatelli, 1989; Gospodarowicz et al., 1986) or amino-terminal extended forms of 154 or 157 amino acids (Baird & Bohlen, 1991). Mature bFGF predominates as a single chain peptide protein of 146 amino acids, with a high (basic) isoelectric point (Gospodarowicz et al., 1987b; Rifkin & Moscatelli, 1989; Baird & Bohlen, 1991), and molecular weight of 24, 22.5, 22 or 18 kD depending upon the site of initiation from the AUG or CUG codons (Rifkin & Moscatelli, 1989). The variants do not arise as a result of posttranslational modifications or degradation (Powell & Klagsbrun, 1991) and are thought to have different functional roles and subcellular distribution patterns (Rifkin & Moscatelli, 1989). Higher molecular weights of bFGF localize preferentially to the nucleus, ribosomal and nuclear fractions. Truncated or lower molecular weight forms (18 kD) are localized primarily in the cytosol (Renko et al., 1990). Truncated bFGF appears as effective as the native form (Gospodarowicz et al., 1987a), indicating that the NH_2-terminal region is likely not involved in the biological activity of bFGF or in its binding to FGF cell surface receptors (Gospodarowicz et al., 1987b).

Basic FGF has some unusual structural characteristics. It contains 4 cysteines, 2 conserved among all members of the FGF family, and 2 which are not essential for biological activity (Rifkin & Moscatelli, 1989). Two sequences characteristic of heparin binding domains are evident at residues 18-22 and 107-110 (bovine pituitary bFGF). Binding to heparin causes significant changes to the tertiary protein structure of bFGF, and protects it against denaturation and proteolytic degradation (Rifkin & Moscatelli, 1989).

5.2 bFGF Expression

Basic FGF has been purified from mesodermal and neuroectodermal-derived tissues in vitro and in vivo. It has been found in all organs, solid tissues, tumours, and cultured cells examined (Gospodarowicz et al., 1987b) and in both normal and hyperplastic cell types under a variety of pseudonyms. Basic FGF has also been noted in chick embryo vitreous fluid, synovial fluid, follicular fluid, and the urine of patients with bladder or kidney cancer (Baird & Bohlen, 1991). Rifkin and Moscatelli (1987) theorize that the bFGF levels found in serum are likely in a biologically inactive state, bound to carrier proteins or associated with blood born carrier cells.

The biosynthesis of bFGF appears to involve a relatively unique mechanism not yet understood (Rifkin & Moscatelli, 1989). By attempting to localize bFGF within the cell, basement membranes, and ECM in vivo and in vitro, researchers hope to gain a better understanding of its mode of synthesis and action.

5.3 bFGF Receptors

Several different forms of plasma membrane receptors which recognize bFGF have been isolated and cloned (Powell & Klagsbrun, 1991). Growth factor receptors are a group of glycoproteins that contain a single extracellular region with one or more ligand binding domains, a single linear hydrophobic region that passes through the membrane bilayer, and a single linear peptide sequence within the cell's cytoplasm (Czech et al., 1991). Their simple design suggests a role in catalyzing signal transduction across the membrane (Czech et al., 1991), though the exact mechanism of this is not yet well known.

FGF interaction with the cell surface receptor is highly specific and bFGF and its receptor will not bind to other growth factors, exlcuding perhaps aFGF, or receptors respectively (Baird & Bohlen, 1991). Basic FGF

surface receptors exist on a variety of cell types and indicate that bFGF may exit the cells in which it is synthesized (Mignatti et al., 1991). The actual number of cell surface receptors for bFGF is speculative. Rifkin and Moscatelli (1989), in reviewing studies of bFGF surface receptors, estimated between 3,000 to 80,000 exist per BHK cell in vitro. An approximate inverse relationship between the number of receptors per cell and the content of endogenous bFGF was noted, suggesting endogenous growth factor down-regulates the bFGF receptor, possibly in an autocrine manner.

Two cell surface protein receptors with different molecular weights have been found to bind members of the FGF family in a potentially competitive and unequal manner (Rifkin & Moscatelli, 1989). The structural homology between aFGF and bFGF enables one to displace the other from a given binding site, however a marked receptor affinity for binding bFGF over aFGF is evident for most tissues studied (Baird & Bohlen, 1991). Mosocatelli (1987) estimated approximately 1 million binding sites for bFGF per bovine capillary endothelial cell, the minority of which (10,000 in number) were estimated as high affinity bFGF binding sites needed to mediate its biological activity.

Vlodavsky et al. (1991), in reviewing the extracellular sequestration and release of FGF, noted that bFGF binding to saturable, high affinity cell-surface receptors stimulated protein kinase activity and activated gene transcription. FGF high affinity binding sites have been found capable of transmitting the FGF signal to the cell in most systems studied to date (Cordon-Cardo et al., 1990), although the exact mechanism is still unknown. Cell surface-bound FGF appears to be slowly internalized, and to either resist degradation (Gospodarowicz et al., 1987a) or degrade very slowly (Baird & Bohlen, 1991). Olwin and Hauschka (1988) reported that cell surface FGF receptors are permanently lost during terminal differentiation in skeletal muscle cells in culture, a process which would ensure that residual FGFs remained extracellular. This

suggests internalization of bFGF plays a role in muscle cellular differentiation.

The predominating low affinity receptors, identified as a large capacity class of heparin sulfate proteoglycans (HSPGs), may be cell-surface associated or membrane-embedded core proteins (Yayon & Klagsbrun, 1990; Vlodavsky et al., 1991). Low affinity receptors are thought to store bFGF molecules that, following cleavage and release of the GAG core protein, may be presented to high affinity cell-surface receptor sites, thereby exerting both autocrine and paracrine effects (Vlodavsky et al., 1991). Low affinity receptors show a preference for aFGF over bFGF (Gospodarowicz et al., 1987b).

Intracellular receptors of bFGF have received much attention since nuclear localization of FGF was documented (Bouche, 1987). Logan (1990) noted that intracellular bFGF is translocated to, and accumulates within the nucleolus where, as a chemical mitogenic messenger, it can facilitate pleiotypic responses. He suggested that within the nucleolus bFGF stimulates nuclear cyclic AMP-dependent protein kinase activity and ultimately, in vitro ribosomal gene transcription. The exact pathway of signal transduction to the cell nucleus is hypothetical. Baird and Bohlen (1991) suggest that different cell types may use different signalling mechanisms, including increased protein phosphorylation, or activation of Na^+/H^+ and other ion channels.

5.4 **Modulators of bFGF Bioactivity**

One factor which distinguishes bFGF from other growth factors is its high affinity for binding to heparin. Basement membranes serve as the "physiologic reservoir for FGFs" (D'Amore, 1990) as do heparin sulfate proteoglycans (HSPG) in the extracellular matrix (ECM) (Rifkin & Moscatelli, 1989; Folkman et al., 1988). The binding of bFGF to heparin and to HSPG is biologically significant. The bFGF-heparin/HSPG interaction localizes bFGF to the cell surface, making it readily

available for target cells. It protects bFGF against the proteolytic degradation characteristic of tissue remodelling, wound healing, neovascularization, and metastasis, thereby improving its function, and serves as an extracellular bFGF reservoir (Baird & Bohlen, 1991). Binding to heparin greatly extends FGF half-life (Gospodarowicz et al., 1987a) and represents an important mechanism for modulating the extracellular activity of bFGF (Mignatti et al., 1991). Binding may also impose conformational changes on bFGF necessary for the optimal interaction of the GF with high affinity cell-surface receptors (Yayon & Klagsbrun, 1990).

The mechanisms that regulate FGF release are unclear. To understand the mode of bFGF action one needs to consider cellular pathways for both exogenous and endogenous FGF. Exogenous, pericellular FGF pathways mediate bFGF bioactivity through specific receptors (Yayon & Klagsbrun, 1990). Endogenous bFGF may be released and deposited in the ECM and basement membranes of cells or cell surface GAGs (Vlodavsky et al., 1991). Then local release of ECM degrading enzymes, such as heparinase and plasmin at sites of tissue remodelling or growth would enhance the release of biologically active FGF (Baird & Bohlen, 1991; Rifkin & Moscatelli, 1989). Cell death, cell lysis and sublethal microinjury have been proposed as additional modes for bFGF release (Rifkin & Moscatelli, 1989) as the application of endotoxins, irradiation or membrane scraping to endothelial cells resulted in significant levels of FGF release (McNeil et al., 1989). Spontaneous leakage into the extracellular space or deposition of FGF containing cytoplasmic bits in the ECM during cell migration have also been proposed (D'Amore, 1990). Receptor bound bFGF may be released by light (photoreceptors in the eye), protamine, or suramin (Schweigerer, 1990).

Dimario et al. (1989) support the role which inflammatory responses and lymphocyte-related heparin-dissolving enzymes play in the release of FGF from the heparin-rich external lamina of muscle cells. Macrophages and

platelets, also evident during inflammatory responses, could theoretically deliver high concentrations of FGF to appropriate sites in a controlled time and manner, possibly as membrane-bound granules (D'Amore, 1990).

Vlodavsky et al. (1991) propose that bFGF stored in the ECM is less active but more stable than the fluid phase bFGF. Release of bFGF when complexed to a heparin sulfate fragment yields a stable form of bFGF, still capable of binding to high-affinity plasma-membrane receptors. Basic FGF complexed to heparin or HSPG appears to interact with the receptor in a manner identical to free bFGF (Rifkin & Moscatelli, 1989). Basic FGF then may be made available via endogenous autocrine and/or paracrine production by the target cells (Rifkin & Moscatelli, 1989; Yayon & Klagsbrun, 1990; Mignatti et al., 1991.)

Protamine sulfate is known to inhibit the mitogenic effects of bFGF by blocking its receptor interactions (Gospodarowicz et al., 1987b). Transforming growth factor beta (TGF_{β}) has multifunctional properties. It can potentiate or inhibit FGF activity depending upon the specific cell type, while having no activity of its own . Together with FGF, TGF_{β} can interact on a cellular level to modulate growth (Gospodarowicz et al., 1987b).

5.5 **Known effects of bFGF:**

The in vitro and in vivo effects of bFGF are known to be both acute and long-term, affecting cell morphology, growth, and responsiveness.

5.51 **In vitro effects of bFGF:**

Early in vitro studies using BALB/c and Swiss 3T3 lines, propose bFGF as a competence factor for normal diploid cells (Gospodarowicz et al., 1987b). The addition of FGF to culture medium maintains vital cellular functions and promotes survival of neuronal, vascular, and endothelial cells (Schweigerer, 1990). Basic FGF further modulates

cellular proliferation by shortening the G1 phase of the cycle, thus reducing the cell doubling time significantly (Gospodarowicz et al., 1987b). It appears to have a variable effect on tumor cells, stimulating proliferation in some cell types while inhibiting proliferation in others (Schweigerer, 1990).

The variable effect of bFGF is also evident during cellular differentiation; not all the cellular effects of bFGF are stimulatory. Basic FGF is known to stabilize the phenotypic expression of cultured cells, such as myoblasts, enabling long-term culturing of cells that normally lose their phenotype over time as they fuse and mature into differentiated myotubes. This ability to delay ultimate senescence of cells and thereby increase culture lifespan 5 to 10 fold has been noted in a variety of cell types (Schweigerer, 1990). In culture, bFGF reduces the number of myoblasts entering the G_0- G_1 cell cycle phase, delaying both their differentiation and subsequent fusion, and in some lineages limiting creatine phosphokinase expression (Linkart et al., 1981; Lanthrop et al., 1985a; Lanthrop et al., 1985b). Internalization of bFGF by the myoblast stimulates RNA polymerase I activity and transcription of ribosomal genes, thereby regulating expression of the cellular oncogenes involved in myoblast proliferation and differentiation. C-fos, a gene involved in promoting cellular differentiation, and c-myc, involved in stimulating cellular proliferation, appear to be particularly affected by the multiple effects of bFGF on gene expression (Schweigerer, 1990).

In vitro, in other cell lines bFGF induces the polarized secretion of extracellular matrix components in vascular and corneal endothelial cells and chondrocytes, and transforms human skin fibroblasts and smooth muscle cells into elongated, bipolar cells with characteristic membrane ruffling (Gospodarowicz et al., 1987a, 1987b). Thus there are both proliferation- and differentiation- related influences of bFGF in vitro.

Other known in vitro effects of bFGF include: stimulation of cellular migration and locomotion (Rifkin & Moscatelli, 1989); modulation

of specific functions in terminally differentiated cell types (eg. synthesis and release of hormones or neurotransmitters, retinal phototransduction) (Schweigerer, 1990); and promotion of tissue organization by stimulating cellular matrix invasion and induction of protein synthesis (plasminogen activator, interstitial and type IV collagenase) (Schweigerer, 1990; Mullins et al., 1991).

5.52 **In vivo effects of bFGF:**

In vivo, bFGF is a very potent angiogenic agent (Gospodarowicz et al., 1986) which has an important role in regulating vascularization during specific angiogenesis-dependent events including reproduction, ischemic responses, tumor invasion, and blood vessel formation and proliferation. Basic FGF induces angiogenic responses during embryonic development, tissue remodelling and wound healing in normal and pathological conditions by modulating endothelial cell proliferation, new capillary sprouting, endothelial cell migration, enzyme production (to modify the surrounding ECM), and new matrix component production (Baird & Bohlen, 1991). It is the primary mitogen present in many organs with pronounced vascular supply (Gospodarowicz et al., 1986), and has been detected in the basement membranes of all sizes of blood vessels (Vladavsky et al., 1991). Uncontrolled expression of bFGF has been implicated in neoplastic cellular transformations and the prominent vascularization characteristic in tumor genesis (Baird & Bohlen, 1991).

Basic FGF may play a significant role in wound healing, a complex process which involves the precise regulation of multiple cellular functions (Schweigerer, 1990), since it is evident at wound sites and in wound fluids. It accelerates healing by attracting cells vital for phagocytosis of debris (macrophage and leukocytes) to the wound site, stimulating the release of matrix degrading enzymes, promoting cellular proliferation (eg. fibroblasts), and inducing the synthesis of ECM components. Basic FGF further promotes wound healing by stimulating local

angiogenic responses, melanocyte and keratinocyte proliferation, re-epithelialization of the epidermis, chondro-ossification, and osseous growth (Gospodarowicz et al., 1987b, Cuevas et al., 1988). This growth factor plays an important role in limb and lens regeneration in specific amphibian species (Gospodarowicz et al., 1986; 1987a; 1987b).

Normal embryonic development is a precisely regulated, inductive, interactive process between the developing tissue cells and the forming ECM. Precisely regulated cellular proliferation and phenotypic stabilization, both mediated in part by bFGF, are required for successful neurulation, somite formation, mesenchymal differentiation and organogenesis. High levels of bFGF have been detected in early embryos, oocytes, fetal brain, and adrenal cortex (Schweigerer, 1990), and the amount of bFGF present, declines with later stages in development. Studies with Xenopus stage 8 blastula cells, where ectodermal explants were exposed to exogenous bFGF, demonstrated a highly specific differentiation of ectoderm into mesodermal structures that could not be imitated by other growth factors (Slack et al., 1987). Animal pole cells in amphibians have likewise demonstrated a highly specific inductive mesodermal response to the bFGF signal (reviewed in Schweigerer, 1990).

The neuronotropic effects of bFGF promote survival and differentiation of specific nerve cell lines from the hippocampal region of the brain cortex (Gospadorwicz et al., 1987b), and induce embryonic CNS development. Baird and Bohlen (1991) note that bFGF stimulates the proliferation of neuroblasts, the proliferation and differentiation of glial cells (astrocytes, oligodendrocytes, Schwann cells), the migration and maturation of astrocytes, and also enhances myelination. Basic FGF further influences the central nervous system cellular response to pathogenic events, and promotes capillary ingrowth into the brain. It has been localized in CNS neurons and cerebellar Purkinje cells, but not in the glial cells surrounding neurons (Cardon-Cardo, 1990)

A possible hormonal regulatory role for bFGF has also been

suggested, not surprisingly as the greatest amount of bFGF purified to date originates from pituitary tissues (Gospodarowicz et al., 1987a) and can be extracted from them (Kardami et al., 1985). Baird and Bohlen (1991) note that while bFGF potentiates thyrotropin releasing factor, it inhibits aromatase activity, testosterone synthesis and luteinizing hormone receptor induction. Thus, both the promotion and the maintenance of vital endocrine capillary networks and gland function are also heavily influenced by bFGF activity.

5.53 **Pathogenic/therapeutic bFGF expression:**

Given the magnitude and range of cellular responses mediated by bFGF, it is plausible that abnormal gene expression of bFGF or faulty signalling pathway components could result in pathogenic cellular stimulation and ultimately in clinical disease. Schweigerer (1990) noted that pathogenic bFGF expression could result from enhanced signalling secondary to amplification of the bFGF gene, from insertion of a functionally active promoter proximal to the bFGF gene, or from cells which contain point-mutated bFGF that are bioactive but escape cellular control (eg. tumor cells). With enhancement of the bFGF signalling pathway, persistent angiogenesis and/or uncontrolled cellular proliferation may occur. These factors are operant in diseases characterized by persistent angiogenesis (diabetic retinopathy, retrolental fibroplasia, rheumatism, abdominal adhesions), or by exaggerated mesoderm- or neuroectoderm- derived cellular proliferation (athersclerosis, rheumatoid arthritis, hepatic cirrhosis, idiopathic pulmonary fibrosis). Basic FGF has been found synthesized in a variety of tumor cells (retinoblastoma, melanoma, osteosarcoma, hepatoma) and may have an autocrine stimulatory effect on tumor development and progression (reviewed in Schweigerer, 1990).

Impaired signalling pathways could also result in the down-regulation or disruption bFGF expression. Considering the known effects

of bFGF on early embryonic development, disturbances in gene expression could result in malformations of varying severity. Abnormal mesodermal proliferation and differentiation, could be lethal early in development, or associated with less pronounced impairments at later gestational dates (Schweigerer, 1990). Faulty expression of bFGF may be associated with developmental disabilities such as infantile or adult progeria (characterized by cataracts, atheroma formation, scleroderma-like skin changes, ulcerations, and diminution of the musculo-skeletal system) and with degenerative neuronal diseases, since neuron synthesis of bFGF is vital for survival and differentiation (Schweigerer, 1990).

Therapeutic enhancement of bFGF expression or, more likely, application of recombinant bFGF potentially provides useful tools for the management of disease. Baird and Walicke (1989) hypothesized potential applications for recombinant bFGF in the management of pathological conditions where increased regeneration, or conversely limited cellular degeneration, is desirable. They speculate that enhanced healing of surgical or traumatic wounds, ulcers, burns, or severe musculoskeletal injuries could result from therapeutic bFGF application as could the development of increased compressive and tensile strength in cartilage and ligaments. Recombinant bFGF could potentially induce revascularization in heart tissue damaged by athersclerosis, prevent the progressive neuropathy of Alzheimer's disease, improve neural recovery following a brain or neural lesion, or even increase the survival of retinal ganglion cells. Recombinant bFGF may also have a role to play in reproductive biology, as perhaps an angiogenic ovarian factor or a developmental morphogen. It is also plausible that recombinant bFGF could play a role in modulating endocrine diseases.

5.54 **bFGF and muscle gene expression:**

The impact of bFGF on in vitro and in vivo muscle cells, as described previously, is significant. In fact, several distinct families

of growth factors are known to exert major effects on the differentiation of muscle cells. Basic FGF and Transforming Growth Factor-beta (TGFß) are potent inhibitors of myogenic differentiation, and Insulin-like Growth Factor (IGF) is stimulatory: together, these factors affect myoblast fusion, muscle-specific gene expression, and postmitotic differentiation in primary muscle cell cultures or immortal muscle cell lines (Florini et al., 1991) and have been shown to stimulate sequential phases of wound repair (Allen & Boxhorn, 1989). Basic FGF promotes myoproliferation and blocks early steps in myogenic differentiation. It is known to stimulate smooth and skeletal myocyte proliferation (Gospodarowicz et al., 1976; 1981) and has been localized in association with the basement membranes, nuclei, and intercalated discs of adult cardiac myocytes (Kardami & Fandrich, 1989; Kardami et al., 1990) where it is known to stimulate cardiac myocyte activity, possibly related to cell-cell communication via gap junctions.

FGF is able to inhibit terminal myogenic differentiation under conditions in which it is not mitogenic. The exact mechanism of bFGF inhibition of myogenic differentiation is still speculative, but likely involves its ability to restrict expression of MyoD and myogenin, myogenic determining genes (Fox & Swain, 1993), or increase cellular oncogene expression of c-fos or c-myc (Florini et al., 1991). It is known that the endogenous expression of bFGF by myogenic cells decreases during cellular differentiation (Vaidya et al., 1991) and that this autocrine and/or paracrine downregulation occurs in parallel with myogenesis both in vitro and in vivo (reviewed in Fox & Swain, 1993). Other proteins known to influence myogenesis demonstrate a similar autoregulation to bFGF during differentiation.

MyoD was the first in a series of four regulatory muscle-specific helix-loop-helix proteins identified in a variety of species, which was found to activate cell transcription, force expression of the muscle phenotype (Bober et al., 1991) and maintain the cell in a differentiated

state (Robertson, 1990). In combination with myogenin, Myf-6, and herculin, MyoD regulates muscle specific gene expression during specification of the myogenic lineage (reviewed in Olson et al., 1991; Beilharz et al., 1992), and is first expressed in early embryonic periods. Levels of MyoD and myogenin expression decline during later gestation, resulting in a relative absence of MyoD and myogenin gene transcription evident in muscle precursor cells of mature, undamaged muscle (Beilharz et al., 1992). Conversely, the increased accumulation of mRNAs encoding for FGF was found to coincide with decreased expression of myogenin, either by suppressing its transcription or decreasing the message stability (Fox & Swain, 1993). Through a variety of mechanisms therefore, increased expression of bFGF maintains the myoblast in an undifferentiated state associated with low levels of MyoD and myogenin expression. According to Fox and Swain (1993), it remains to be demonstrated whether the control of expression of the muscle regulatory genes exerted by FGF occurs as a result of its direct effect on gene transcription or by a more indirect mechanism, which may or may not be operative in vivo. This is of clinical significance as studies of enhanced expression of MyoD and myogenin have demonstrated their unique ability to convert non-muscle cells (such as fibroblasts) into myoblasts (Robertson, 1990). A potential therapeutic role for bFGF is suggested, based upon its ability to influence muscle specific gene expression in the DMD population, in which transfection studies using donor fibroblasts and a MyoD expressing retrovirus have been found to create potentially large populations of transformed cells suitable for myoblast transfer therapy (Tapscott et al., 1990).

The specific expression of muscle regulatory genes in activated, replicating skeletal muscle precursor cells has been studied as a quantitative measure of both growth and regeneration in normal and mdx striated skeletal muscle. Beilharz et al. (1992) found heightened mRNA levels of both MyoD and myogenin evident in mdx muscles during the phase of active dystrophy and regeneration (21 to 40 days), decreased to a

fairly constant though elevated level in comparison to intact control muscle samples in adult mouse populations. The authors maintain that elevated levels of MyoD and myogenin mRNA expression evident in adult mdx skeletal muscle suggest an ongoing rather than transient phase of muscle necrosis and regeneration in this strain. This is consistent with earlier observations that adult mdx hindlimb muscle demonstrates persistent, mild myofibre lesions (Tanabe et al., 1986) in small myotubes regenerated inside older external lamina sheaths (Anderson et al., 1987) but contrasts with the work of DiMario et al. (1991) who proposed that fibre regeneration is not persistent in adult dystrophic (mdx) mouse skeletal muscle. Di Mario et al. (1991) based their conclusion on analysis of fetal myosin mRNAs and embryonic MHC expression in adult dystrophic skeletal muscle which in fact demonstrated a longer period of expression of neonatal and embryonic myosin than evident in control populations.

5.55 **bFGF and dystrophic muscle:**

Knowing therefore, that upregulation of bFGF results in inhibition of terminal differentiation in muscle through downregulation of MyoD and myogenin gene expression, and that bFGF itself functions as a potent mitogen, the possibility of bFGF playing a role in promoting mdx muscle regeneration has also been investigated.

DiMario and Strohman (1988) found that satellite cells from mdx hindlimb muscle display an increased sensitivity to FGF in comparison to satellite cells from the normal mouse muscle or fibroblast cells from either muscle group. They proposed that this heightened sensitivity to FGF permits rapid myofibre regeneration in the mdx hindlimb muscle in vivo without parallel fibroblast hyperplasia. However, this study was not well controlled in aspects of tissue culture technique, nor in comparison with control mouse myoblasts, and has not been repeated by others. Later work by DiMario et al. (1989) related significantly elevated levels of FGF in mdx hindlimb muscle extracelluar matrix (ECM) to an increase in both

satellite cell and regenerative activity evident in dystrophic muscle, which they felt was sufficient to enable the mdx model to display a benign phenotype despite dystrophin deficiency. The mdx mouse skeletal muscle demonstrated an amplified concentration of endomysial and basal lamina-bound FGF, although these authors did not detect any of the dystrophic lesions in mdx muscle sections.

Anderson et al. (1991) did demonstrate distinctive patterns of bFGF distribution through immunofluorescence labelling (with a different antibody to bFGF) in degenerating and regenerating areas of mdx hindlimb and cardiac striated muscle at the light microscopic level. Basic FGF was localized at the periphery, over nuclei, and less intensely, in the sarcoplasm of control striated fast- and slow- twitch hindlimb muscle. Presumptive myosatellite cells labelled strongly for bFGF, confirming earlier reports of bFGF gene expression by satellite cells (Alterio et al., 1990). Dystrophic muscle sections demonstrated significantly more bFGF in recent areas of degenerating sarcoplasm and also over myotubes during new fibre formation. The anti-bFGF labelling was greater in mdx than control muscle for both hindlimb and cardiac tissues. Muscle extracts for mdx hindlimb and cardiac tissues also contained significantly more bFGF than control counterparts. Interesting was the observation of increased availability of bFGF epitopes prior to mononuclear infiltration and phagocytosis in dystrophic tissue, suggesting, as the authors note, that bFGF may promote myofibre repair in mdx hindlimb tissue by a variety of mechanisms. These could include bFGF acting as a chemotactic factor released following injury to attract responsive cells; bFGF providing contact guidance for cells converging on areas of recent injury; and/or bFGF stimulating mononuclear infiltrative cell proliferation and differentiation to mediate the regenerative process. The authors conclude that a correlation exists between local concentrations of bFGF and the regenerative processes of skeletal muscle: greater levels of bFGF were evident in slow-twitch than fast-twitch hindlimb skeletal muscle which

coincide with their differences in regenerative capacity.

The hypotheses that differences in the amount or distribution of bFGF in skeletal hindlimb muscle correlates with successful regeneration following dystrophic insult, was further examined using human, canine, and mdx dystrophin-deficient muscles. Anderson et al. (1993) used immunofluorescence to identify differences in anti-bFGF labelling between biopsies taken from patients with a range of myopathies including DMD and the related Becker muscular dystrophy (BMD), and from both normal and dystrophic canine and mouse tissues. They noted intense bFGF label both at the myofibre periphery and in the ECM in mdx and control mouse tissue which was not replicated in the human or dog sections. Endothelial and smooth muscle cells at all ages in human, dog, and mouse muscles (dystrophic and control) also stained brightly for bFGF, likely related to endothelial cells being a known site for both FGF synthesis and the angiogenic action of bFGF. Greater levels of bFGF were evident in the mononuclear cells within the ECM than in peripheral myonuclei in muscle samples for all species, and in degenerating than intact myofibres. The authors conclude that the high extracelluar, peripheral staining for bFGF in mdx limb muscle might stimulate a local proliferation of the muscle precursor cell (mpc) population following dystrophic insult and that this in turn could effect the remarkable regenerative response of those mdx muscles.

Studies at the LM level have identified distinct and elevated pericellular, nuclear, and extracelluar staining patterns for bFGF in mdx skeletal hindlimb tissue. The increased expression of bFGF evident in this animal model for DMD is felt to represent one mechanism which mediates the remarkable regenerative capacities evident in mdx hindlimb tissue despite a persistent absence of dystrophin. Of interest then would be the localization and quantification of bFGF in mdx diaphragm tissue, in which myofibre degeneration is much more persistent, and muscle is eventually almost replaced by fatty and fibrotic tissue (Stedman et al.,

1991). If there were reduced levels of bFGF expression evident in mdx diaphragm corresponding to control diaphragm, they would be consistent with earlier observations which correlated a) limited bFGF expression in DMD with poor myoregeneration following dystrophic insult, and b) high levels of FGF in mdx limb muscle which does regenerate from dystrophy.

6.0 IMMUNOGOLD ULTRASTRUCTURAL LOCALIZATION:

Accurate localization and quantification of bFGF in discrete tissues and cells, would enable us to learn more about its function, storage, and method of synthesis and delivery to target sites. At the electron microscopic (EM) level, immunocytochemistry, which makes use of antibody-antigen reactions inherent in the immune system, proves a valuable tool for this purpose.

6.1 The antigen-antibody reaction:

An antigen is a molecule which when encountered, is identified as "foreign" by the host, resulting in the initiation of a specific, protective, multifaceted, immunogenic response (Abbas et al., 1991a). Antigens have a unique molecular and/or conformational portion, known as a determinant, which is recognized in turn by a specific antibody (Bozzola et al., 1991).

Antibodies represent a superfamily of structurally related glycoproteins, produced in a membrane-bound form by B lymphocytes and released to tissues and plasma, which mediate the protective effects of humoral immunity. Antibodies demonstrate high specificity, or ability to recognize and distinguish between a tremendous range of antigenic structures, with differential marked affinity in their strong binding to specific antigens (Abbas et al., 1991a). They are found in distinct locations throughout the body including membrane-bounded compartments, plasma, immune effector cell surfaces, and collectively are referred to as immunoglobulins (Ig).

Ig molecules are similar in structure. The common Ig core consists of two identical short arms each composed of one light chain bound to one heavy chain. These short arms are in turn "hinged" to a central region where the two heavy chains bind together. This results in a "y"- shaped configuration where the "short arm" N-terminal domains form the variable regions containing the antigen binding sites. Enzymatic cleavage severs

the Ig molecule into three segments, the two shorter fragments which bind antibody (Fab) and the central, single crystallisable (Fc) fragment (Bozzola et al., 1991). Igs are divided into numerous physicochemically distinct classes and subclasses, each with a diversity of amino acid sequences at their Fab sites (Abbas et al., 1991b).

Antibodies prove useful to identify and localize the anatomical distribution of a specific antigen within a given tissue or cellular compartment. To do this, antibodies are harvested from animals such as rabbit, mouse, or goat, that have become immunized in a natural or, more commonly, artificially induced manner which involves repetitive injections of a specific antigen (Bozzola et al., 1991). Polyclonal antisera, containing a mixture of antibodies against different determinants on the antigen are produced. Monoclonal antibodies, on the other hand bind to a single determinant of the antigen, are produced typically from distinct hybridoma cell lines. Antigens from different species or molecules with varied functions but similar structural determinants, will cross-react, making the harvested antibody useful for labelling antigens in other tissues (Abbas et al., 1991b). When a visible label, such as a gold particle is attached to the harvested antibody, it becomes possible to infer the location of a designated antigen using immunocytochemistry techniques (Bendayon, 1986).

6.2 **Colloidal Gold Immunocytochemistry:**

Ultrastructural immunolabelling techniques are a sensitive method to locate and quantify specific antigenic determinants, important for their characterization (Bendayan, 1986). Postembedding immunogold methods are one preferred approach, which aim to maintain the essential, delicate balance between antigen recognition by the antibody and morphological preservation (Bozolla & Russel, 1991; Herrera, 1991; Park et al., 1989; Ferrari et al., 1989). The alternative, cryo-ultramicroscopy, requires very low temperature processing of frozen tissue to maintain structure,

but has the advantage of better retention of antigenicity of target epitopes. Successful immunolabelling depends upon a myriad of factors including tissue fixation and processing, antibody characterization and selection, etching and labelling techniques (Bozolla et al., 1991). Conditions for optimal labelling must be developed empirically to obtain high morphological and antigenic preservation (Bendayan 1987). Both a critical degree of antigenic expression to clearly identify a reliable reaction, and an antibody-tag complex (used to visualize the antibody locations) of high affinity and specificity are required to bind the tag effectively to the antigen.

Proper tissue fixation and processing directly impacts the success of specimen immunolabelling (Herrera, 1991; Bendayon 1987). To minimize denaturing of the antigenic determinant, low concentrations of glutaraldehyde (<1%) or paraformaldehyde have been used with success (Ferrari et al 1989; Bendayon 1983). Osmium, used to increase membrane stabilization and tissue contrast, may alter or mask the antigenic sites in some tissues (Varndell & Polak, 1987), necessitating careful appraisal of results achieved (Bozzola et al., 1991). Johnson and Bettica (1989) linked poor label penetration to the presence of osmium and to the limited effectiveness of sodium metaperiodate etching techniques used to expose antigenic sites of tissues embedded in epoxy resins. Tissue dehydration, infiltration, and embedding steps, derived to preserve antigenicity, must be discerned empirically and individually for each specific tissue type and labelling agent of interest.

Pre- or post-embedding labelling procedures each have unique inherent advantages and disadvantages (reviewed in Bozzola et al., 1991). In post-embedding labelling, the staining procedure is carried out on ultrathin tissue sections (silver or pale gold interference colours) mounted on nickel grids. Many new hydrophilic resins such as Lowicryl and LR White have been developed to allow enhanced antibody penetration (Herrera 1991), and appear to produce good labelling results (Stirling

1990; Shida & Ohga 1990; Bendayon 1987). If epoxy resins are used, an initial etching procedure prior to immunolabelling is required to expose the antigenic sites buried in the plastic. Hydrogen peroxide (Bozzola, 1991), sodium metaperiodate (Bendayon 1983, 1986, 1987), and sodium ethoxide (Johnson et al., 1989) have all been suggested as appropriate etching agents. The etching process could prove destructive to the antigen under investigation (Varndell & Polak 1987) so care must be taken not to compromise tissue antigenicity or integrity during the etching period. Thorough rinsing prior to subsequent staining is required to remove all residual traces of the solvent.

Blocking steps typically recur throughout the labelling protocol. During blocking, the tissue is exposed to normal or non-immune serum and/or albumin proteins which bind to nonspecific antibody sites. This improves the specificity of the subsequent colloidal gold labelling by blocking access to low and medium affinity antigenic sites. Ovalbumin and skim milk are routinely used as blocking agents, and when modified with the addition of Tween-20 (a detergent) and sodium chloride, become suitable diluents for the antibodies and gold reagents as well (Johnson et al., 1989).

The primary antibody, prepared or purchased specifically for the tissue antigen, is diluted and applied to the grid-mounted sections. A tag may be applied to the primary antibody for a direct labelling approach, however signal amplification may be desirable in which case inclusion of a secondary antibody proves advantageous.

Following incubation, unbound antibody is washed away, blocking recurs, and a secondary antibody is introduced to magnify or amplify the primary antibody label. The secondary antibody itself may contain an electron-dense tag, or subsequently after additional washing and blocking procedures is linked to a tag in suspension such as colloidal gold. Colloidal gold suspensions link relatively stable, discrete, highly electron-dense, non-cytotoxic gold particles to Igs, protein A, protein

G (Varndell & Polak, 1987; Bozzola et al., 1992), or protein AG (Bendayon, 1991). Protein A-colloidal gold displays low, nonspecific labelling properties and precise antigen detection (Slot et al., 1989). Protein A-colloidal gold allows for clear visualization of the surrounding tissue structure and good quantification of the bound determinant sites.

Protein A and Protein G bind the Fc portion of some Igs with varying affinities, a factor which impacts the selection of individual colloidal suspensions (Stirling, 1990). The gold particles contained within the colloid are available in a variety of sizes (from 5 nm to 20 nm routinely), making the multiple labelling options feasible. Smaller particles, though more difficult to visualize, demonstrate less steric hindrance (Ferrari et al., 1989), a higher efficiency of labelling and better resolution of the target protein's distribution (Park et al., 1989; Stirling, 1990).

Following gold labelling, the sections must be rinsed thoroughly to remove unbound gold particles, and then contrast stained with lead citrate and uranyl acetate. The immunolabelled sections are dried thoroughly, the grids demagnetized, and then viewed with a transmission electron microscope.

Immunocytochemistry experiments require a battery of controls for the staining, blocking, and tagging steps to reveal potential localization artifacts and to minimize experimental error (Bozzola, 1991). Omission of the primary or secondary antibody, demonstrates antibody specificity. Pre-immune serum used in place of the primary antibody demonstrates if any component other than the specific Ig is responsible for the antibody binding which is evident in sections. Adsorption, in which the primary antibody is removed from solution following binding to an aliquot of excess antigen, should result in a solution which is no longer capable of labelling the antigen when the routine protocol is implemented. Adsorption confirms that it is the primary antibody and not the diluting

solution that ultimately binds the gold tag to the antigenic determinant; use of a specific pre-sorbent molecule which is identical to the epitope of interest furthur confirms the molecular identity of labelled sites.

7.0 PROJECT HYPOTHESES:

From a review of the literature, the following conclusions were drawn: a) Successful myoregeneration following dystrophic insult, evident in Mdx mouse hindlimb (soleus) muscle, is significantly compromised in mdx diaphragm tissues, resulting in a progressive histopathology similar to that evident in DMD; b) An identical genetically-based sarcolemmal protein deficit ultimately results in markedly divergent phenotypic expression within two tissue types from the same animal model, suggesting that other factors (mitogenic, angiogenic, and/or chemotactic) may compromise the regeneration of diaphragm muscle; c) Basic fibroblast growth factor (bFGF) plays a vital role in mediating both myogenesis and muscle repair in striated skeletal muscle through its known mitogenic and angiogenic properties. Since the mdx soleus contains significantly more bFGF than control muscle and also regenerates successfully from dystrophy, a tissue which did not regenerate in mdx mice (diaphragm) was chosen to test the hypothesis. d) Immunocytochemistry is an efficacious tool for the localization and quantification of specific proteins (such as bFGF) at the ultrastructural level in muscle tissue. Based on these conclusions it is hypothesized that:

1) Precise localization and quantification of the bFGF protein at the ultrastructural level is possible by means of immunogold labelling for bFGF in mdx striated muscle.

2) Greater amounts of bFGF are present in control diaphragm striated muscle tissue, which demonstrates ongoing successful myogenesis, than in dystrophic (mdx) diaphragm muscle, in which myogenesis is compromised.

7.1 Specific Objectives:

1) To develop an effective technique using immunogold Protein A immunocytochemistry to localize and quantify the presence of bFGF in mdx and control skeletal muscle.

2) To apply this method to study muscle ultrastructure, and generate a labelling index (LI) of gold particles per unit area in defined myogenic cellular compartments.

3) To study statistically any differences found in the LI between muscle strains, muscle types, and cellular components which are involved in muscle regeneration (myoblasts, fusing myoblasts, central and peripheral myonuclei, satellite cells) and tissue repair (fibroblasts, endothelial cells) and the extracellular matrix.

8.0 METHODS:

In this study a post-embedding protein A-colloidal gold immunocytochemistry technique was developed to visualize the bFGF antigenic binding sites in diaphragm and hindlimb (soleus) skeletal muscle from mdx and control C57Bl/ScSN mice aged 6-7 weeks. This technique was based on the known affinity of Protein A for IgG antibodies, the effectiveness of colloidal gold particles as an electron dense marker, and the stability of the complexed protein A-colloidal antibody label (Bendayon 1986; 1987). The initial tissue processing for electron microscopy followed established protocols as described below. The immunogold labelling process however, was developed empirically, by extensive testing of previously published labelling methods and many control procedures, prior to its implementation in this study.

8.1 Processing for electron microscopy:

Mdx mice (C57BL/10 ScSn mdx) and their normal age-matched control mice (C57Bl/10ScSn) were bred by brother-sister matings from original breeding pairs (Bulfield et al., 1984) and housed according to the Canadian Council on Animal Care in the University of Manitoba Central Animal Care Facility. Diaphragm muscles were removed from six-week-old control mice and from seven week old mdx mice under 1:1 ketamine and xylazine anaesthesia (.03cc/20g). The muscles were dissected whole, pinned immediately through tendon insertions and ribcage into natural resting length positions, and immersed in 1.5% glutaraldehyde (in Sorenson's phosphate buffer) at room temperature for ten minutes. The muscle tissues were then trimmed into blocks with a razor blade to remove tendon, bone, and sites of procedural trauma. Leaflets of diaphragm muscle sections were dissected perpendicular to the ribcage from the ventrolateral costal region near the insertion of the phrenic nerve (Stedman et al., 1991).

Primary specimen fixation continued by immersion of blocks in 1.5%

4°C buffered glutaraldehyde for two hours, followed by two ten minute rinses with 0.1M Sorensen's phosphate buffer (SP). Tissues were stored overnight at 4°C in SP containing 5% sucrose.

Post-fixation in 1% osmium tetroxide (in SP) for two hours at room temperature preceded dehydration through increasing concentrations of ethanol (30% to 100%) and then methanol. Muscle tissue blocks were placed for 10 minutes each in 1:1 methanol: propylene oxide followed by 100% propylene oxide to complete the dehydration process.

Resin infiltration of the tissues was initiated with a 1:1 propylene oxide: Epon 812 mixture for three hours duration on a rotator. Specimens were placed in labelled EM flat embedding molds filled with pure Epon, mixed fresh prior to use, and oriented for either cross or longitudinal sectioning. Molds were left for twenty-fours hours in a fume hood, and then polymerized at 60°C for 48 hours.

Thick transverse and longitudinal sections were cut from each block, stained with toluidine blue, and photographed using the UFX-IIA Nikon Labophot microscope and TX-400 B & W film for orientation prior to viewing by the TEM (Phillips 300).

Resin blocks were trimmed and sectioned to pale gold interference color and were collected on cleaned 200 mesh nickel grids (JBS # s251), which had been rinsed in glacial acetic acid (3 minutes), 100% ethanol (one minute), and five rinses of double distilled water (Johnson & Beattica, 1989). Tissue sections mounted on grids were dried, demagnetized and stored for later use.

8.2 **Immunogold labelling protocol:**

Post-embedding gold labelling protocols were performed by floating the grids, section side down, on droplets of room temperature solutions in closed chambers (petri dish cover on clean parafilm). Grids were blotted between each step but not allowed to dry until the labelling procedure was completed. Slow spinning of the grids on a magnetic stir plate (Varndell

& Pollack, 1987), gentle stream rinses, and dipping techniques were used during the extensive rinsing procedures. Fresh OA solution (1% Ovalbumin and 1% skim milk powder in 0.01M Phosphate-buffered saline (PBS)) and OAT solution (0.05% Tween-20 and 30 mg/ml sodium chloride added to OA solution) were made and filtered extensively just prior to use. The use of anti-capillary forceps and regular demagnetizing of both forceps and grids (Speiss et al., 1987), proved helpful and were included in the final protocol.

To begin the immunogold labelling process, grids were floated on double distilled water (ddH_2O) for five minutes and then etched with freshly prepared saturated aqueous sodium metaperiodate (NaMp) (0.1gm/ ml PBS) for one hour (Bendayan, 1983; Johnson & Bettica, 1989) to unmask potential bFGF antigenic sites. Grids were blotted and washed with ddH_2O (five minutes) and PBS (five minutes followed by 10 second stream rinse) to remove all traces of NaMp. Grids were then double blocked using OA solution for five minutes (Johnson & Bettica 1989), and then 0.15M glycine (Bendayan, personal communication) for twenty minutes to reduce nonspecific staining and block low affinity binding sites.

Following blocking, grids were exposed to basic fibroblast growth factor antibody (bFGF Ab), provided and characterized as highly specific by Kardami (Kardami & Fandrich, 1989, Kardami et al., 1990) and previously reported (Anderson et al., 1993) at a 1:100 dilution in OAT for two hours at room temperature. Grids were washed in three 5 minute rinses of OA solution to remove unbound antibody. A secondary goat anti-rabbit immunoglobulin serum (Atlantic Antibodies, Sigma) diluted 1:100 in OAT was applied to enhance the signal achieved by the primary bFGF Ab. Following a two hour incubation period, the grids were washed in three 5 minute rinses of OA solution to remove unbound serum and again provide a protein block of the low affinity binding sites.

Protein A linked to 10 nm colloidal gold particles (Sigma) was diluted 1:100 in OAT and used as the electron dense tag for the secondary

antibody. Grids were exposed for one hour at room temperature to the protein A-gold colloid, followed by extensive rinsing with OA solution (5 times), PBS (three times), and ddH_2O (10 second gentle stream rinse followed by fifty rapid dips). Grids were dried, demagnetized and stored overnight. A complete summary of each staining run was recorded (Table 2).

Contrast staining for EM viewing followed an established protocol involving exposure to uranyl acetate for two hours and washing in ddH_2O followed by double strength lead citrate (.00375 gm./12.5 ml ddH_2O) for 3 minutes. Grids were rinsed for five minutes each in O.01M NaOH followed by ddH_2O, dipped rapidly fifty times into beakers of ddH_2O dried thoroughly and demagnetized. Unlabelled grids were coded by a second observer (JEA) to effectively double blind the grids prior to viewing on a Phillips 300 TEM.

Muscle sections were scanned under low power on the TEM to locate myonuclei and sites of cellular infiltration and/or active dystrophy. Higher magnifications (step 8 to 10, equivalent to x3630 to x5940 according to manufacturer) were required to confirm the type and location of the myonuclei and to visualize bound 10 nm. gold particles. Micrographs of areas of interest were taken using roll film. The date, magnification, photograph code, grid code, and summary of observations were recorded for each photograph on a form developed for this purpose. The sites photographed were then illuminated with an intense beam in the electon microscope to confirm that the particles noted were in fact gold, by their consistent size, precisely round shape, and great electron density (Bendayon, 1986). As this process potentially resulted in tissue distortion, it was employed only <u>following</u> photography of a visual field in situations where signal clarity was questioned. The film was developed and contact prints made for orientation and selection, prior to formal data collection.

8.3 **Development of immunogold protocol:**

Significant experimentation was required in the first phase of this research project to develop the final immunocytochemistry protocol unique to this particular tissue type and antibody. Many variables were assessed and multiple experimental trial runs were needed to determine optimum conditions and ensure satisfactory control procedures had been evaluated. The results of the initial trails are summarized on Table 3. Since previous work with immunolocaliztion for bFGF in dystrophic tissue was done on hindlimb muscles, the preliminary experiments and observations were established in soleus muscle. Only when specificity and sensitivity were reproducible and satisfactory was the diaphragm tissue stained.

Cytoskeletal integrity appeared adequately preserved by immersion fixation in this study, therefore perfusion fixation was discontinued. Lower concentrations of glutaraldehyde (1.5%) appeared to maintain morphology and antigenicity (Bendayan, 1983) while higher (3%) concentrations resulted in decreased antigen localization.

The tissue embedding resin selected was changed from Araldite, used during initial trials, to Epon 812 which proved more stable to both labelling and EM viewing procedures. In particular, the Epon 812 appeared to withstand intense illumination/heat with minimal tissue distortion.

To minimize the potential for contamination, nickel grids were cleaned with a regime of glacial acetic acid, ethanol, and distilled water. The grids appeared cleaner under EM observation, than those washed only in absolute ethanol or distilled water. However, grids were more prone to corrosion and etching if not rinsed sufficiently, particularly if old (ie. not fresh) sodium metaperiodate (NaMp) was used to etch sections (see below).

To improve tissue adherence, grids with sections were initially heated overnight at 40-50^{o}C (Johnson & Beattica, 1989). This practice was found to be of marginal value and discontinued in later trails.

In attempts to minimize environmental contamination and solution

evaporation during the labelling procedure, closed chambers were required. Glass covered, wax-lined petri dishes or cell culture box lids proved effective but susceptible to contamination with repeated use. Sheets of Parafilm covered by a petri dish lid provided a suitable working surface.

Etching with a diluted stock solution of sodium metaperiodate (NaMp) resulted in corroded grids as the stock solution gradually turned acidic. NaMp, freshly prepared and filtered just prior to use, eliminated this problem. Experiments using a double etching protocol that included the addition of sodium ethoxide (Johnson & Bettica 1989), resulted in fragile sections prone to tearing. As the antigen accessibility did not appear to improve significantly by this double etching procedure, the use of sodium ethoxide was discontinued.

At several steps during the protocol the tissue was exposed to a blocking solution containing albumin. The initial protein blocking solution containing 1% ovalbumin in 0.01M PBS was improved through the addition of skim milk powder (Johnson & Beattica, 1989), resulting in greater apparent specificity of stain. A second blocking step, 0.15M glycine for a twenty minute period, was included during the final trials and enabled significantly higher concentrations of the primary antibody to be used (from 1:400 to 1:100). This resulted in good visualization with minimal background staining.

Experiments completed with refrigerated OA and OAT stock solutions demonstrated their rapid decomposition and bacterial contamination and resulted in poor labelling. Good specificity was obtained when the solutions were mixed and filtered just prior to use, or by using stock solutions stored fresh frozen in premeasured vials at -20°C.

Filtering of all solutions was very important to minimize potential sources of contamination. The OA/OAT solutions were centrifuged, Buchner filtered (medium grade filter paper), and millipore filtered (8 and 2.5 microns) prior to use. All other solutions were millipore filtered prior to use, with the exception of the final ddH_2O rinses. Difficulties in

filtering the high protein OA/OAT solutions with millipore filters resulted their elimination from the final working protocol.

The primary bFGF antibody was tested at multiple dilutions including 1:20, 1:25, 1:40, 1:60, 1:80, 1:100. 1:160, 1:200, 1:250, 1:300, 1:400, 1:500, 1:600, 1:800, and 1:1000. Initially the lower dilutions resulted in significant background staining and a low specificity of label. A 1:400 dilution of bFGF Ab in OAT provided good specificity with low background labelling and was selected as optimum, although later trials which included a secondary blocking agent enabled 1:200 and 1:100 concentrations to be used effectively. The introduction of OAT in lieu of 1% ovalbumin/PBS as the diluent for the primary antibody, secondary antibody and protein A-colloidal gold also improved specificity. As noted by Stirling (1990), the addition of Tween-20 proved extremely effective in reducing non-specific gold probe reactions.

Initial trials did not include the use of a secondary antibody between applications of the primary antibody and protein A-gold to sections. Labelling under those conditions was clear but very sparse. With the addition of a secondary goat anti-rabbit antibody (diluted 1:100 in OAT) to the staining protocol, successful and amplified labelling was evident. Table 1 provides a schematic of the final immunogold labelling process.

The use of 20 nm. gold particles enabled easy visualization of the antigen binding sites during early trials; however, penetration was limited. The introduction of smaller 10 nm. gold particles resulted in increased particle penetration and antigen accessibility but proved significantly more difficult to locate by the TEM and on printed micrographs. Trials in which Protein G was substituted for Protein A-colloidal gold, did not demonstrate improved reactivity, as was anticipated and the use of Protein G was discontinued.

8.4 **Experimental Controls:**

Multiple control experiments were completed to verify the specificity of the labelling achieved by the final immunogold protocol. Control procedures included: a) omission of the primary bFGF antibody, b) preabsorption of the primary bFGF antibody with excess bFGF (Gibco), c) omission of the Protein-A colloidal gold tag, and d) use of preimmune rabbit serum (Vector) in lieu of the bFGF antibody. Controls a and c were run with each staining procedure from the onset of the project, while controls b and d were run during procedures after the final gold-labelling protocol was established. As previously stated, all grids were coded and the identities of photographs established only after the morphometric analysis was completed.

8.5 **Morphometric and Data analysis:**

Micrographs of myonuclei and mononuclear cells for analysis were selected from contact prints and following review of observation notes. Negatives which contained images of presumptive myoblasts, fusing myoblasts, satellite cells, central nuclei, peripheral nuclei, fibroblasts, endothelial cells, and mononuclear infiltrative cells of known magnification x3630 to x5940, were enlarged and printed to similar contrast at a 5"x7" size on resin-coated photographic paper (Kodak). The individual photographs were then grouped according to final magnification (19,500x, 25,000x or 32,000x) and principle cell type, as evaluated by two independent observers using strict inclusion/exclusion criteria. Presumptive myoblasts were identified in particular based on the description provided earlier in this paper: a prominent, central nucleus, enlarged nucleoli, relatively scant cytoplasm, abundant ribosomes, Golgi, RER system, multiple mitochondria, and possibly a small accumulation of muscle filaments in non-muscle, non-fibroblast, non-endothelial cells.

Other cell types of interest in this study were of both myoblast lineage (including myoblasts, fusing myoblasts, central nuclei, and

satellite cells) and non-myoblast lineage (fibroblasts and endothelial cells). For each type of cell, nuclear and cytoplasmic compartments were examined, in addition to areas of endomysial and eipmysial ECM. The areas of sarcoplasm evident between peripheral myonuclei and the external lamina were assessed separately from other regions of sarcoplasm.

Photographs were excluded from final analysis if the two observers failed to definitively or consistently identify the cell type(s) depicted; if sections appeared torn, distorted or immediately adjacent to grid bars; if visible regions of contamination or dirt were evident; or if the overall quality of the photograph was compromised (eg. poor focus, cloudy or obscured portions of visual field, damaged negative, poor print contrast).

A digitized computer graphics tablet with the Sigma-Scan program (Jandel) was used to assess the actual nuclear, cytoplasmic, and extracellular compartmental areas of each working photograph. Individual calibrations were entered into the computer for each of the three photograph magnifications prior to scanning for the area in μm^2. Cellular compartments were outlined in pen on the coded photographs, numbered, and traced in order. These steps were required to enable a later "gold particle count per μm^2" to be determined with accuracy for each compartment.

Individual gold particles were localized under conditions of high illumination and magnification on the micrographs. Particles were identified, circled, and classified as individual particles or small clusters (2-8 particles) depending upon their proximity to each other. Gold particles located within twenty microns of each other (twice the particle diameter) were designated as a cluster. Gold particles located at least twenty microns from each other were scored as individual units of gold. Each gold count was repeated on at least two separate occasions to ensure accuracy and check reproducibility. The gold particle count was then entered with the corresponding cellular compartment area following

decoding of micrographs, using a standard computer spreadsheet (Quatro Pro and Lotus 1-2-3). Spreadsheet column headings included: micrograph code number, animal strain, muscle type, antibody dilution, and TEM magnification followed by a complete listing of the area(s) and gold counts for each cell type and compartment (nucleus, cytoplasm, sarcoplasm, ECM) evaluated. This enabled a final labelling index (LI) to be generated, that calculated the number of gold particles per micrometer^2 for each area of interest. The LI was derived using a macro with the following formula, which weighted each cluster as containing on average, 3 gold particles:

$$LI = \frac{\text{Single particles (number)} + 3\text{x(cluster number)}}{\text{area in } \mu m^2}$$

As the working photographs were decoded, and the observations were entered into the computer spreadsheet, data was sorted according to animal species, muscle type, and principle cell type. Labelling indexes were compared both within and between the two animal strains using the NWA Stat-Pak statistics program. Two- and three-way ANOVA statistical tests and Duncan's tests were used to determine the statistical significance of findings. A "p" value of less than .05 was used to reject the null hypothesis that there were no significant differences in the LI for bFGF labelling between the muscle cell populations and/or between the two strains. a MacIntosh computer and Cricketgraph were used to graph the LI data.

9.0 RESULTS

Results suggest pronounced differences exist across muscle types (hindlimb and diaphragm), cell types (myoblast, peripheral nuclei, central nuclei, satellite cells, fibroblasts, endothelial cells) and animal strains (mdx and control) with respect to ultrastructural morphology. In addition, the bFGF LI generated through this study proved significantly different both across cell types and muscle types, and between the animal strains, supporting the project hypotheses. General observations related to these findings and the development of an effective immunolabelling technique for mdx and control muscle tissue are summarized separately below.

9.1 Immunogold Labelling Technique:

An effective tool for ultrastructural localization of bFGF in mdx dystrophic skeletal muscle using immunocytochemistry was developed following extensive experiments. The final immunogold protocol (Table 2) was refined from a series of over thirty successive trial runs (Table 3) and resulted in good tissue preservation, penetration, high specificity of the gold label, and minimal background staining (Figure 5C). These variables are important criteria in determining the technical success of the final immunogold protocol which was developed.

During the development phase of this project it became apparent that a myriad of factors potentially influence the immunocytochemistry process. Table 4 summarizes observations of specific variables which were found to impact the final signal clarity. Each variable was considered independently throughout the development phase of this project and multiple control procedures were implemented to minimize their effects (reviewed previously).

Etching with sodium metaperiodate for one hour gave good exposure of the antigenic sites embedded within the Epon 812 epoxy resin, as evident by the consistently labelled cellular compartments (nuclear, cytoplasmic,

extracelluar) in cells of various types (Figures 7,8, & 9 containing areas of differing tissue electron density). Double etching resulted in fragile grids and sections prone to tearing (Figure 12C) and was discontinued.

Double blocking of the muscle tissue sections appeared to mask the low affinity receptor sites effectively and improve label specificity (compare figure 6C with 9A, 9B). Effective gold labelling of bFGF epitopes was evident with minimal background staining with a 1:400 (bFGF in OAT) plus OA block, however further signal amplification was desired. This was achieved by the introduction of a second block using 0.15M glycine, and a 1:100 (bFGF:OAT) dilution which resulted in improved tissue penetration, signal amplification (more label in similar or identical areas), clarity in localization of bFGF epitopes (resulting from denser labeling on antigenic sites), and particle resolution (Figure 5).

Blocking solutions proved unstable due to their high protein content which could also result in increased nonspecific binding of Protein-A gold, and the partial masking of the visual field during TEM scanning. It was important that blocking solutions were mixed fresh and filtered extensively just prior to their use, and a low protein-binding filter paper in a Buchner filter proved sufficient for this purpose. Alternately, the use of filtered, previously frozen blocking agents proved satisfactory (Figure 8).

The introduction of a secondary goat anti-rabbit antibody significantly amplified the visible signal markedly. To confirm that the colloidal gold tag was indeed recognizing the bFGF epitope following the introduction of this secondary Ab, control runs in which the primary Ab was omitted were included. The omission of the primary bFGF Ab in trials containing the secondary goat anti-rabbit Ab, resulted in an absence of visible signal (Figures 5d, 12b).

Other control procedures which were implemented included presorbtion of bFGF Ab with excess human recombinant bFGF antigen (Ag) (Gibco), and b) use of preimmune rabbit serum in lieu of bFGF Ab. The complete absence of

gold particles on alternate sections treated in the same experiment run with presorbed primary antibody confirmed the specificity of the label to the primary bFGF antibody (compare 6D with 9A,9B). There was only low level, diffuse background labelling when sections were incubated with preimmune rabbit serum. The initial presorbtion trial in which the antibody-antigen combination was reacted for two hours prior to incubation of sections, failed to inhibit all signs of labelling. However, this random, nonspecific labelling was later reduced or eliminated when the Ab-Ag complex was refrigerated overnight, prior to use, suggesting that the success of the Ab-Ag presorbtion process is in part time dependent.

Use of Protein A-colloidal gold containing 20 nm particles to visualize the bound Ab-FGF (1:100 bFGF:OAT), was found to give a very limited labelling of tissue sites (Figure 6A). The introduction of 10 nm gold particles resulted in greater numbers of visualized binding sites in a single run on alternate sections after using the identical primary and secondary antibody dilutions. The smaller size particles (10 nm versus 20 nm) were much more difficult to locate (compare 5A with 5C, 5A with 8A).

Micrographs were enlarged to 5"x7" final working copies in order to measure both the individual cellular compartmental areas and make the corresponding corresponding gold counts. Cellular compartment areas were scanned and the areas tabulated confirmed by frequent and random repetition of measurements. Gold counts were repeated for each photograph and randomly checked for consistency and accuracy by an independent observer, who found results to be consistent and within 5% of original counts. The calculated labelling index (LI) gave a reasonable identification of the total number of gold particles per micrometer^2 of cellular compartment area. Since single clusters of 2-8 particles were designated as containing 3 particles on average, the index (LI) is likely an underestimation of the total particles. Use of the index enabled a standardized comparison to be made across strains in all cell types observed in diaphragm striated muscle.

Two observations should be made prior to discussing the statistical analysis of the indices. First, it is important to note that the population of fusing myoblasts and centrally located myonuclei evident in this study appeared to be unique to dystrophic mdx tissue and could not be correlated with a similar cell type in the control strain in that control muscle was not regenerating (compare Figure 1D with 1A). Second, the results of the LI drawn from this study are based primarily upon observations of control and mdx diaphragm striated muscle. Preliminary comparisons between the mdx soleus and diaphragm muscles have been included however, as they display clearly two divergent responses of mdx striated muscles to the dystrophic insult. To date very little has been reported on the mdx diaphragm and bFGF distribution has not been studied in mdx muscle at the EM level. Therefore comparisons with prior LM studies of bFGF in mdx soleus muscle (Anderson et al., 1991; Anderson et al., 1993) provided vital preliminary information from which this project was developed.

9.2 Tissue Morphology

The ultrastructure of control diaphragm (DIA) tissue is comparable to that of any mature skeletal mammalian muscle, apart from considerations of muscle architecture. In cross section, control DIA demonstrated essentially homogeneous, dense, polygonal myofibres containing numerous mitochondria, myofibrils and contractile elements with a definitive sarcomere array, peripheral myonuclei, and blood vessels (Figure 1A). The satellite cells were sparse in number (as reflected by the low "n" value in the tables), though readily identified based on their distinct appearance and para-sarcolemmal location (Figure 3A). Interstitial and endomysial fibroblasts comprised the most readily apparent non-muscle cell type, followed by endothelial cells. Of interest were small pockets of fat and fibrous tissue noted interfasicularly, extrinsic to intact myofibres in control DIA samples (Figure 1B). The appearance of periodic pockets of

collagen and adipose extracelluar infiltration in the control muscle were prevalent enough to mislead this observer, when making preliminary conclusions based on TEM viewing of double blinded specimens, that the control tissue was in fact dystrophic. Control muscle however, did not demonstrate many areas of free myoblasts or inflammatory cells, the presence of fusing or centrally migrating myoblast populations, or any intracellular accumulations of fatty tissue as evident in mdx tissues (compare Figures 1A and 2A).

Mdx muscle ultrastructure in contrast, demonstrated significant extracellular accumulations of mononuclear infiltrative cells and adjacent regions of myofibre damage and repair, in both the diaphragm (DIA) and hindlimb (SOL) muscle of 6-7 week old mice (Figures 2A, 3C). In both mdx muscles, segmental necrosis had initiated episodes of myofibre degeneration and attempts at regeneration. During the early stages of cell death/lysis, the myonucleus assumed a pyknotic appearance (Figure 1C), accompanied by structural disruptions such as sarcomere fraying or splitting, loss of individual myofilaments and swelling of mitochondria (Figure 2D) and vacuolation of the sarcoplasmic reticulum (SR) and T-tubule vesicles (Figure 2E). With myofibre degeneration, a diversity of mononuclear cell types infiltrated the necrotic zone. At the EM level, these infiltrative cells were observed to include large numbers of presumptive myoblasts, fusing myoblasts, fibroblasts, and macrophages, with somewhat lower numbers of lymphocytes, mast cells, and polymorphonuclear leucocytes evident (Figure 1D, 2A, 3C). Early attempts at myoregeneration were successful, as evident by the concurrent appearance of migratory myoblasts, fusing myoblasts, myotubes, and centrally nucleated myofibres in dystrophic DIA samples (Figure 1D, 2A). Once centrally nucleated however, DIA myocytes were also noted to display myofibrillar disarray and structural compromise (Figure 2B), suggesting that a second wave of damage to the same segment of these fibres was possible. Myofibrils continued to appear frayed with poorly organized

sarcomere banding, and were found in environ of very low amounts of glycogen and abnormal mitochondria following one initial phase of myogenic repair (Figure 2D). The SR swelling, characteristic of the initial necrotic insult, appeared to persist in regions, and may have further limited the successful reformation of adjacent sarcomeres (Figure 2E). The second wave of damage to previously regenerated fibres (Figure 1D) again involved infiltrative mononuclear cells, necrotic debris and fibrosis. The significant accumulation of collagen described in the mdx DIA, appeared early on in the disease process in the ECM (Figure 2C), though fibrosis was most pronounced near the perimysium surrounding fascicles. Fibrosis was evident in the endomysium, defined for the purposes of this study as the myofibre external lamina and interstitial endomysium, although to a lesser extent. Collagen infiltration appeared very much more pervasive in the mdx diaphragm than in any other tissue studied in this project. Signs of concomitant adipose cell infiltration were evident at this stage of development, and lipid droplets were noted intracellularly in myofibres (Figure 2D).

At the ultrastructural level, the initial stages of segmental necrotic insult, mononuclear infiltration, myoblast migration, fusion, and myofibre regeneration were indistinguishable in mdx soleus muscle from that described for the mdx diaphragm (compare Figures 1A & 4D, 3A & 1D, 3B & 2A). During active dystrophy, the mdx soleus interstitium also contains a dense heterogeneous assortment of infiltrative cells which phagocytize debris and repopulate areas of necrosis (Figure 3C). Myoblasts invade in synchrony with many inflammatory cell types (Figure 4C) and fuse with each other or to surviving segments of myofibres inside the original external lamina sheath (Figure 10B,C) to reestablish myofibre continuity (Figure 3A and 4A). Unlike the mdx diaphragm however, the soleus myofibres reorganize and appear more resistent to further rounds of dystrophic insult, although such are reported (Anderson et al., 1987). Structural integrity appears to be reestablished in a gradual but

successful manner (compare Figures 4A and 4B). Characteristic banding of the sarcomere is re-aligned both within and between the individual myofibrils in a fibre, resulting ultimately in a morphology characteristic of adult striated skeletal muscle apart from the appearance of central nuclei (Figure 4B insert). Mdx soleus muscle escapes the interstitial fibrosis and adipose infiltration characteristic of the dystrophic diaphragm (Figure 4B) and interestingly, appears to escape further rounds of degeneration, at least at this age. Signs of subsequent degeneration were not apparent in centrally nucleated mdx soleus muscle at six weeks-of-age. The mechanism by which this hindlimb muscle is able to escape further dystrophic insult despite the persistent absence of the dystrophin protein product is as yet unknown, though these observations perhaps support the theory for work-related muscle injury secondary to dystrophin deficiency (Petrof et al., 1993).

Also of interest were the appearance of neuromuscular junctions in newly regenerating skeletal muscle. Figure 12C depicts a myofibre undergoing significant degeneration, though still maintaining an intact neuromuscular junction (NMJ). At higher magnifications it is possible to observe truncation of the secondary synaptic folds in regenerating striated muscle fibres. In general mdx NMJ of regenerated fibres appear to lack the complexity evident at normal NMJ sites since synaptic clefts are shallow and secondary folds are shortened, irregular, and widely spaced (Figure 12D).

The actual stages of the myogenic repair process were observed and recorded at the ultrastructural level during the course of this study. Following cell necrosis and degeneration, many different inflammatory mononuclear cells were attracted to the degenerating tissue. These included mast cells (Figures 4C and 11A), polymorphonuclear leukocytes (Figure 11B), macrophages (Figure 11C, 1D, 3C) and lymphocytes (Figure 11D, 2A). Also evident within this inflammatory cell population were mononuclear myoblasts in varying stages of differentiation (Figure 1D),

presumably attracted to the wound site, possibly by a chemotactic signal such as bFGF.

Myoblast stem cells, thought to arise from activated satellite cell populations, were evident initially in close association with the inflammatory infiltrate (Figure 4C). At the EM level, presumptive myoblasts were recognized by the presence of morphological features including an oval nucleus, prominent nucleolus, scanty cytoplasm with plentiful ribosomes, and well-developed but short RER cisternae (Figure 4C). As the myoblasts begin to differentiate and synthesize contractile proteins, a random and then parallel accumulation of intermediate filaments was observed beneath the plasma membrane was observed (Figure 10A). The myoblast appeared to undergo a series of phenotypic transformations to assume an elongated appearance which included the accumulation of dense heterochromatin in the nucleus, and the presence of an increasing number and complexity of cellular organelles within an enlarging cytoplasm (Figure 10B). Fusion with adjacent myoblasts to form myotubes (Figure 10B), and with the sarcolemma of existing myofibres (Figure 3C) were evident as two distinct mechanisms by which reconstitution of myofibres was initiated. The fusion of cells, following close approximation often within the external lamina, evolved by complex, highly interdigitating limiting membranes (Figures 10B, 10C). As definitive myotubes were reformed, polymerization of the protein filaments was inferred by the observation of their longitudinal orientation into more typical sarcomere arrays. Mitochondria also appeared to undergo transformation as they elongated and became oriented in close association between the individual myofibrils. After fusion, the myonuclei appeared to migrate centrally as contractile filaments were synthesized and deposited at the myofibre periphery (Figure 2A). With the restoration of both sarcolemmal and sarcoplasmic integrity, regenerated myoblast nuclei appeared vesicular with large nucleoli as noted previously (Figure 1D), in a prominent central position within myofibres, surrounded

by an organized array of contractile elements (Figure 10D).

9.3 Results from Gold Particle Labelling:

The bFGF labelling index (LI) derived during this study was applied to determine if there were statistically significant differences between mdx and control animals for most cell types and compartment spaces assessed. Cell types most clearly labelled for bFGF in either strain included myoblasts, endothelial cells, fibroblasts, satellite cells, and peripheral nuclei. Nuclear and cytoplasmic compartmental LIs were evaluated individually for each cell type and a comparison was made also between extracelluar and intracellular/sarcoplasmic bFGF LIs.

Initial impressions generated while collecting data from the working copies of colloidal gold-stained muscle tissue micrographs, indicated that visible differences existed between control and mdx muscle tissue bFGF, although this was only confirmed after micrographs were decoded. Greater amounts of bFGF were evident on control than on mdx cells for the majority of cell and compartment types. These included fibroblasts (Figures 5A, 5B), peripheral nuclei (Figures 7A, 7B), myoblasts (Figures 8A, 8B), and endothelial cells (Figures 9A, 9B). It was difficult to ascertain if there were visible differences in particular regions of nuclear and cytoplasmic localization of bFGF, though clearly elevated levels of bFGF were evident in the ECM when compared to the sarcoplasm. For all tissues examined, gold particles were often observed to be bound to collagen (Figures 5A, 5C), with greater amounts of bFGF visualized adjacent to the perimysium than within the interstitial endomysium (compare Figures 5A, 7A). This would be consistent with earlier reports of intense pericellular staining for bFGF evident in mdx hindlimb muscle at the LM level (Anderson et al., 1991; Anderson et al., 1993).

Initial impressions also indicated that, irrespective of animal strain, certain cell populations demonstrated preferential binding for bFGF. Circulating myoblast cells in particular appeared to present with

the greatest amount of gold-tagged bFGF epitopes, followed by endothelial cells. As results were compiled, the myoblast population was delineated further into four distinct subgroups according to the degree of differentiation, for purposes of statistical analysis. This enabled a comparison to be made of the LI of freely migrating myoblasts (defined as having been activated, possibly dividing, and then withdrawn from the cell cycle, and, committed to the muscle lineage), fusing myoblasts (defined by the presence of fusing adjacent membranes), central nuclei (defined as myoblasts which have completed a cycle of myoregeneration), and satellite cells (defined previously as a visibly distinct resting precursor population of myoblast stem cells in mature striated skeletal muscle which lie between external lamina and sarcolemma). Initial impressions suggested that there was a progressive decline in the amount bFGF evident in these different myoblast populations which correlated with the stages of initial differentiation, fusion, migration and quiescence. This impression was later confirmed statistically as discussed below.

Macrophages were amongst the mononuclear cells that appeared to label well for bFGF within dystrophic striated muscle. To a lesser extent, but also labelled, were mast cells, PMN, and lymphocytes (Figure 11). Myelin sheaths and neuronal axons demonstrated the presence of bFGF in very much smaller amounts than evident in myonuclei, as did the region of a synaptic cleft (Figure 12 A, 12D), also in agreement with previous observations by LM (Anderson et al., 1991). Together, these observations suggest a multimodal and multicellular distribution of bFGF across tissue types and cellular compartments within normal and dystrophic skeletal muscles. These observations appear to be consistent with what is reported in the literature about the many roles bFGF may play in regulating tissue repair through modulation of cellular proliferation and differentiation.

A relative absence of bFGF-gold labels was evident within the lumens of blood vessels lumen (Figure 5C), or over erythrocytes (Figure 9A) and mitochondria (Figure 7A, 7B). This was interpreted to support the

specificity of the bFGF label as applied by this technique and protocol (as the literature suggests these sites do not demonstrate bFGF), and was used as a measure of nonspecific background staining during the protocol development. The relative absence of gold particles was also evident on micrographs taken from sections subjected to control procedures (Figures 5D, 6D, 12B), confirming again a high specificity of the colloidal gold tag to the bFGF antigen and the specificity of the developed protocol.

9.31 **Labelling Index Analysis:**

A series of statistical tests was completed on the raw data generated in this project to test the initial impressions of labelling. A probability of <0.05 was established as the point at which the null hypothesis would be rejected. Two and three way ANOVAs, Duncan's Multiple-range test, and unpaired t-tests were used to determine the statistical significance of the LI results. The individual statistical tests completed are described in brief below, and have been summarized in a composite manner in Tables 5A (DIA) and 5B (SOL).

Initially, a two-way ANOVA test was used to compare nuclear and cytoplasmic localization of bFGF in mdx and control diaphragm migrating myoblasts to ascertain if a) greater levels of bFGF are found in myoblasts during the successful maintenance of a muscle or a myogenic response and b) if there was a difference between nuclear and cytoplasmic localization of bFGF. The latter comparison was made in all cell types studied, with the aim of clarifying further the potential source and/or route of entry of bFGF in the cell since significant differences between intra- and extra- nuclear localization of bFGF might provide important information concerning the autocrine, intracrine, or paracrine regulation of bFGF for a given cell type. Results of this ANOVA indicated a statistical significance ($p=0.003$) between the labelling index of the two mouse strains, with control circulating myoblasts demonstrating greater amounts of bFGF than mdx myoblasts. There was however, no difference between the

cytoplasmic and nuclear distribution of bFGF within either strain ($p=0.57$).

A three-way ANOVA test looked at differences in the nuclear and cytoplasmic bFGF between control and mdx diaphragm myoblasts and fusing myoblasts to determine if the presence of bFGF decreases significantly during the early phases of myoregeneration. Results demonstrated a significant difference between the myoblast populations in different strains ($p=<0.001$), with control diaphragm exhibiting notably higher levels of bFGF than mdx diaphragm. Within the mdx diaphragm muscle itself, greater amounts of bFGF were evident in the circulating myoblast population than in the fusing myoblasts, confirming initial impressions. There was no statistical difference found between nuclear or cytoplasmic LI within the three cell types ($p=0.46$).

A comparison was then made of the bFGF LIs between the four distinct mdx diaphragm myoblast subgroups to ascertain if the trend towards decreasing levels of bFGF evident during myoblast maturation was in fact persistent into fully differentiated regenerated muscle. A one-way ANOVA confirmed statistically significant differences existed between each of the four stages of the myonuclei ($p=.01$). Further analysis using a Duncan's Multiple-range test indicated the major significant difference ($p=.05$) to lie between the levels of bFGF evident in pools of mononuclear extracellular myoblasts (most immature) and the intracellular central nuclei (most mature). In addition it was noted that satellite cells tended to have a lower bFGF LI than migrating myoblasts, however the relatively small number of observations likely precluded this difference from reaching statistical significance. However, this and the previous ANOVA test, supported the observation that the bFGF content of mdx myoblast nuclei diminishes significantly following migration to the site of regeneration.

To further clarify this impression, a comparison was then made between the nuclear and cytoplasmic bFGF LIs for each of the four myoblast

subgroups in mdx diaphragm. A two-way ANOVA suggested there might be differences between the cell types, although again the very small number of satellite cell observations appeared to limit the statistical significance of such ($p=0.07$). Consistent with earlier findings, there was no significant difference evident between the nuclear and cytoplasmic bFGF LIs for these cell types ($p=0.81$).

To assess differences in the nuclear and cytoplasmic content of bFGF in two myoblast populations (unbound myoblasts and satellite cells) between mdx and control diaphragm muscle a separate 3-way ANOVA was completed. Satellite cells and circulating myoblasts only could be compared between the two groups, since fusing and centrally nucleated myoblasts were unique to the dystrophic muscle in this study. Borderline statistical significance was achieved ($p=.08$), again limited by the relatively small number of satellite cell observations made. Both mouse strains displayed more bFGF in myoblast poopulations than the satellite cells, although this was not stastically different between nuclear or cytoplasmic localization ($p=.77$). This unfortunately small number of satellite cells, however does appear to be representative of population size as described in current literature (Grounds et al., 1991). A large number of satellite cells was observed and photographed in this study. However, they were excluded from final statistical analysis as they were not stained with the final protocol itself. Consequently, a large pool of cells was used for preliminary development of the technique and for observations of morphology but were discounted from statistical analysis of LIs.

To confirm these initial results which suggest that bFGF appears equally distributed between the nuclear and cytoplasmic compartments of discrete cell types, two two-way ANOVA tests were completed which analyzed the nuclear and cytoplasmic LIs in cells thought to synthesize and/or store bFGF. A comparison between control and mdx endothelial cell compartments revealed significantly greater amounts of bFGF in control

than mdx diaphragm muscle endothelial cells (p=.005), but no difference was noted between compartments (p=.53). A significant difference was not obtained during the comparison of fibroblast cells between the strains (p=0.17) or between compartments (p=.33), although there appeared to be more bFGF evident in control than mdx fibroblast cells irrespective of nuclear and cytoplasmic localization.

To verify the observations that bFGF localization within the cell nucleus was not significantly different from that in the cell cytoplasm, a three-way ANOVA was completed that compared nuclear and cytoplasmic bFGF in mdx and control endothelial, fibroblast, and myoblast populations. These three cell types represent the most frequently observed mononucleated cell populations within actively dystrophic muscle in this study, which by comparison would tell us about differences in bFGF distribution between myogenic and non-myogenic cells. Interestingly, significant differences were observed between strains (p=0.0000) and cell types (p=0.0031) though not between nuclear and cytoplasmic compartments (p=.3895). The greatest amount of bFGF (nuclear and cytoplasmic) was found in control myogenic cells (circulating myoblasts), then, in descending order, in control endothelial cells, control fibroblasts, mdx circulating myoblasts, mdx endothelial cells, and lastly mdx fibroblasts. A significant interaction was evident between strain and cell type (p=.02). This means that for the control cell types, differences in bFGF were larger than between the mdx cell types.

Peripheral muscle nuclei (PN) represent a population of stable, non-dividing myonuclei evident in normal and dystrophic striated skeletal muscle. The bFGF content of peripheral nuclei and the sarcoplasm located between their nuclear border and the external sarcolemma (designated ECM cytoplasm or →→ECM in the tables) were analyzed using a two-way ANOVA to determine if initial impressions that more bFGF was observed in the ECM cytoplasm than in the nucleus or remaining muscle sarcoplasm were accurate. Statistical results failed to confirm significant differences

for diaphragm muscle between mouse strains (p=.80) or cellular compartments (p=.90), since the bFGF label only tended to be higher in control peripheral nuclei than in mdx.

Statistical analysis next compared the bFGF LI of mdx and control diaphragm sarcoplasm to determine if intracellular accumulations of bFGF are reduced in tissue which is morphologically compromised. An unpaired t-test confirmed a one-sided significance of p=0.002: significantly less bFGF was evident in dystrophic than control sarcoplasm, perhaps accounting in part for its limited regenerative capacity following repetitive dystrophic insult.

The intracellular bFGF content in diaphragm muscle for both strains was then compared to that of the extracelluar matrix (ECM). The ECM serves as a significant physiological reservoir for bFGF, which once bound to the abundant heparin sulphate proteoglycans found in ECM collagen, becomes relatively stable. It was of interest therefore to extend the previous comparison of the intracellular levels of bFGF in normal and dystrophic muscle to include bFGF levels in the ECM, most notably to determine if the dystrophic diaphragm, which demonstrates much more collagen than control, would in fact bind greater amounts of bFGF. A two-way ANOVA was completed which found significant differences between both the animal strains (p=.01) and between the sarcoplasmic and ECM accumulation of bFGF (p=.001). Control diaphragm demonstrated significantly more bFGF both within the sarcoplasm and in the ECM than mdx, although in both strains significantly more bFGF was labelled in the ECM than in the sarcoplasm. Interestingly, the dystrophic diaphragm muscle which demonstrated significantly more extracellular fibrosis and collagen infiltration and theoretically a greater ability to bind bFGF, demonstrated significantly less bFGF than its control counterpart. This suggests that the amount of endogenous bFGF produced and sequestered by control diaphragm muscle tissue is greater than that evident in mdx, or conversely that the turnover of bFGF in mdx ECM is higher than in control

muscle.

In combination, this series of statistical tests yielded results consistent with the preliminary observation of decoded micrographs. There were greater amounts of bFGF evident interstitially, extracellularly, and within most types of myonuclei in control than in mdx diaphragm muscle tissue. This suggests that bFGF may play a role in the maintenance of muscle integrity, and that reduced levels of bFGF are evident in one muscle tissue which exhibits stages well into the process of dystrophy progression. Of interest then, would be a comparison of mdx diaphragm bFGF LIs with those of mdx hindlimb soleus muscle. Both tissue types experience a common myofibre insult secondary to dystrophin deficiency; however, only the mdx soleus demonstrates the capacity to regenerate.

The immunogold labelling technique for bFGF was developed and applied on hindlimb muscle tissue initially to confirm LM findings. The focus of this study was the morphology of diaphragm muscle and the distribution of bFGF in that muscle, which reproduces the degenerative changes of DMD and is therefore of great clinical interest. Observations included below regarding the bFGF LIs in stained sections of soleus muscle were taken from those sections processed at the same time as diaphragm muscle by the final staining protocol. The comparison of the DIA and SOL muscles in mdx and control populations presented below thus represents only a preliminary and very limited study which, while interesting, must be interpreted with caution, particularly in comparing to diaphragm bFGF LIs.

9.4 **Labelling indices (LI): diaphragm and hindlimb:**

Preliminary attempts to compare the bFGF content in dystrophic hindlimb (SOL) and diaphragm (DIA) muscles were limited by the narrow field of soleus muscle observations which met the full inclusion criteria. The immunogold labelling protocol was originally developed on sections of two mdx hindlimb muscles (extensor digitorum longus and soleus), allowing

some interesting preliminary observations to be made although the statistical significance of such is limited. The morphological differences between mdx SOL and DIA muscle were described earlier.

9.41 **Comparison of Control and mdx Soleus LIs:**

As shown in Table 5B, similar statistical tests were applied to assess the differences between control and mdx soleus cell types and compartments. Given the caution regarding the limited data pool from which results were drawn, the following observations were made. More bFGF appeared to label in mdx than in control hindlimb tissue. This is consistent with earlier reports (Anderson et al., 1991) and is interesting considering the enhanced regenerative capacities of the mdx soleus compared to control muscles (Zacharias & Anderson, 1991). Duncan's Multiple-range test confirmed that there was significantly more bFGF was evident in endothelial cells, peripheral muscle nuclei, and in the cytoplasmic compartment between the peripheral nucleus and the external lamina (ECM cytoplasm) in mdx SOL than in control SOL muscle ($p<.05$). The stronger labelling evident in the dystrophic soleus endothelial cells furthur supports this location as a recognized site of bFGF synthesis. Likewise, the large amount of bFGF evident in the mdx sol ECM may be related to its enhanced production, secretion, storage, and/or liberation in actively regenerating rather than quiescent tissues, suggested by DiMario and Strohman (1988) and Anderson et al.(1991). What is unusual however is the significantly elevated bFGF labelling of mdx soleus peripheral nuclei (PN) and adjacent cytoplasm, which contrasts markedly from the consistently low levels of bFGF evident in the same areas in each of the three other muscle types examined (mdx DIA, control DIA and SOL). The importance of the enhanced staining for bFGF in the peripheral nuclei and adjacent sarcoplasm is unclear, but may suggest that PN are not in fact as "quiescent" as presumed in regenerated mdx soleus muscle fibres. Indeed many other structural features of immaturity in mdx muscle

including myogenic regulatory gene expression (Bielharz et al., 1992), muscle fibre typing (Anderson et al., 1988), nuclear location (Anderson et al., 1988), contraction speeds (Anderson et al., 1988) and tropomyosin phosphorylation (Heeley & Anderson, 1993) are reported.

Significant differences were also evident between the individual myoblast populations in control and mdx soleus muscle ($p<.05$), with more bFGF evident in each of the four myoblast subgroups in the mdx compared to the control strain. There was also a significant difference in the bFGF LIs between myoblast and non-muscle cells (endothelial cells and fibroblasts). Similar to those findings reported earlier for the DIA, the greatest amount of bFGF was evident in endothelial cells followed in descending order by myoblasts and fibroblasts. Also consistent with findings from the diaphragm was a significant interaction between cell type and strain for both muscle (myoblasts and peripheral nuclei) and non-muscle (endothelial cells and fibroblasts) cells. The differences between nucleear and cytoplasmic bFGF LIs across all cell types and compartments were not significant, as for diaphragm muscle.

Both control and mdx soleus muscles demonstrated that signicantly more bFGF was labelled in the ECM than was internalized within the muscle sarcoplasm ($p<.01$). This, too, is consistent with results from the DIA, and indicates that extracellular sequestration of bFGF is more prominent than intracellular accumulation of this growth factor in many types of straited skeletal muscle. Table 6B presents in graph form these preliminary results which suggest that the mdx SOL muscle generally demonstrated much more gold-labelled bFGF than the control SOL across all cell and compartment types.

9.42 **Comparison of Mdx Soleus and Diaphragm LIs:**

Initial comparisons were also made between successfully regenerating (SOL) and poorly regenerating (DIA) muscle in the mdx mouse, as presented in Table 6C. Results indicate that much more bFGF was evident in the mdx

soleus than the diaphragm. This would be consisent with observations of the differences in regenerative capacity previously noted between the two muscle types.

The labelling indices of the the four myoblast subgroups were compared between the mdx soleus and diaphragm muscles using a two-way ANOVA. Results failed to show a statistically significant difference between the hindlimb or diaphragm myoblasts ($p=.37$), likely due to the limited data. However, there was a significant and consistent difference between the LIS for individual myoblast subgroups (in descending order: migrating, fusing, central nucleated, satellite cells) ($p=.05$). Again there was no significant difference between nuclear and cytoplasmic bFGF LIs.

Table 6C suggests that the amount of bFGF labelled in the hindlimb satellite cells and central muscle nuclei is greater in the diaphragm counterparts, however further testing is required to verify this interesting suggestion that there is ongoing activation of bFGF in SOL but not in DIA muscle precursors and regenerated myonuclei. The differences in bFGF labelling between the mdx diaphragm and soleus displayed in Table 6C appear larger in endothelial cells, peripheral nuclei, and ECM, where much greater LIs are evident in the soleus than in the diaphragm.

Preliminary observations therefore appear to suggest that there are greater bFGF LIs are evident in mdx soleus than in mdx diaphragm tissues, this includes labelling of intracellular and ECM compartments, and mononuclear myoblast nuclei in particular. It also appears that, in general, the greatest amount of bFGF was found in mdx SOL muscle followed, in descending order, by control DIA and SOL, and finally mdx DIA. The precise quantity and distribution of bFGF within the soleus, and between soleus and diaphragm cannot be compared reliably, based on the limited data, although preliminary statistical tests indicated significant differences (Tables 5B, 6B, 6C). Clearly the firm documentation which was provided for the diaphragm (Tables 5A, 6A) is needed to confirm

observations derived from this study and others on the soleus (Anderson et al., 1991; Anderson et al., 1993). Although preliminary observations of bFGF in hindlimb skeletal muscle are interesting and quite distinct from those of the diaphragm, the discussion of results will be confined to the diaphragm, which has been studied in greater detail.

9.5 **Summary:**

The statistical findings comparing bFGF distribution in dystrophic and nondystrophic diaphragm muscle are summarized on Tables 5 and 6. Significantly greater bFGF LIs were evident in control than mdx diaphragm for the following cell types and compartments analyzed: circulating myoblasts, satellite cells, endothelial cells, muscle cytoplasm (sarcoplasm) and extracellular matrix. Greater amounts of bFGF were evident in cells of myogenic lineage than in nonmyogenic cells, and control cell types showed significantly greater variation between cell types than was evident for mdx diaphragm cell types. There were no statistical differences between the bFGF LI of nuclear and cytoplasmic cellular compartments.

Also observed was a significant decrease in the bFGF LI with the increased level of differentiation between the myoblast population subgroups for both strains, with the greatest LI in circulating myoblasts prior to fusion. Although these observations were limited by a relatively small sample of satellite cells, they do correlate with the known effects of high levels of bFGF that promote myoblast proliferation over differentiation. These data represent the first known attempt to correlate bFGF with myoblast differentiation and fusion at the ultrastructural level, and also the first EM study of bFGF in mdx skeletal muscle tissues.

Preliminary observations comparing control and dystrophic hindlimb (SOL) and diaphragm (DIA) muscle indicate significant interactions exist between mouse strain and specific muscle cells (myoblast, peripheral

nuclei), non-muscle cells (endothelial cells, fibroblasts) and cell compartments (sarcoplasm and ECM). The amount of bFGF evident in the mdx diaphragm is significantly compromised in comparison to that evident in the mdx SOL and in both control muscle types, suggesting a strong correlation between the amount of bFGF present and the integrity of the muscle. Large amounts of bFGF are evident in actively regenerating muscle and lesser amounts in relatively quiescent or stable muscle, with the least amount of bFGF evident in muscle tissue that is unable to overcome dystrophic insult through myoproliferation, at least according to the immunostaining protocol which was developed, applied, and quantified in this study. These conclusions would support the initial hypotheses.

10. DISCUSSION:

This discussion will examine the results of this study in relation to each of the specific objectives cited previously. It will also attempt to address the implications of these findings to the clinical management of those afflicted with Duchenne muscular dystrophy. Unless otherwise stated, the muscle type in question is diaphragm. This is for two reasons: 1) little is known about the mdx diaphragm and therefore it was the principle focus of this study, and 2) preliminary results indicate that bFGF labelling indices for mdx hindlimb tissue are consistent with earlier studies of bFGF localization at the LM level, and more importantly, are notably divergent from those evident in mdx diaphragm.

10.1 Development of technique:

The first of three specific objectives for this study has been met through the development of a technique which is effective in localizing and quantifying the presence of bFGF in mdx and control skeletal muscle at the ultrastructural level using immunogold Protein A immunocytochemistry. The final protocol clearly labelled bFGF epitopes in control and mdx skeletal muscle tissue with low background staining. This was achieved by a combination of titrating the concentration of the primary antibody, increasing the incubation time, and treating the sections with two blocking solutions prior to immunolabelling. The immunogold labelling proved both sensitive and specific as evident by signal quenching following control procedures which included: use of pre-immune rabbit serum; omission of primary antibody; and presorption of the primary antibody with excess bFGF. Label specificity was also indicated by a consistent absence of gold particles over distinctive cellular compartments thought to lack bFGF (mitochondria, vessel lumen), and from non-tissue regions of resin sections.

Bendayon et al. (1987) noted that the nature of tissue fixative, embedding medium, and conditions of embedding can interfere with colloidal

gold immunolabelling. Muscle tissue cytoskeletal integrity appeared well preserved following immersion fixation in 1.5% glutaraldehyde followed by postfixation in 1% osmium tetroxide and routine progressive dehydration in ethanol, methanol, and propylene oxide. Although osmium fixation has been linked with the potential destruction of antigenic sites (Bendayon & Zollinger, 1983), its inclusion in this protocol significantly enhanced the visualization of cytoskeletal morphology, important in determining cell compartment boundaries.

Embedding specimens in epoxy resin may mask or alter antigenic sites. Epon 812 was selected for use in this study however, based on reports of its stability during processing and scanning and its suitability for immunolabelling procedures that require high resolution (Bendayon et al., 1987). Results suggest that etching of resin embedded sections with sodium metaperiodate prior to immunolabelling did expose the antigenic epitopes as reported (Bendayon et al., 1987). However, the exact percentage of bFGF antigen sites which are uncovered by etching is only speculative, and since the etching process may potentially denature surface antigens, it should be used cautiously.

Variations in skeletal muscle tissue density and composition may cause variations in both the depth/density and integrity of the epoxy resin covering the bFGF epitopes. Therefore it is possible that a single consistent etching step may unmask surface antigenic sites in a variable, almost random manner dependent upon the plane of section, and may not be truly representative of the tissue in vivo. However, the relative consistency of labelling observed between strains, cell type, and compartments in this study, the relatively low statistical standard errors in diaphragm data, and the excellent correlation with light microscopic studies of the same nature (Anderson et al., 1991) suggest that the etching procedures included in the final protocol did result in consistent and reproducible epitope exposure despite variations in tissue density and composition. The larger range of standard errors evident in the ECM (non-

cellular areas) of both tissue types may be attributed to the combination of endomysial and perimysial (interstitial) ECM areas rather than inconsistent labelling in a single compartment.

The introduction of newer low temperature embedding media such as Lowicryl and acrylic-based resins such as LR White designed specifically for immunocytochemical techniques, have been reported to result in enhanced retention of surface antigenic sites combined with adequate morphological preservation (Stirling, 1990). They should be considered for comparison in future projects of this nature. However, these alternative resins require completely different processing and polymerization, and a new protocol would have to be developed and tested extensively to determine if the intensity of the specific label under study was improved. Conditions of optimal labelling must be worked out empirically for each class of antigen, tissue binding site, and embedding medium used. Tissues processed by a cryoultramicrotome demonstrate good retention of labelling properties, but morphological preservation, and therefore surface antigenicity may be compromised during that type of processing.

Alternate approaches to enhance bFGF labelling may be possible through the introduction of a monoclonal rather than polyclonal antibody for bFGF. However the greater specificity of monoclonal antibodies and consequent binding to the highest affinity sites, may result in a lowered density of the probe and label (Stirling, 1990). Alternately, one could consider the use of a polyclonal antibody which recognizes a broader range of bFGF peptides and variants than that characterized for the antibody used in this study (Kardami et al., 1990; Anderson et al., 1991; 1993). The bFGF antibody used in this protocol is characterized as highly specific for bFGF and recognizes the majority of the amino terminus (residues 1-24), though not all the variants of bFGF that may actually exist in the muscle tissue. This could lead to an underestimation of the amount of bFGF present. Kardami et al., (1990) recommended the use of

several different antibodies to immunolocalize bFGF in given tissues, although they noted a greater consistency in immunoflourescence staining for bFGF in skeletal muscle than for smooth or cardiac muscle. Some underestimation was given to these experiments in that presorbed controls had Ag-Ab reaction for up to 18 hours (overnight), while sections were only "stained" for 2 hours by the primary Ab to bFGF. Such sections would thus show label preferentially over the more rapid binding higher affinity sites.

The use of different antibodies for bFGF has been demonstrated to result in variations of immunolabelling patterns in mdx hindlimb muscle (as discussed for the comparison of reports by Anderson et al.,1991 with DiMario and Strohman, 1988). Different bFGF antibody preparations could be tagged with gold labels of varying sizes, perhaps mapping bFGF epitopes in a more composite manner than when a single preparation is used.

Additional methods for potentially amplifying the final signal could include introduction of a Protein G or Protein AG colloidal gold substrate, thought to bind with greater affinity to the goat immunoglobulins of the secondary antibody (Stirling, 1991), or through application of silver enhancement techniques to magnify the generated gold label (Bendayon, 1991). Pre-embedding immunolabelling techniques, in which immunoreagents are allowed to penetrate into the specimen prior to the completion of fixation, have been found to be particularly useful for antigens sensitive to embedding procedures. A comparison of muscle tissues labelled both pre and post-embedding could provide further information regarding the stability and specificity of the bFGF immunolabel achieved in this study, though extensive testing would be required to develop a reliable pre-embedding protocol specific to these tissue and antigen types. Given the success, albeit arduous, of the labelling generated by this post-embedding immunocytochemistry protocol developed for bFGF in mdx striated muscle, the value of such an exercise would be questionable.

Gold particles of smaller size are known to demonstrate less steric hindrance (Stirling,1990). The introduction of 5 nm gold particles, therefore may produce enhanced tissue penetration and in turn better signal generation. Observations made during the development of this protocol, which compared the labelling produced by 20nm and 10 nm Protein A gold particles however, indicated that conclusive localization of the numbers and sites of gold labelled epitopes is significantly more difficult in this particular muscle tissue when smaller gold tags are used. Heterochromatin, nuclear membranes, and cellular inclusions in mdx and control osmicated muscle sections at times masked the presence of 10 nm gold particles due to the competing background electron density of the organelles. The localization and quantification of gold particles that are even smaller may require the tissue to be non-osmicated. This in turn however would severely limit both the study of tissue morphology and the clear distinction of cellular compartments and contents required to generate a labelling index. Bendayon et al., (1987) in reviewing the effects of tissue processing on colloidal gold cytochemistry concluded that for all methods examined, gold particles remain essentially at the surface of sections and that exposure of the binding sites by the cutting procedure is in fact one of the prime determinants of successful quantitative evaluation.

10.2 **Review of tissue morphology:**

The second specific objective of this project was to study the muscle ultrastructure of mdx and control hindlimb and diaphragm muscle and then to generate a labelling index of gold particles per unit area in defined myogenic cellular compartments. Morphological analysis was completed on micrographs of control and mdx hindlimb and diaphragm striated muscle enlarged from x9,000 (for overview of tissue sections) to x24,000 (to enable accurate analysis of cell type and compartments), although figures were reduced for the purposes of this thesis. The

control muscle, both diaphragm and hindlimb, presented in cross section as dense, homogeneous, polygonal myofibres containing numerous mitochondria, a definitive sarcomere array, and essential typical mammalian cytoarchitecture, as reviewed earlier in this paper and by the work of others (Anderson et al., 1987).

The assessment of the morphology of the mdx hindlimb muscle micrographs was consistent with earlier reports citing the unusual ability of mdx hindlimb muscles to overcome the effects of dystrophic insult through successful myoproliferation and regeneration (Anderson et al., 1987; Anderson et al., 1991; Grounds and McGeachie, 1992; Anderson et al., 1993). The mdx hindlimb skeletal muscle demonstrated significant dystrophic insult between 6-7 weeks of age, as evident at the ultrastructural level by marked segmental fibre necrosis and vacuolation, swelling of the sarcoplasmic reticulum, myofibril fraying, hypercontraction and disruption of the sarcomeres, mononuclear cell infiltration, and degeneration of both centrally and peripherally nucleated myofibres (Grounds et al., in press; Anderson et al., 1987). At the ultrastructural level infiltrative mononuclear cells were characterized by the presence of migratory presumptive myoblasts (muscle precursor cells which lack cytoplasmic protein filaments), fusing myoblasts, mast cells, macrophages, polymorphonuclear leucocytes, and lymphocytes. In synchrony, these mononuclear infiltrative cells are known to facilitate successful skeletal myoregeneration through phagocytosis of necrotic material and the proliferation and fusion of muscle precursor cells (Grounds and Yablonka-Reuveni, 1992).

Following the spontaneous onset of limb muscle destruction in mdx mice and mononuclear cellular infiltration, the phases of myofibre regeneration were evident in hindlimb muscle at 6-7 weeks, with the concurrent presence of myoblasts which were migrating, differentiating, and fusing to form multinucleated syncytial myotubes separate or continuous with stumps of surviving myofibrils (Robertson et al., 1990).

Satellite cells, which are the principal source of muscle precursor cells (Mauro, 1961; Grounds, 1991) were evident between the basal lamina and sarcolemma of myocytes in numbers that were consistent with previous reports estimating their representation at 4-7% of the total myonuclei in healthy adult tissue (Snow, 1981).

Mdx hindlimb muscle, when compared to control hindlimb muscle, demonstrated greater numbers of migrating presumptive myoblasts, fusing myoblasts, and mononuclear infiltrative cells, consistent with a tissue undergoing significant necrosis and repair. Satellite cell activation and myotube formation can occur in the absence of the infiltrating leucocytes (Grounds and Yablonka-Reuveni, in press), and in this study examples of myoblasts without leukocyte infiltration were observed in regions of active dystrophy and repair. Mdx hindlimb muscle on cross section demonstrated significant central nucleation, a diversity of fibre diameters, and a notable lack of adipose tissue infiltration or fibrotic change in the endomysium, again consistent with earlier reports (Anderson et al., 1987; 1991; 1993; Grounds & McGeachie, 1992).

The neuromuscular junctions in DMD frequently show ultrastructural abnormalities which include focal degeneration of the junctional folds, simplification of the postsynaptic cleft and/or widening of the synaptic cleft (reviewed in Nagel et al., 1990). Similar observations were evident in mdx hindlimb neuromuscular junctions which, following myoregeneration, appeared distinctly truncated with a reduction in synaptic folding and redistribution of post-synaptic molecules such as acetylcholinesterase (Lyons & Slater, 1991). This junctional remodelling was thought to be associated with the vulnerability of the plasmalemma secondary to the dystrophin deficiency, and interestingly was not associated with impaired neuromuscular transmission (Nagel et al., 1990). Very similar changes in NMJ structure were seen in mdx diaphragm muscle in this study.

Control diaphragm muscle did not demonstrate the degenerative or regenerative histological changes evident in dystrophic tissue. This

meant that there were no fusing myoblasts or centrally nucleated fibres present for comparison to mdx muscle, although a low incidence of central nuclei (up to 1-2% total myonuclei) has been reported in normal skeletal muscle secondary to normal wear and tear (Zacharias & Anderson, 1991).

There has been much speculation regarding the potential myriad of factors that might influence the exceptional sustained muscle regeneration evident in mdx hindlimb muscle. Grounds and Yablonka-Reuveni (in press) proposed that regenerative capacities typified by mdx hindlimb muscle are not a unique property of mdx mice per se, but rather are species-specific. This conclusion was based upon observations made following experimental injury in control and dystrophic muscle tissue from a variety of animal species in which the mdx and control parent mouse strains were felt to demonstrated significantly upregulated myoregeneration, although precise statistical analysis was limited. Whether these species-specific differences are due to inherent differences in the proliferative capacities of muscle precursor cells, the influence of development on the dystrophic process, or the impact of the host environment (eg. growth factors) on new muscle formation (Anderson et al., 1993) is as yet unknown. This theory of species-specific proliferative differences however fails to explain why the dystrophic diaphragm of the same mdx mouse strain demonstrates a notably impoverished myoregenerative response, and suggests that other factors may be involved in mediating the exceptional limb muscle repair.

Studies of control and dystrophic hindlimb report that although it is difficult to determine the absolute numbers of muscle precursor cells present in vivo in striated muscle, it appears their proliferative capacity diminishes with factors such as age and repetitive cycles of necrosis and degeneration (Grounds & Yablonka-Reuveni, in press; Zacharias & Anderson, 1991). Whereas differences relating to aging fail to explain the differences evident between mdx hindlimb and diaphragm tissues in this study, it is plausible that the repetitive cycles of dystrophic insult and

regeneration, more prevalent in mdx diaphragm muscle, are the causative reason for an inhibition of the proliferative capacity of muscle precursor cells (both satellite and interstitial), more significant in the diaphragm, resulting ultimately in an expressed phenotype similar to DMD.

In summary, observations of cytoskeletal morphology of the hindlimb muscle in control and mdx dystrophic mice are consistent with earlier publications (Dangain and Vrbova, 1984; Anderson et al., 1987; 1991, 1992; Grounds and Yablonka-Reuveni, in press) and provide a good base from which to compare and contrast hindlimb skeletal muscle ultrastructural histopathology with that of the mdx diaphragm about which very little is known.

Recent publications have noted the mdx diaphragm to display an exceptionally divergent response to dystrophic insult compared to its hindlimb counterpart muscles, such that the mdx diaphragm is felt to reproduce the degenerative skeletal muscle characteristic of DMD (Stedman et al., 1991; Dupont-Versteegden and McCarter, 1992). Both studies conclude mdx diaphragm muscle is more greatly perturbed by dystrophic insult than hindlimb muscle, and extrapolate that this may have important clinical implications which make the mdx diaphragm an excellent model for human DMD. The paucity of studies focusing on the mdx diaphragm made it an absorbing and fascinating tissue on which to focus this study.

At the EM level control diaphragm muscle demonstrated muscle architecture comparable to that observed in control hindlimb sections, as reviewed above, with the addition of somewhat greater connective tissue representation than in hindlimb muscle. Mdx diaphragm muscle, however, was readily apparent to be morphologically distinct from both control muscle and the mdx hindlimb counterpart. Unlike mdx hindlimb muscle, the mdx diaphragm (DIA) demonstrated persistent and invasive dystrophic damage despite ongoing attempts at myoregeneration. The observations of Stedman et al., (1991), in their landmark paper introducing the mdx diaphragm as a viable model for human clinical DMD, showing previously regenerated

central nucleated myofibres undergoing successive rounds of necrosis with significant fatty and fibrotic infiltration, were confirmed by this study. However, not all the observations made in Stedman's initial paper were supported by observations generated in this study. Concurrent foci of myofibre degeneration, necrosis and limited regeneration were evident throughout the mdx diaphragm with signs of regeneration persisting to 7 weeks, which is well past the 30 days noted by Stedman. A wide variation in fibre size and architecture, and significant connective tissue proliferation, thought to occur by 6 months of age, were in fact prevalent in regions throughout the mdx diaphragm by 6-7 weeks of age. Consistent with the earlier report however, the dystrophic lesions in the diaphragm were indistinguishable from those evident in hindlimb muscle, and the initial histopathology was very similar to that described previously for mdx hindlimb muscle.

A clearly visible difference in the quantity and density of collagen was evident between the two mdx muscle types, and between control and mdx diaphragm muscle. The most dense and most pervasive interstitial fibrosis and fatty infiltration was evident in mdx diaphragm, although some pockets of interstitial fibrosis and fatty infiltration were found in control diaphragm tissue. This is consistent with the work of Marshall et al., (1989) who noted a marked accumulation of collagen in both the endomysium and perimysium of dystrophic muscle as compared to age-matched control, although their work focused on the mdx soleus and was not supported by work in other labs. It is known that in muscle tissue, the ECM plays an important physiological role in maintaining the quiescent state of satellite cells and in regulating muscle precursor proliferation and fusion (Grounds, 1991). Changes in the composition of the extracellular matrix have been reported to adversely influence new muscle formation by changing the balance of ECM composition in favour of the proliferation of fibroblasts and adipocytes at the expense of muscle precursor cells (Robertson et al., 1990). This hypothesis is supported by observations

described for mdx diaphragm tissues in the present study. Increased fibrosis may also limit myoregeneration by affecting the physical juxtaposition and appropriate longitudinal orientation of myoblasts prior to fusion and the formation of myotubes (reviewed in Marshall et al., 1989).

In addition to enhanced fibrosis, mdx diaphragm muscle demonstrated significantly elevated mononuclear cell infiltration, similar to the histopathology described previously for actively dystrophic muscle. Mdx diaphragm muscle, during the phase of active dystrophy demonstrated the presence of many myoblasts, possibly distinct from the reduced proliferative capacity shown by DMD myoblasts grown from muscle biopsies (Blau et al., 1983).

Gold-labelled bFGF was most prominent in the myoblast mononuclear population, although fusing myoblasts/myotubes, macrophages, mast cells, and PMN leucocytes expressed bFGF in lesser amounts. It is known that phagocytosis of necrotic debris is a vital component of the regenerative process and invading macrophages in both mdx and control diaphragm tissues did contain bFGF to varying extents. It has been suggested that macrophages may also mediate myoregeneration through delivery of bFGF in an effective spatial-temporal manner to sites of injury, thereby promoting successful myoregeneration in a second more localized manner.

10.3 **Review of Labelling Index:**

10.31 **Technique:**

The labelling index which was generated to represent overall labelling of gold particles in cell compartments was effective and consistent in distinguishing control from mdx diaphragm, though it represents conditions of deliberate underestimation. A conservative approach was taken in data collection, and a majority of the micrographs were discounted from final morphometric and statistical analysis as they failed to meet all of the inclusion criteria. Inclusion criteria for this

project required micrographs to be: cell types identified by the consensus of two independent observers prior to decoding; immunolabelled following only the final working protocol; free of contamination, debris or processing artifacts including tears, knife marks, chatter, negative scratches; focused sharply such that cellular membranes and gold particles were sharply defined; contrast stained and printed in a manner that enabled precise distinction of cellular and compartmental borders yet did not mask the electron dense gold tags by competing background densities (evident for example in nuclear heterochromatin, cellular inclusions, or lead precipitates); and printed at magnifications from x18,000 to x24,000. Micrographs of undifferentiated presumptive myoblasts were often excluded from final analysis as they demonstrated ambiguous morphology which prevented definitive consensus agreement between observers.

There are many factors with the potential to impact the labelling index. Errors during the processes of data collection and manipulation in an appropriate statistical format cannot be discounted, although several measures were taken to minimize potential sources of these handling errors. These included the double blinding of muscle sections prior to viewing on the TEM, maintenance of strict inclusion criteria, and random checks by a second observer to verify the consistency of both the gold count and the final LI generated. All the micrographs which were analyzed were felt to be representative of the tissue type of origin. There is however, always the possibility that the cells which reached full inclusion criteria represented only a distinct portion of the total muscle to be studied. To minimize this possibility tissues were sampled in a consistent manner from the mid-belly of muscle fibres following procedures described previously (Anderson et al., 1987; Stedman et al., 1991).

The generation of the labelling index ascribed a value of three gold particles to each gold cluster counted. This represented a conservative estimate of cluster content, which ranged from two to eight particles. If a larger number had been used to represent the gold particle count in the

each cluster, this would have furthur magnified the differences in the results between the control and mdx populations. This reason, also supports the premise that the labelling index represents a conservative estimate of the bFGF tissue content.

Any of the variety of factors discussed previously under the review of methodology have the potential to impact upon the accuracy of the final LI (Table 4). The processes of EM fixation and immunolabelling affect epitope visualization and likely result in a much more restricted definition of label than that evident in LM immunoflourescence studies. Nonetheless, the localization and quantification of bFGF at the periphery, nuclei, and sarcoplasm of striated hindlimb muscle is in quite good general agreement with previous reports (Anderson et al., 1991; Kardami et al., 1990).

However, the truly exciting product of this EM study is the much greater detail of labelling and the greatly enhanced resolution of cell identification and localization of bFGF-Ab binding in these tissues. At the ultrastructural level, preferential localization for bFGF were evident for both strains and all muscle types studied, over nuclear heterochromatin and on perimysial and endomysial collagen. The strong labelling of myosatellite cells and of small recently-formed mdx skeletal muscle fibres reported for mdx hindlimb skeletal muscle (Anderson et al., 1991) was not observed in the mdx diaphragm. In so much as the myogenic responses of the mdx diaphragm are significantly compromised, it is logical that a significantly lower LI would be found for its cell types and compartments, if the labelling index positively correlates with regenerative capacity. The finding of greater amounts of bFGF in mdx soleus muscle and control diaphragm which demonstrate sustained successful myoregeneration and maintenance respectively, is consistent with earlier studies, although the preferential expression of bFGF in mdx over control hindlimb muscle is reversed when one considers diaphragm muscle. Therefore it is important when reviewing publications on mdx skeletal

muscle to clearly ascertain the source of the muscle (ie. hindlimb vs. diaphragm) prior to the interpretation of results.

10.32 **Interpretation:**

The localization of lower bFGF in most mdx diaphragm cell types and compartments may act to allow terminal differentiation and reduce the proliferative stimulus to muscle precursor cells, in turn decreasing the sustainable viability of the myofibres (Linkhart et al., 1981; Brunette & Goldfine, 1990). In comparing the myoblast populations, it is interesting to note that the largest labelling index, indicative of the greatest amount of cellular bFGF, was found in migrating presumptive myoblast populations prior to their differentiation and fusion. It was also observed that the amount of bFGF detected by immunogold labelling decreased following myoblast differentiation and fusion into myotubes, and was at its lowest following migration of the myoblasts into a central position within the myofibre, a new and important finding in this study. The spontaneous inhibition of bFGF expression has been attributed to down-regulation of the bFGF receptors by either autocrine or paracrine methods (Fox & Swain, 1992), and has been speculated to carry on for one or two generations. Down-regulation of bFGF synthesis in turn would permit expression of myogenic genes and result in final commitment to the muscle lineage and the production of muscle-specific proteins such as contractile filaments vital to muscle function (Beilharz et al., 1992).

Lower LIs for bFGF in mdx diaphragm myofibres were evident both intrinsically (within the peripheral nuclei and sarcoplasm) and extrinsically (within most infiltrative mononuclear cells and in the ECM). This may relate to the apparently lower level of maintained proliferative stimulus to myoblast stem cell populations in mdx diaphragm muscle, possibly including both satellite cells and discrete non-muscle cell types with an identified potential to express myogenic phenotypes (fibroblasts, adipocytes, pericytes) (Grounds, 1990). The diminished proliferative

stimulus in turn might further limit the potential reservoir of cells which can respond and regenerate new muscle following a dystrophic insult in the immediate locale.

The LI determined for endothelial cells in this study also demonstrated marked bFGF labelling compared to fully differentiated muscle cells, irrespective of strain or muscle type. This correlates well with the known role of endothelial cells in bFGF synthesis, and may relate to their impact in normal tissue maintenance and vascularization of new tissues.

The extracelluar matrix of the diaphragm in either strain also demonstrated high bFGF LIs, with lower bFGF labelling evident in mdx muscle. Earlier work by DiMario and Strohman (1988) correlated greater concentrations of FGF in the endomysium with increased regenerative capacities, and this observation appears not inconsistent with observations of diaphragm muscle (ie. intact muscle in control versus dystrophic muscle in mdx. Possibly more specific testing of this idea would study control and mdx diaphragm at an earlier age (prior to dystrophy) or after an imposed injury to both.

Earlier reports showed intense cytoplasmic anti-bFGF immunolabelling in degenerating mdx cardiac and skeletal tissues when compared to control or intact nondegenerating mdx fibres (Anderson et al., 1991). In addition newly regenerating fibres in mdx skeletal muscle were identified by their strong bFGF labelling in mdx muscles which was greater than in surrounding mdx skeletal or control fibres. Such relative staining levels were in fact reversed in this study: the control diaphragm generally expressed more bFGF in intact fibres, myoblasts and non-muscle cells. This staining in view of the failure of the mdx diaphragm to demonstrate sustained recovery following persistent dystrophic insults, supports the position that greater amounts of bFGF are evident in healthy skeletal muscle, either intact (as in the control diaphragm) or regenerated (as in the mdx hindlimb). Whether these differences reflect an increased synthesis of

bFGF or increased accessibility of bFGF in intact or regenerated muscle is unclear. Also uncertain is the difference in epitope detection between the two slightly different polyclonal antisera (produced by two rabbits) against two samples of the same bFGF peptide (Anderson et al., 1991 vs. Anderson et al., 1993 and present study). What is known is that the increased bFGF expression precedes and likely promotes myoregeneration by acting as a chemotactic agent for invading mononuclear cells and phagocytes, by providing contact guidance to cells converging at the site of injury, and by stimulating the proliferation and differentiation of migratory cells at the lesion site (reviewed in Grounds 1991; Anderson et al., 1991). These roles for bFGF may have important clinical implications in the development of future therapies directed towards DMD and are discussed in greater detail below.

The bFGF LIs for diaphragm muscle tissue indicate that the synthesis and accumulation of bFGF occurs pervasively throughout the regenerating muscle tissue in mdx muscle and in normal tissue, and not in unique pockets, such as close association with satellite cells. This is an important difference from previous reports, such as one by Bischoff (1990), who demonstrated that focal injury in myofibres releases a localized competence factor, thought to be bFGF, that specifically activates satellite cells. The presence of additional serum factors however were required for further satellite cell proliferation and differentiation, indicating that there is an orchestrated series of events, mediated by local and humoral responses to injury, necessary for the entire repair process. Exposure to bFGF in particular sites or levels, when combined with other growth factors and hormones, has been shown to be one mechanism for regulation of satellite cell activity (reviewed by Allen & Rankin, 1990; Chen & Quinn, 1992). The significant amounts of bFGF localized in control diaphragm ECM and endothelial cells therefore, have the potential to activate quiescent satellite cells and improve their response to bFGF through receptor-mediated mechanisms in a

paracrine manner. It is also possible that the lower LI in mdx than control endothelial cells hints at impaired angiogenesis in the mdx DIA which would have a negative impact on muscle repair. Muscle tissue which demonstrates successful myoregeneration should exhibit a more prolific satellite stem cell pool which can respond to the mitogenic effects of bFGF and also in turn, synthesize bFGF (Grounds, 1991; Anderson et al., 1991).

The bFGF LIs were largest in mononuclear, undifferentiated myoblasts in either strain, consistent with the knowledge that bFGF upregulates muscle precursor cell proliferation. A gradual and persistent decline in bFGF LI was evident during the phases of differentiation (through fusion to differentiation and quiescence). Following fusion and central migration of the myoblast nuclei, the relative amount of labelled bFGF was lower in myoblasts of both strains. However it is still unknown whether the bFGF labelled in this study was made by those myogenic cells or simply acting in those sites after originating in non-muscle cells. This question is currently addressed in the lab using in situ hybridization techniques to study mRNA transcribed from the bFGF gene.

10.4 **Implications and Speculation:**

The findings of this study, while intriguing from a basic research standpoint, also have clinical significance when reviewed in light of current efforts underway to develop therapies to ameliorate the devastating sequelae of DMD. Colbert and Curran (1991) noted that the medical, rehabilitative, and psychosocial concerns of those with DMD are extensive and unique because of the progressive nature of the disease and the age group involved. The prolonged course of the illness has a financial and psychosocial impact on the individuals, their families and significant others, and society (Bartalos, 1991). Extending the quality of life for those with DMD by medical, pharmacological, and technological advances, has also identified the need to target therapy to systems

associated with human interaction, self-care, productivity, and leisure. Respiratory insufficiency and muscle weakness limit the social and physical participation of individuals with DMD in each of these areas within the first decade of their lives. Ultimately cardio-respiratory insufficiency and failure prove lethal (Colbert & Curran, 1991). Therefore it is of prime importance in DMD to target early intervention toward preserving strength and integrity in the heart and diaphragm muscles, rather than in the limb muscles per se. This project involving an animal model for DMD, represents one attempt to study in greater detail the morphology of the dystrophic diaphragm, and better understand of the role of a powerful myogenic growth factor, bFGF, in the disease process. This study has implications for the mdx animal model and myoregeneration, as well as to current therapy approaches to DMD therapy.

An interesting but perplexing question remains as to what factor(s) evident in mdx hindlimb muscle are absent or compromised in the mdx diaphragm, which make the latter susceptible to rampant fibrosis and fatty infiltration characteristic of DMD? Successful myogenesis is dependent upon a complex series of interactions involving among other things, discrete cell types, growth factors, hormones, proteases, angiogenesis, and the ECM. Although bFGF is only one component of the overall process, it has been cited as a vital mitogenic, angiogenic, and competence factor for skeletal muscle tissues (Florini & Magri, 1991). Differences in bFGF expression between mdx hindlimb and diaphragm skeletal muscle tissues may reflect intrinsic differences in the synthesis and sequestering of bFGF, or conversely may reflect a rate of protease-mediated bFGF turnover that differs between the muscle types.

Two important conclusions are generated through morphological and statistical analysis of the bFGF labelling indices generated in this study. The first is that the pattern of cellular localization of bFGF epitopes does not appear to differ significantly between the mouse strains or tissue types, and is consistent with the patterns visualized with

immunoflourescence at the LM level in earlier studies from this lab (Anderson et al., 1991; 1993). The second conclusion is that the quantity of bFGF evident in skeletal muscle varies significantly both between the animal strains and within the dystrophic muscle types. Greater amounts of bFGF were detected in regenerating or intact skeletal muscle than in actively dystrophic regions in degenerating diaphragm myofibres. In the control diaphragm, endothelial cell and myoblasts contained the largest amounts of bFGF/μm^2 of section area, followed in descending order by the ECM, the sarcoplasm, fibroblasts, satellite cells and peripheral nuclei. In the dystrophic diaphragm, the largest amounts of bFGF/μm^2 were in the ECM, followed in descending order by myoblasts, endothelial cells, fibroblasts, satellite cells, central nuclei, fusing myoblasts, and peripheral nuclei. As well there was no significant difference between the amounts of bFGF detected in nuclear vs. cytoplasmic compartments of any cell type studied. This is interesting given what is known about the storage and activation of bFGF.

The sites of synthesis of bFGF remain elusive, although satellite cells, endothelial cells, and macrophages are known to express limited quantities of this growth factor, at least in vitro. In vivo, very recent work in the lab has shown that fusing myoblasts in new myotubes express bFGF mRNA (Garrett and Anderson, unpublished observations). As bFGF lacks a signal sequence essential for secretion outside the cell, it is thought to be released into the ECM by sub-lethal cell injury and cell lysis and/or alternatively secreted already bound to heparin sulphate proteoglycans (HSPG). As the labelling indices failed to demonstrate a significant difference between nuclear and cytoplasmic localization of bFGF in diaphragm skeletal muscle, they do not elucidate potential nuclear sites of bFGF synthesis which could be targeted therapeutically. However one micrograph (Figure 10D) at high magnification appeared to show radial arrays of bFGF-gold labelling in the central nucleus of a regenerated fibre, which suggests that nuclear proteins may organize the binding of

FGF to DNA. However, the bFGF LIs indicate significantly greater levels of the growth factor in the ECM than in the sarcoplasm in both normal and dystrophic skeletal muscle, likely bound to low affinity, but highly abundant receptors associated with HSPG. Future confirmation of bFGF receptor locations at the presumed sites of action can be made only by inference from immunolocalization techniques, in parallel with in vivo in situ hybridization methods to visualize mRNA expression of those genes. Given the specificity for the bFGF-Ab characterized by this study which did not distinguish between nuclear and cytoplasmic compartments, it can be assumed only that gold label was present on bFGF epitopes exposed on the muscle tissue surfaces. It is likely that these epitopes are associated with both high and low affinity bFGF receptors, as well as within bFGF molecules along the path of synthesis, storage, secretion and action, so the label is not indicative of the site of action.

The significant binding of bFGF to collagen in the ECM (and therefore to HSPG) is likely an important reservoir of this growth factor for muscle tissue. As reviewed earlier, when bFGF is mobilized from the ECM HSPGs, it binds to high affinity cell surface receptors (130 kD proteins) and is rapidly translocated into the cell nucleus where it generates a "growth signal". While this study offers evidence of intra and extracellular localization, none of the autocrine, paracrine, or intracrine mechanisms which might modulate the bioactivity of bFGF in skeletal tissues is clearly ruled out by this work.

The consistently low bFGF LIs evident in dystrophic diaphragm muscle therefore are interesting, considering the muscle displays both extensive fibrosis (and therefore HSPG) and persistent non-lethal cell injury and lysis. Theoretically, therefore, these findings should correlate with an increased quantity of bFGF being localized extracelluarly in dystrophic skeletal tissue when compared to nonfibrotic, intact healthy muscle if the rate of synthesis and secretion were equal. In contrast, lower extracellular bFGF was found in dystrophic than normal healthy muscle.

This suggests that the synthesis of bFGF is under markedly divergent feedback regulation between control and mdx diaphragm tissues and as well suggests that the composition of the dystrophic diaphragm may be distinct and important. Perhaps bFGF on low affinity HSPG receptors is exposed to heightened levels of proteases or muscle enzymes in the dystrophic diaphragm, to result in less stable and therefore less "active" bFGF following expression and release in the dystrophic diaphragm.

Given the understanding that bFGF is a vital mitogen for muscle repair and regeneration, it is interesting to consider how a change in bFGF expression could relate to the development of future therapies for DMD. Current research efforts into myoblast transfer therapy and gene replacement, two key therapeutic approaches, emphasize the importance of influencing conditions that regulate muscle regeneration (as reviewed in Grounds, 1990). It is known that multiple factors modulate the proliferation of muscle precursor cells (mpc), including exercise, passive stretch, innervation, trauma, and the presence of soluble growth factors (Allen & Rankin, 1991; Anderson et al., unpublished observations). It is also known that the process of muscle regeneration after injury and myoblast transplantation, involves revascularization, cellular infiltration and phagocytosis of necrotic material by macrophages, and proliferation of mpcs, (Grounds, 1990). Clinically, there are several important issues to be addressed during attempts to facilitate the repair of damaged (dystrophic) muscle. Some of these include obtaining an adequate population of myoblasts; delivering and maintaining the myoblast population where regeneration is required; providing a matrix for proliferation, orientation and differentiation of myoblasts; and facilitating vascularization into areas of new growth (Caplan et al., 1988) As reviewed earlier, each of these processes is known to influenced in part by bFGF. Therefore, exogenous application of varying concentrations of bFGF in association with other growth factors and hormones known to regulate mpc proliferation and differentiation (such as

IGF and thyroid hormone) could potentiate successful myogenesis following both myoblast transfer therapy and gene transcription therapy. Alternately, by altering myoblast sensitivity to bFGF in vitro, one might impact the myogenic process in vivo by mechanisms along the autocrine pathway. This could be tested by treating mdx muscle with bFGF-Ab to prevent effective regeneration, presuming the mice were immunosuppressed during treatment.

To potentiate the effects of exogenous application of bFGF one would need to develop a mechanism which upregulates the high affinity cell surface bFGF receptors. This could facilitate more rapid internalization (possibly preventing protease digestion) of bFGF from the ECM along the paracrine pathway. Parallel to the enhancement of high affinity receptor activity, would be the need for concomitant activation of low affinity receptors that bind bFGF within the ECM. Increasing the physiological reservoir of stabilized bFGF in the ECM without further proliferation of fibrotic tissue, possibly by heparin injections, would provide dystrophic muscle with a needed source of bFGF that would be continuously mobilized to interact with cell surface receptors. This could prove important in promoting, among other things, successful myoblast transfer and persistent regeneration in DMD tissues.

10.6 **Addressing the question:**

The question persists as to what factor(s) are absent or compromised in the mdx dystrophic diaphragm that makes it susceptible to the rampant fibrosis and degeneration characteristic of human DMD. Further studies that compare the mdx diaphragm with the hindlimb soleus muscle, which demonstrates a contrasting and pronounced regenerative capacity, are clearly needed. Also needed are further studies that address the perplexing clinical issue of why mdx mice demonstrate normal longevity, in contrast to individauls with DMD, despite significant diaphragm pathology similar to DMD.

There are multiple factors which, in combination, may explain the different phenotypes evident in mdx hindlimb and diaphragm muscle. The organization of the diaphragm muscle differs from that of the soleus in terms of its development, innervation, structure and lack of stationary insertions. The embryological origin of the diaphragm is from four sources (the septum transversum, the pleuroperitoneal membranes, the dorsal mesentery of the esophagus, and the body wall (Moore, 1991) rather than the single source of the soleus progenitor populations derived from somitic mesoderm. Ordalh (1992) suggests two distinct myogenic lineages exist in the somite; one giving rise to the axial muscles and the other giving rise to the limb musculature. As not all muscle precursor cells demonstrate the same proliferative capacities, the different embryological origins of the two muscle types are likely to contribute to differences in disease expression.

Diaphragm muscle fibres are arranged into a distinctive segmental leaflet organization, connected at either end to a mobile surface which moves upwards and down in addition to lengthening and shortening. Unlike the soleus muscle, the insertion points of the diaphragm muscle are not typically stationary. This places different mechanical stresses on each diaphragm myocyte than those placed on the soleus fibres, and may exacerbate work-induced muscle injury. The work performed by the diaphragm is thought to be greater than of any other muscle in the mdx mouse (Stedman et al., 1991; Petrof et al., 1993). In contrast to limb muscle the diaphragm is required to maintain a more or less constant work rate throughout life for reasons of survival (Petrof et al., in press). A large work load and rate in combination with membrane fragility due to dystrophin deficiency, and saturation of the muscle regenerative capacity, may overcome the relative protection afforded by smaller fibre size in the mdx diaphragm and lead to its ultimate degeneration (Petrof et al., 1993).

Histologically both the soleus and diaphragm are characteristic of

striated skeletal muscle. However they each possess unique fibre types which may contribute to the differential disease expression evident in the mdx mouse and DMD tissues. Rapid declines with age in the ability of the mdx diaphragm to generate active tension, and of the individual myofibres to shorten and to withstand membrane stress during force development have been reported. Such functional deficits were linked to the high rates of respiratory failure evident in patients with DMD (Dupont-Versteegden & McCarter, 1992; Petrof et al., 1993). Also reported are the observations that adult mdx diaphragm muscle demonstrates a 35% net loss in the sarcomeres, severe loss of tissue compliance and elevated intracellular calcium levels leading to increased protein degradation and in turn, a decrease in respiratory function (reviewed in Dupont-Versteegden & McCarter, 1992; Stedman et al., 1992). Similar observations are anticipated within the DMD population.

Not all dystrophin deficient muscles express a similar phenotype. Small-calibre skeletal muscle fibres and cardiac tissue appear to exhibit minimal dysfunction in those with DMD and in mdx mice (Karpati et al., 1988). Matsuma et al., (1992) proposed that the significant increase of dystrophin related proteins (DRPs) evident in mdx but not control skeletal muscle tissue could compensate for the dystrophin deficiency by retaining dystrophin associated sarcolemmal proteins (DAPs) in the extrajunctional regions of the sarcolemma. They note that DAPs appear preserved in small skeletal and cardiac muscle but did not mention limb muscles, and proposed that upregulation of DRPs, leading to retention of DAPs, might be a potential therapy for DMD. The presence of DRPs in the neuromuscular junctions and sarcolemma of the dystrophic diaphragm warrants investigation, based on the present findings. Hypothetically one might expect to find greatly reduced DRP, and therefore DAP, content in the mdx diaphragm when compared to the soleus, which could also explain part of the difference in myofibre integrity between the two mdx muscles.

A question of great clinical interest however, is why, despite

significantly compromised respiratory function, mdx mice demonstrate normal longevity. The compensatory recruitment of accessory respiratory muscles, the prevention of overstretch myofibre injury by increased interstitial fibrosis and muscle stiffening, and the slowing of twitch kinetics combined with enhanced type I MHC expression have been proposed as distinct mechanisms that promote survival of the mdx mouse. Petrof et al. (1992) reported that although the maximal twitch and tetanic tension in the mdx diaphragm were reduced to 15 and 20% respectively of control values, there was a concomitantly substantially enhanced muscle endurance and an eight-fold increase in type I myosin heavy chain (MHC) expression. The known influence of low bFGF on satellite cell senescence and on subsequent MHC expression could also affect muscle function.

In conclusion, the process of myogenesis during muscle repair is highly complex, involving a series of carefully orchestrated events modulated in part by the interaction of growth factors, hormones, the ECM, and mononuclear infiltrative cells. Appropriate levels of bFGF are one vital component of this process with known effects on cell proliferation, gene expression, and differentiation. Results of immunogold localization of bFGF showed significant differences in the relative amount but not distribution of bFGF between the mdx dystrophic diaphragm, which demonstrates histopathology comparable to that of DMD, and its healthy control counterpart. These results may have implications for the development of new therapies for DMD including myoblast transfer therapy and gene transcription therapy, and suggest the need for further application of this technique and others in the study of degenerating and regenerating dystrophic muscle.

11.0 FIGURES and TABLES

Figure 1: Micrographs of control (A,B) and mdx (C,D) diaphragm muscle.

Figure 1A: Control DIA demonstrating dense polygonal myofibres, containing the characteristic sarcomere array and numerous mitochondria surrounding a small vessel with endothelial cell (e) in interstitium. (X5460).

Figure 1B: Interfasicular pockets of adipose tissue in Control DIA. Note borders of adipocyte (→) and internal accumulation of debris. (X4065).

Figure 1C: Myofibre demonstrating the early stage of cell death following dystrophic insult in mdx DIA. Note the pyknotic central nucleus (**CN**), vacuolation of sarcoplasmic SR, swollen mitochondria, and disruption of sarcomeres (→). (X8300).

Figure 1D: Fibre degeneration during the stage of early regeneration by a centrally nucleated (**CN**) mdx DIA myofibre. Note the significant mononuclear infiltration including: a fibroblast (**f**) synthesizing collagen; a macrophage phagocytozing necrotic debris to assist early repair process (**mΦ**); myoblast (**m**) migrating to site of injury to synthesize new myofilament proteins; and early myotube formation (**mt**). The central nuclei from an earlier round of muscle repair are evident in a fibre which is undergoing a second round of dystrophy. The larger CN is vesicular and contains a prominent nucleolus. Note the presence of endothleial cells (**e**) in the endomysium. (X5500)

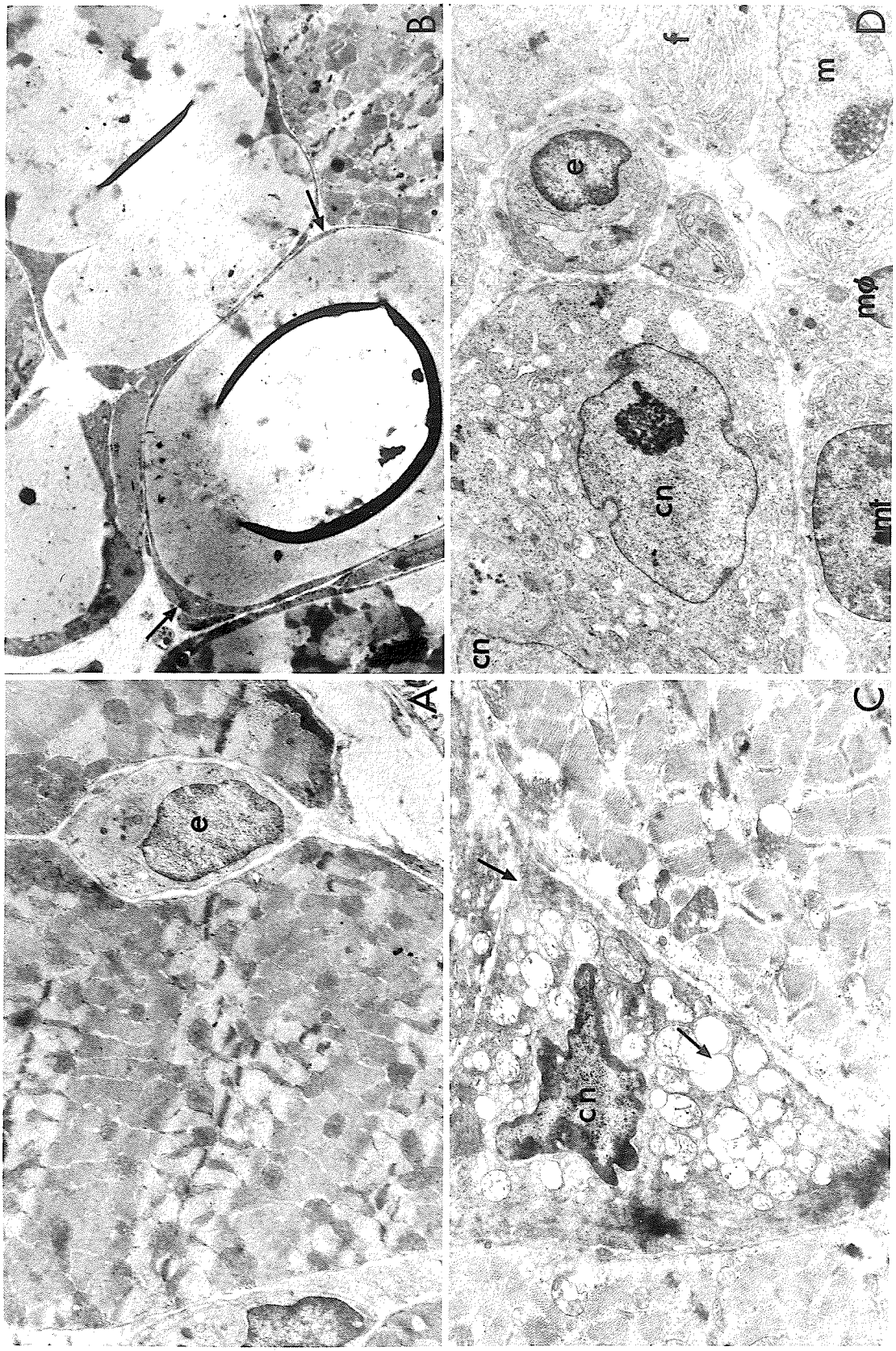
A
e
B
C
cn
D
e
cn
mf
mφ
m
f
cn

Figure 2: Micrographs of mdx diaphragm myofibre ultrastructure.

Figure 2A: Significant infiltration and myofibre degeneration indicates a second wave of damage has occurred in previously repaired, centrally nucleated (**cn**) mdx DIA muscle. Infiltrative cells include: fibroblast (**f**), lymphocyte (**lo**), macrophage (center of photo), myoblast (**m**), and myotube (bottom left). (x5500).

Figure 2B: Central nucleation, characteristic of myoregeneration, in mdx DIA. Note poorly organized sarcomere bands near areas of the fibers with few organelles, low glycogen content and iregularly shaped mitochondria. (x7700).

Figure 2C: Mdx DIA demonstrating marked fibrosis in the endomysial extracellular matrix (ECM). (→) indicates collagen bundle. (x7700).

Figure 2D: High magnification of mdx DIA myofibrils in a degenerating fibre shows disrupted sarcomeres, myofibril splitting (→), swollen mitochondria (★), and a lipid droplet (l). (x13,000).

Figure 2E: High magnification of mdx DIA sarcoplasm demonstrating good preservation of lipid bilayers in sarcoplasmic reticulum (→) and triads as well as of the myofilaments. Note the vacoulation of SR. (X41,000).

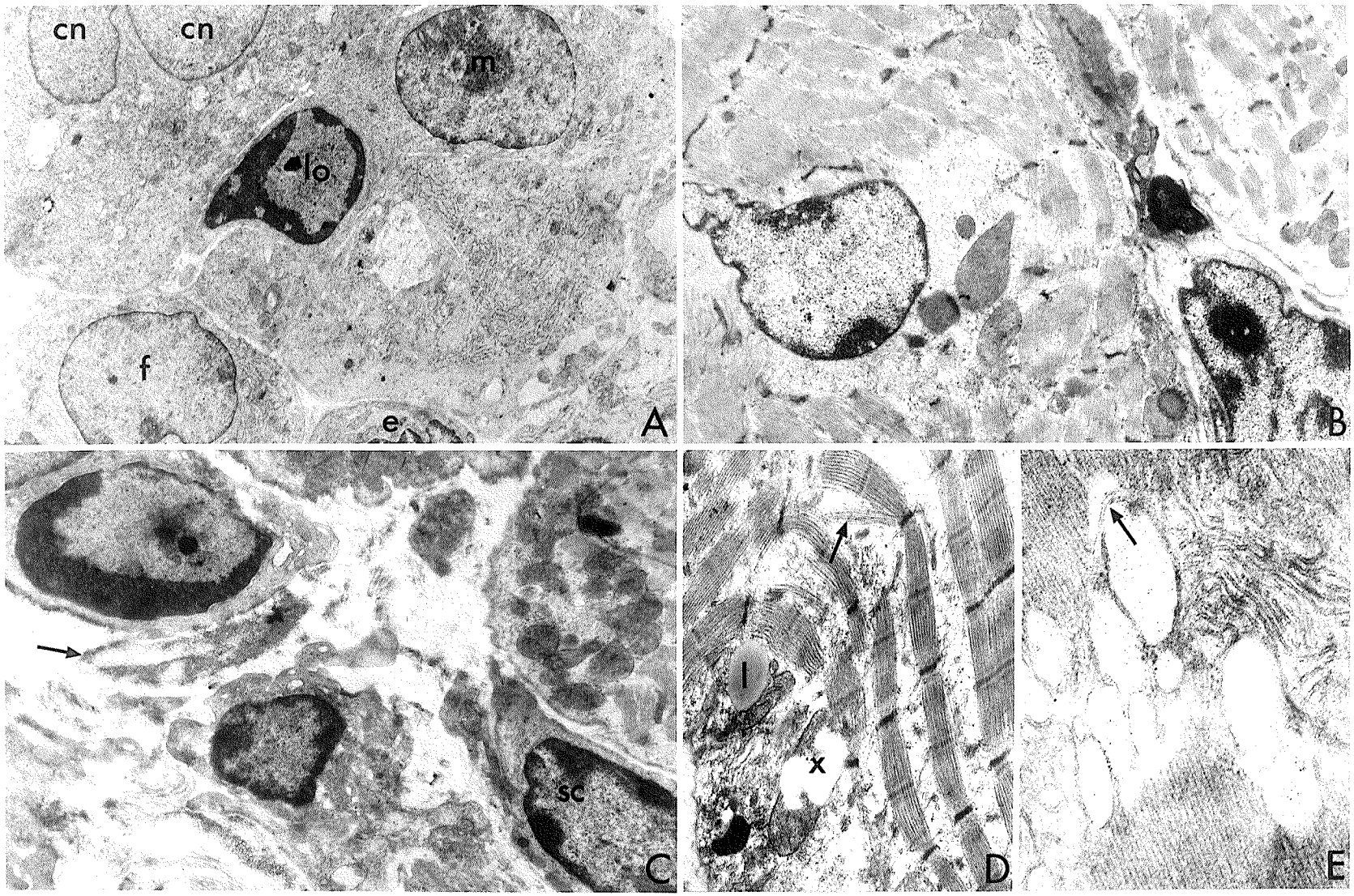
cn
cn
m
lo
f
e
A
B
C
sc
D
I
x
E

Figure 3: Micrographs of degenerating mdx soleus muscles.

Figure 3A: Focal segmental necrosis is evident as pervasive myofibre degeneration in this 6 to 7-week-old mdx soleus (SOL) muscle (★). Satellite cells (**s**) lie between the external lamina and the sarcolemma, the reserve pool of muscle precursor cells. Fibroblasts (**f**), an endothelial cell (**e**), and a myoblast (center left with large nucleolus) infiltrate the damaged region. (X5200).

Figure 3B: An area of mdx SOL adjacent to the previous figure (3A), demonstrates a peripheral nucleus (**pn**) in an intact fibre, and extensive collagen deposition in the endomysium. Note a myoblast has reached this area which contains many fibres with disrupted myofibrillar organization. (X7100).

Figure 3C: This micrograph of a SOL from 7-week-old mdx, during the phase of active dystrophy, demonstrates a dense accumulation of heterogeneous mononuclear infiltrative cells to phagocytose and repopulate the necrotic tissue. Adjacent to intact regions of muscle (top right & bottom left), external lamina sheaths (→) contain degenerating fibres, with macrophages (**mϕ**) and myoblasts. (X4400).

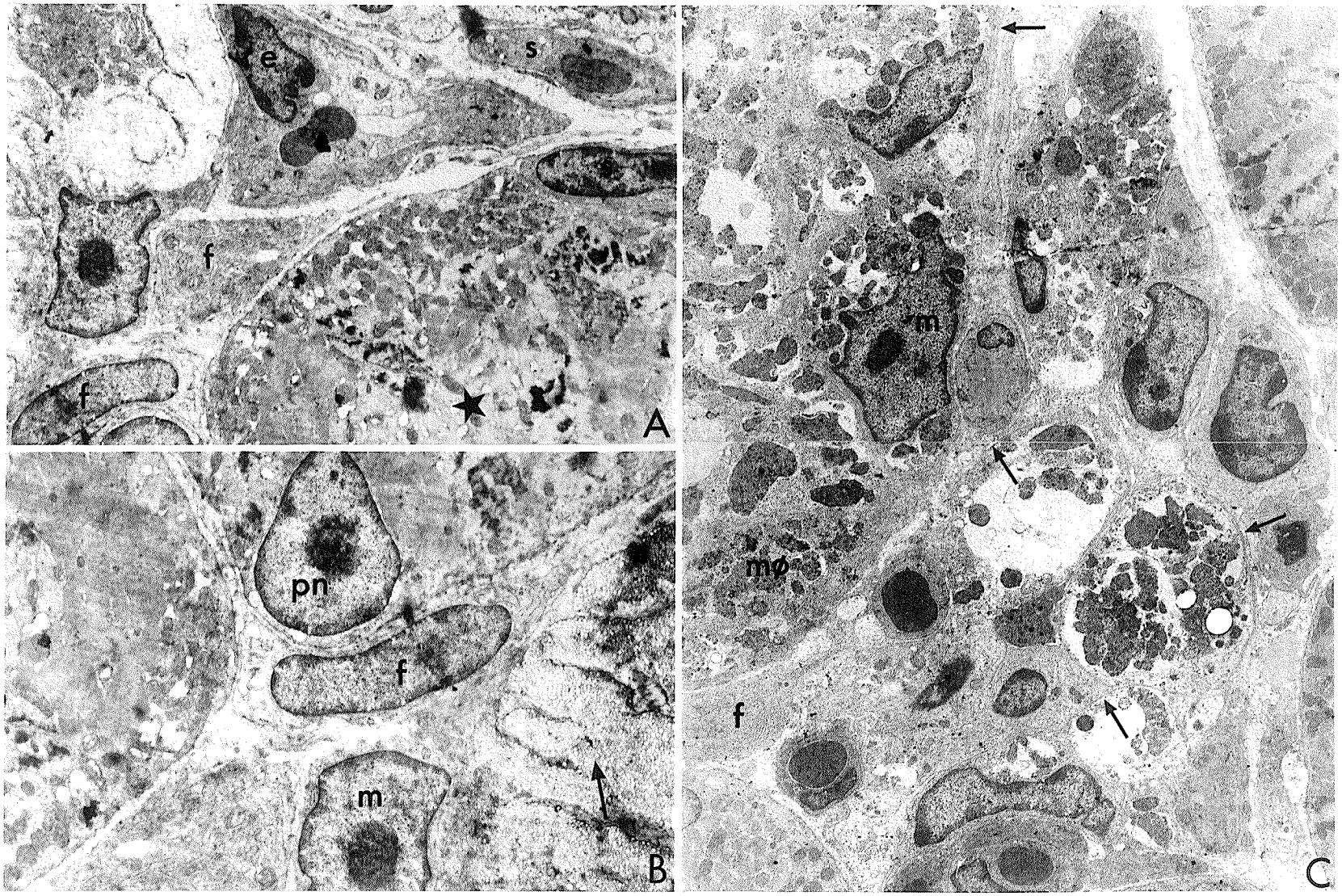
e
s
f
f
A
pn
f
m
B
m
mø
f
C

Figure 4: Micrographs of mdx (A,B,C) and control (D) soleus muscle.

Figure 4A: This series of plates shows that structural integrity of mdx SOL myofibres is reestablished in a gradual process. A centrally nucleated (**cn**) myofibre demonstrates both cross and longitudinal sections of fibrils early in the disruption of this fibre. (X4000).

Figure 4B: Following successful regeneration, the mdx SOL demonstrates the typical characteristics of adult striated skeletal muscle although fibres are central nucleated (**cn**). These regenerated myofibres show good structural integrity along with restoration of sarcomere banding. The endomysium contains blood vessels (**bv**), and a mast cell (→). The inset at higher magnification, demonstrates the well-preserved Z band, I band, and mitochondria in these fibres. (x4100 & x23,700).

Figure 4C: A mast cell with granules shown inside the external lamina (→) of a degenerated mdx SOL myofibre, and a myoblast (**m**) attracted to the site of damage. The myoblast demonstrates a large oval nucleus, prominent nucleolus, and scanty cytoplasm, characteristic of its cell type in an unfused precursor state. (X8300).

Figure 4D: Myofibres of an intact control SOL muscle demonstrating characteristic polygonal fibres around a blood vessel (**bv**), quiescent peripheral nuclei (**pn**), and the absence of mononuclear cells or fibrotic infiltration into a region of endomysial connective tissue with very scant collagen deposition. (X1300).

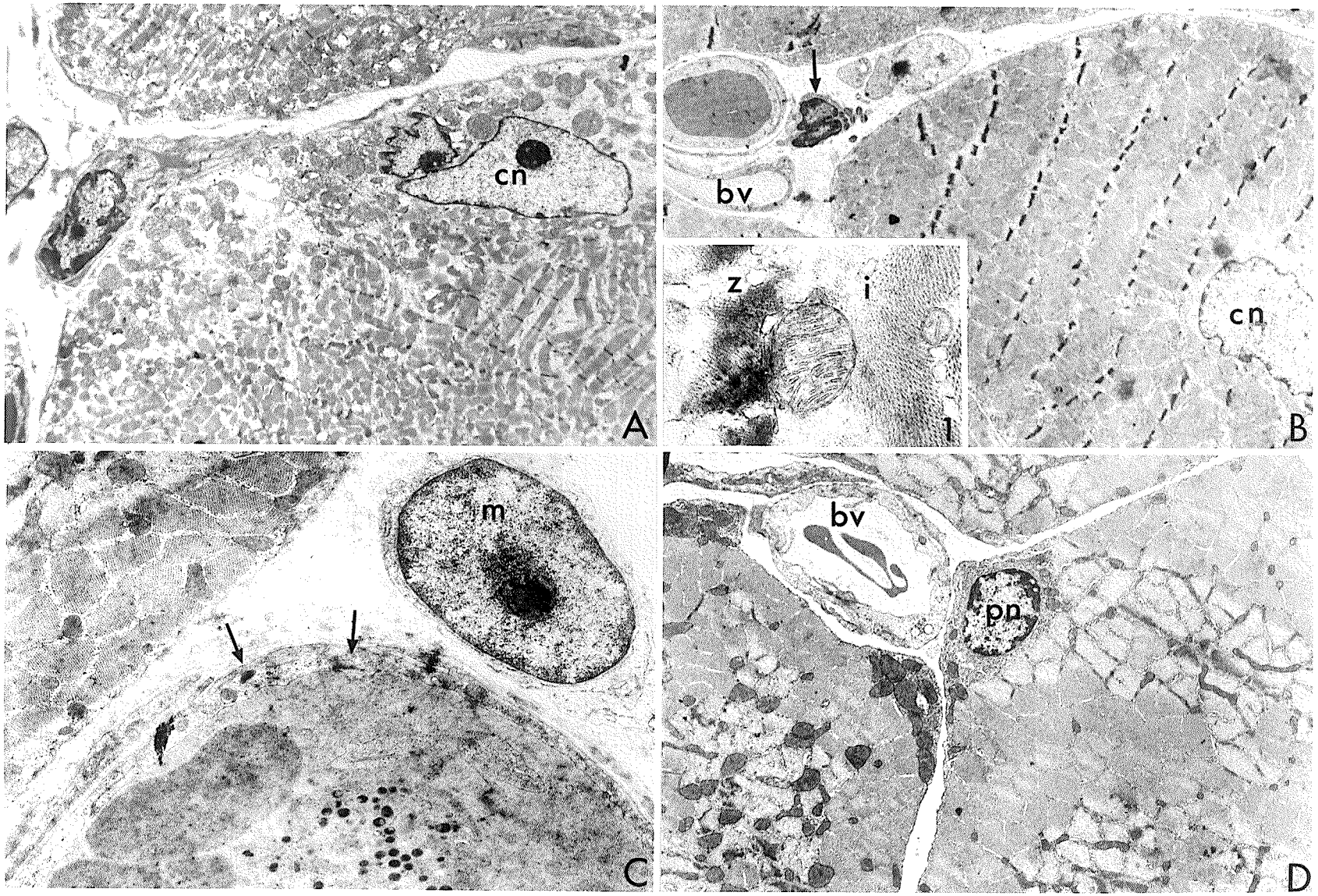
cn
A
bv
z
i
l
cn
B
m
C
bv
pn
D

Figure 5: Micrographs of fibroblasts and an endothelial cell from control and mdx diaphragm to demonstrate gold immunolabelling and its removal by omission of the primary antibody (D).

Figure 5A: A control DIA fibroblast is shown adjacent to the perimysium and a collagen deposit in the ECM. Circles indicate some of the dense bFGF labelled with 10 nm Protein A-gold evident in this tissue type (x25,000).

Figure 5B: An mdx DIA fibroblast also from the region of the perimysium, processed in same manner as 5a (above), demonstrates many fewer particles labelling bFGF. All gold particles are circled on this photograph. (X25,000).

Figure 5C: This micrograph demonstrates good tissue preservation and label penetration after immunolabelling with the final protocol developed on control DIA muscle. Note the selective gold labelling for bFGF over ECM collagen (**c**), and on the endothelial and fibroblast cells, but minimal background staining over the acellular vessel lumen (★). (X25,000).

Figure 5D: This control DIA fibroblast was in a section which was processed without the primary bFGF antibody demonstrates an absence of gold particles, indicative of the specificity of the label for the bFGF epitope. (X25,000).

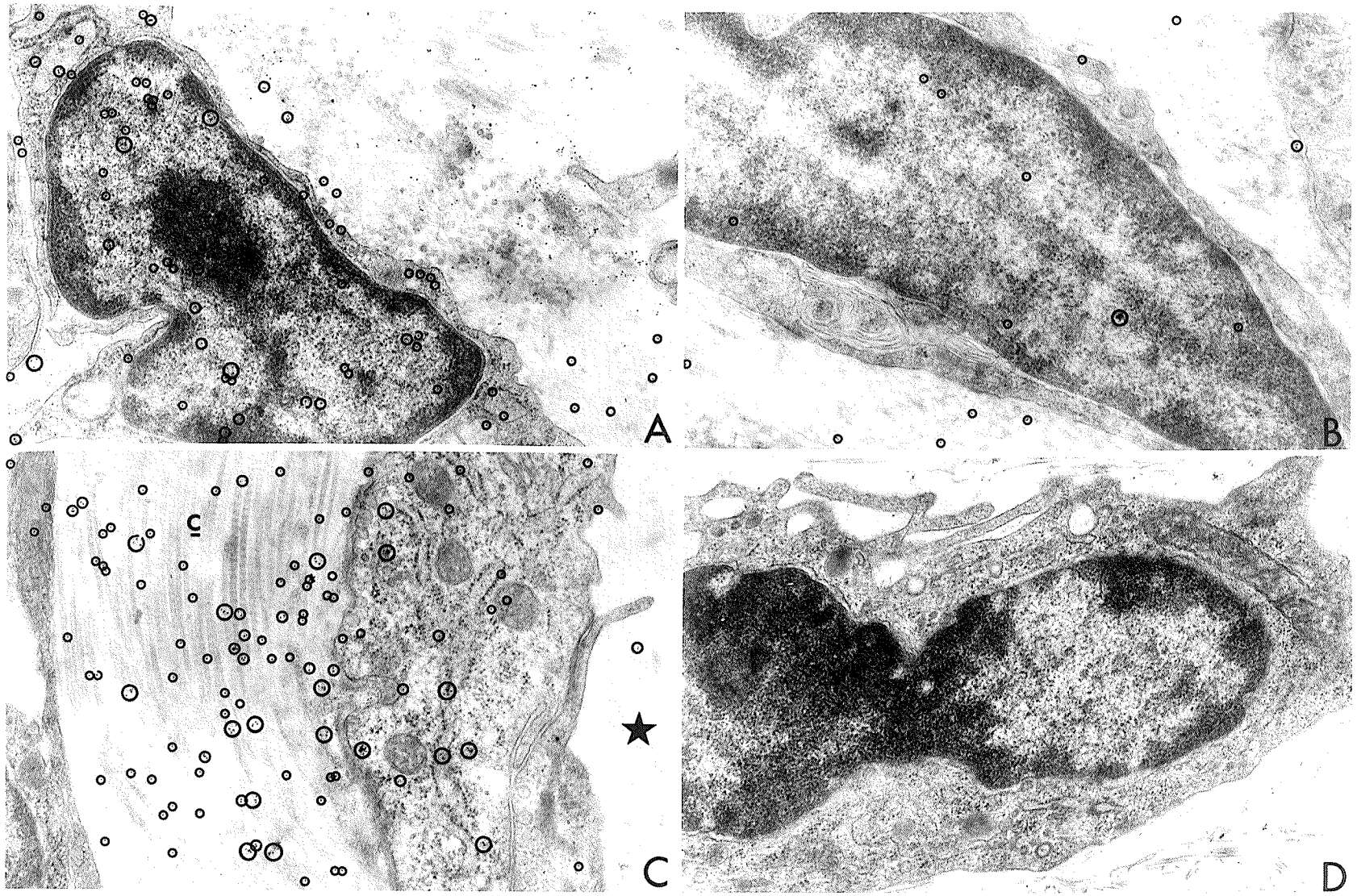
A
B
C
C
D

Figure 6: Micrographs of endothelial cells which demonstrate changes in the immunostaining protocol which affect specificity of label.

Figure 6A: An endothelial cell from the mdx DIA, surrounded by collagen (c) processed with 1:100 dilution of the primary antibody, a secondary goat anti-rabbit antibody, and 20 nm Protein A-colloidal gold. The 20 nm gold particles are easier to visualize (see circles), but their limited tissue penetration has restricted the extent of labelling. (X25,000).

Figure 6B: This is an example of a micrograph excluded from morphometric analysis as it did not meet all the inclusion criteria. Tissue was processed with a 1:25 diltuion of primary antibody, and demonstrates clumps of extensive nonspecific staining (→) which crosses cell boundaries. (X25,000).

Figure 6C: This endothelial cell from a mdx SOL muscle was labelled after incubation in a single blocking agent, and then a 1:250 dilution of the primary antibody. The micrograph was excluded from morphometric analysis as it demonstrates nonspecific gold labelling over an area of contamination (→). Small and larger clusters and single particles are also present (circled). (x25,000).

Figure 6D: An enothelial cell from a control DIA muscle demonstrates a nearly complete absence of label from all compartments following overnight presorption of the primary antibody with excess bFGF antigen (human recombinant bFGF, Gibco). The absence of gold particles confirms the specificity of the label for bFGF. The single gold particle (circled) is an example of the typically low level of nonspecific background staining. (X25,000).

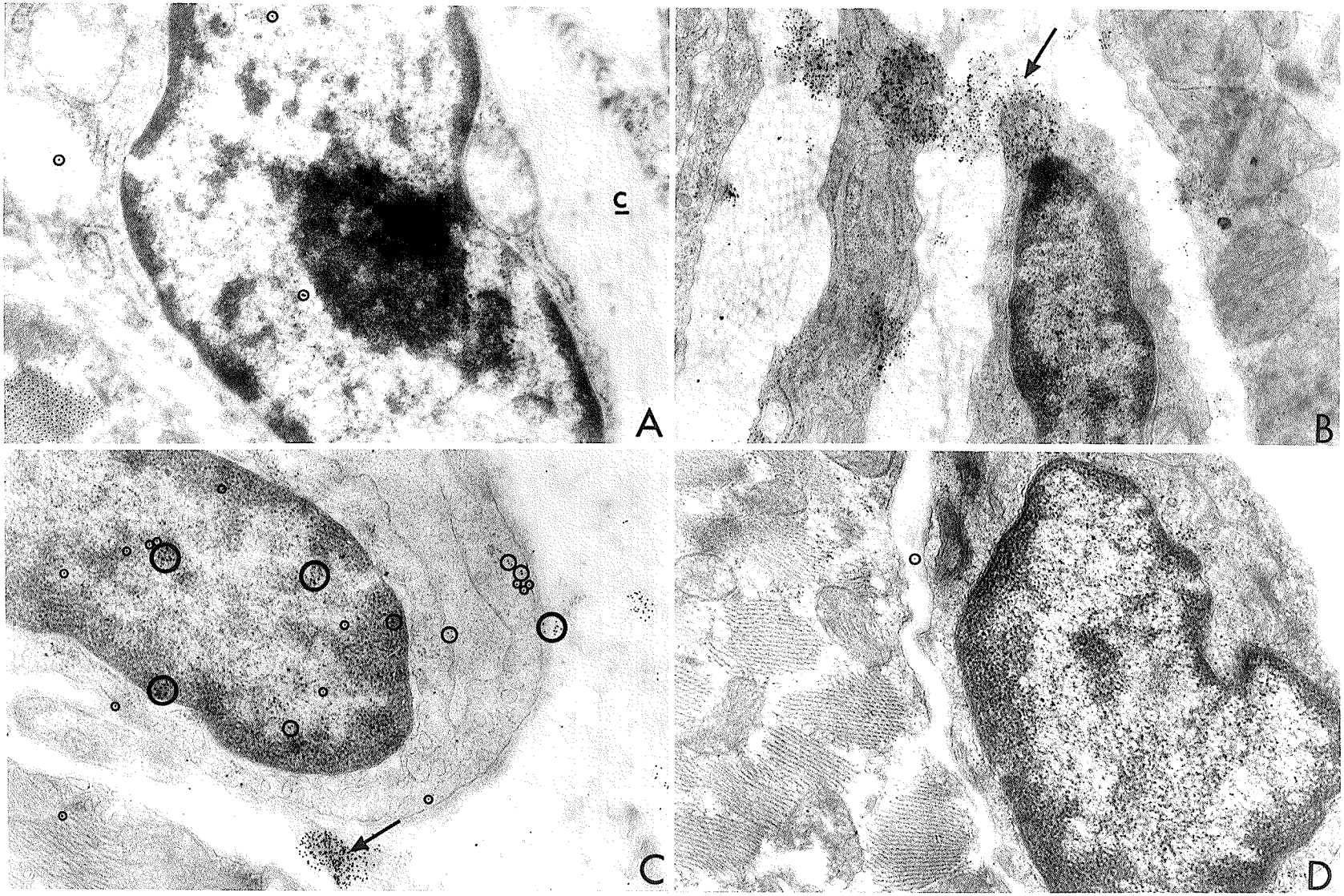
c
A
B
C
D

Figure 7: Micrographs of peripheral nuclei from mdx (**A**) and control (**B**) diaphragm muscle demonstrating bFGF gold-labels (as indicated by small circles) after staining with the final protocol. More gold particles are noted in control (B) than mdx (A) intact muscle. Note the relative absence of collagen in the dystrophic and control muscles 1) close to the endomysium and 2) between the intact non-degenerating myofibres. The absence of gold labels over mitochondria indicates minimal background staining for this tissue type. (X26,300).

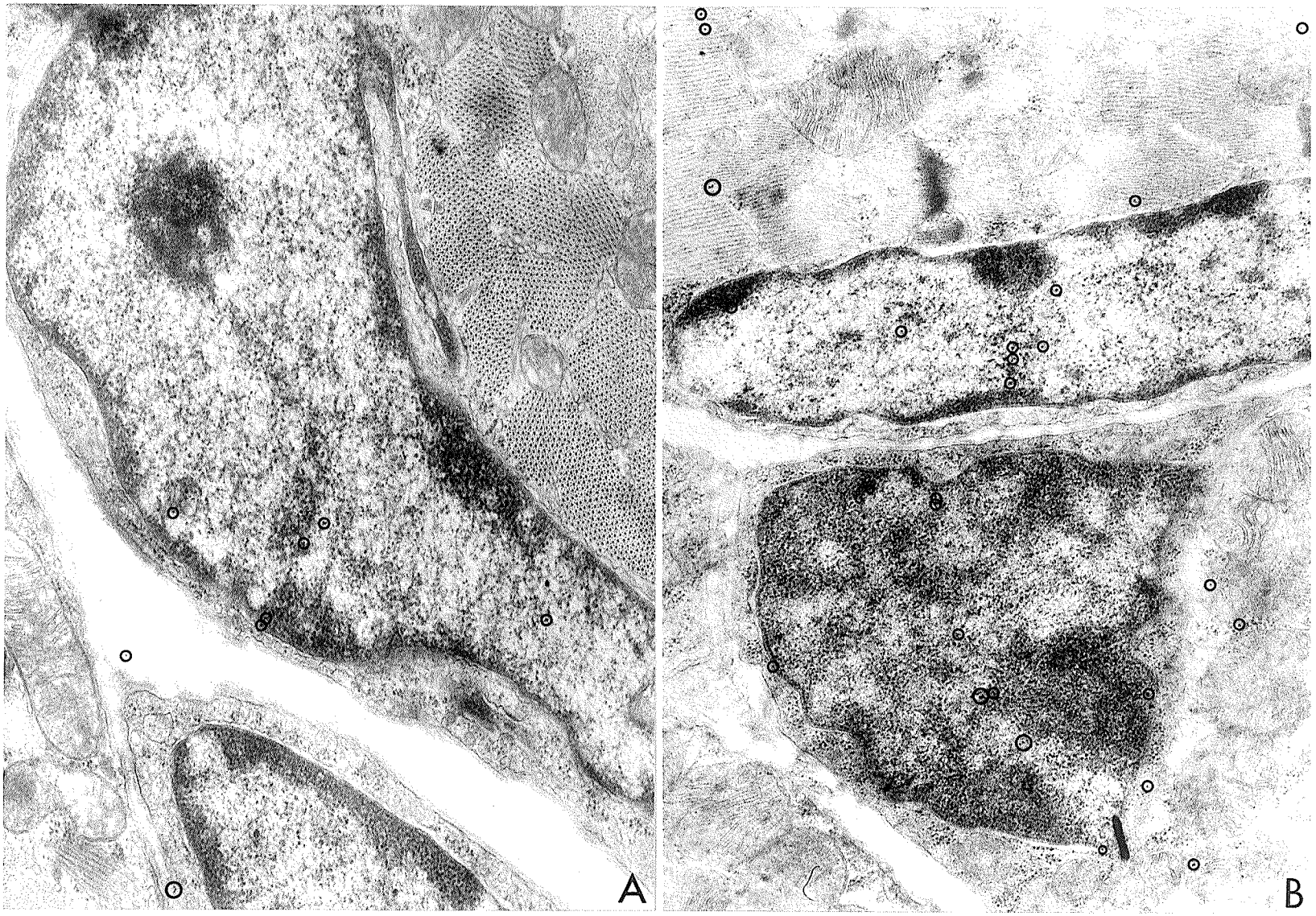
A
B

Figure 8: These micrographs of myoblasts from mdx (**A**) and control (**B**) DIA demonstrate gold-labelled bFGF (as indicated by the small circles). Note the reduced bFGF evident in dystrophic (A) versus control (B) DIA, and the large accumulations of gold label on collagen (B bottom). (X33,850).

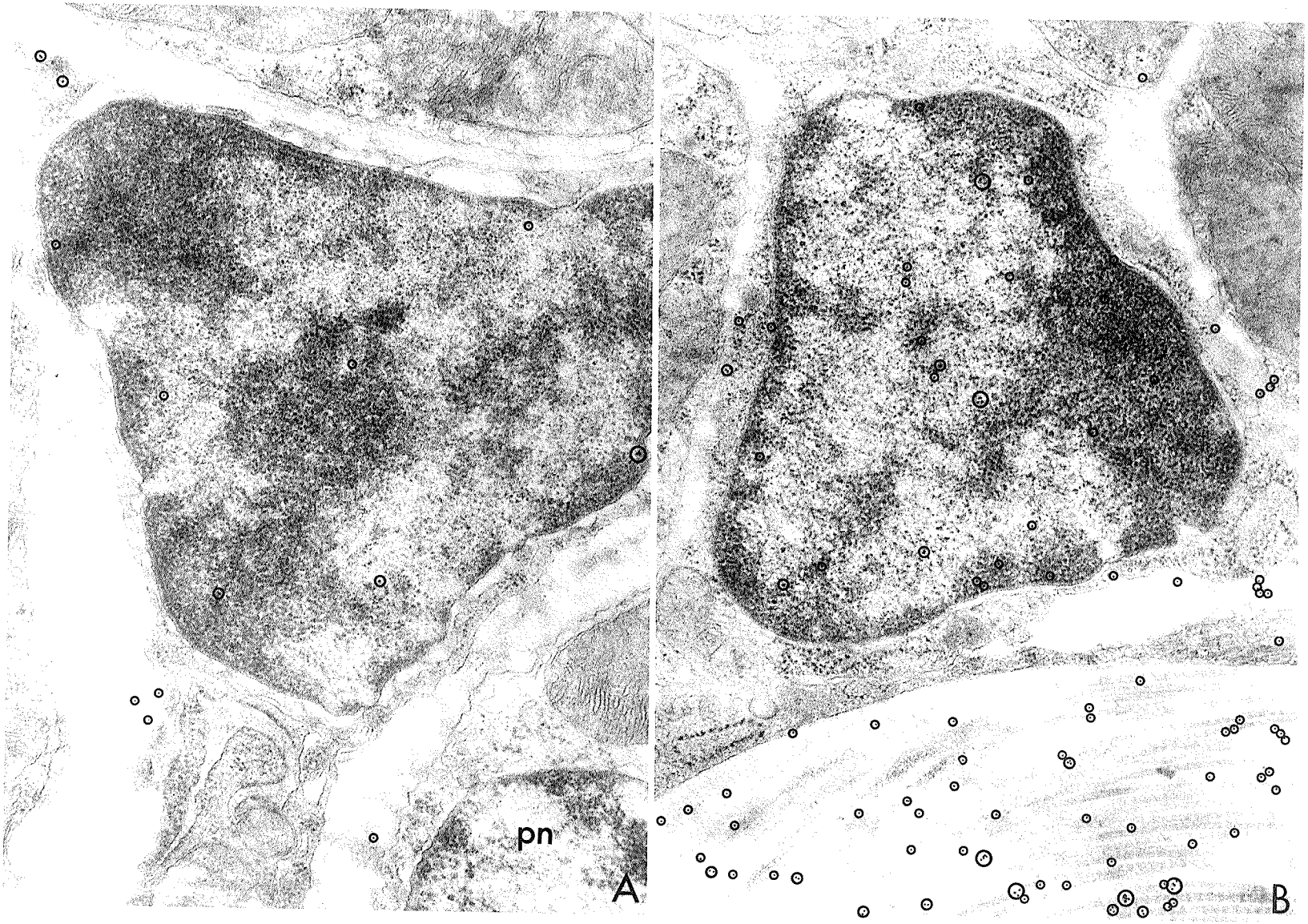
pn
A
B

Figure 9: Micrographs of endothelial cells from mdx (**A**) and control (**B**) DIA demonstrate gold-labelled bFGF (as indicated by the small circles). Note the absence of label over the vessel lumen and erythrocyte, indicative of the relatively specific localization of bFGF. Although the mean LI may not appear represented by the control micrograph (b), this image provides a good example of the difficulty in visualizing 10 nm gold particles on tissue with high competing background contrast, such as over heterochromatin. On the original working microraph several additional gold particles and clusters were visible over the control cell heterochromatin. (X34,500).

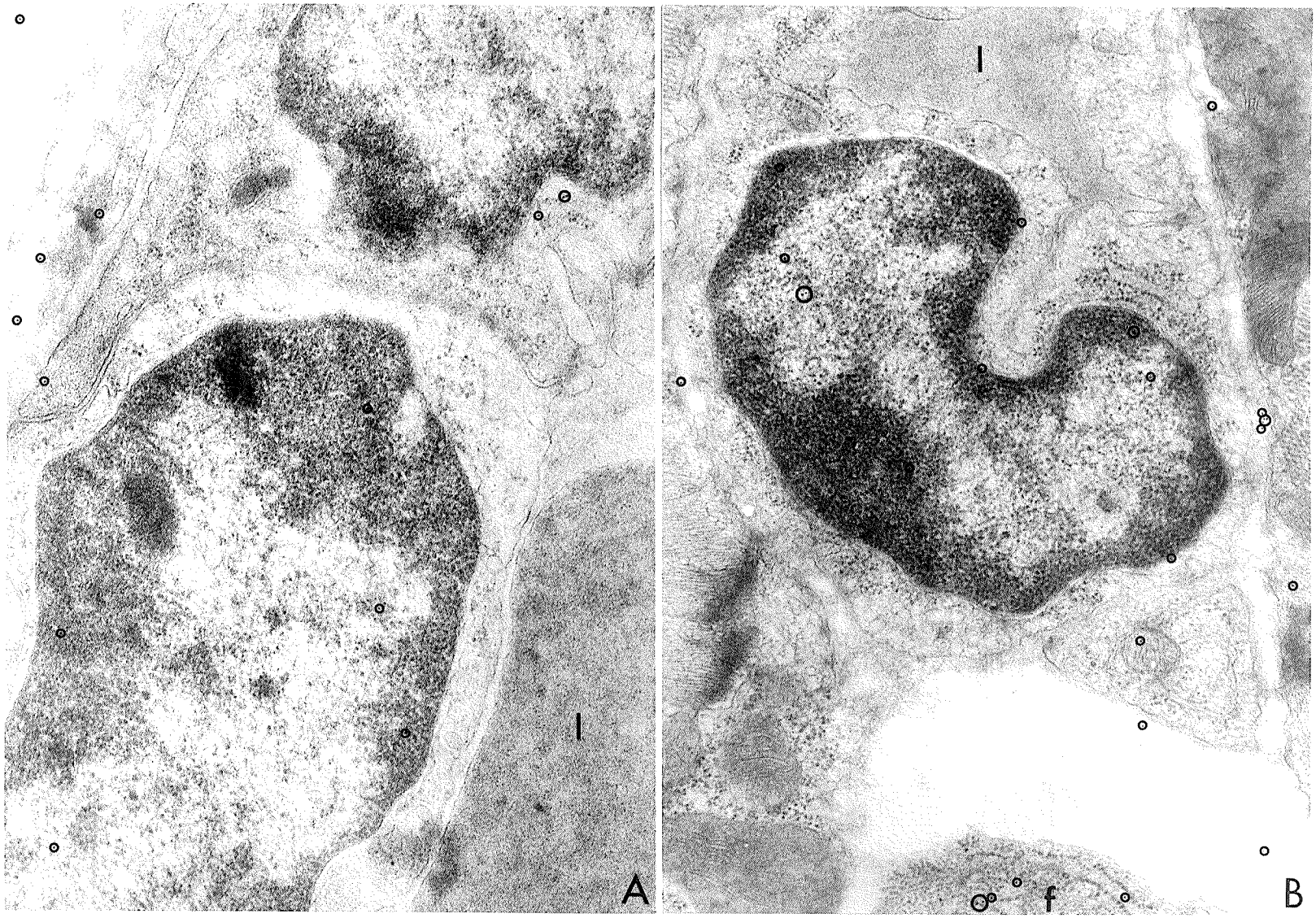
I
A
I
f
B

Figure 10: A series of micrographs which demonstrate different structural stages in muscle regeneration.

Figure 10A: A myoblast (muscle precursor cell) which has synthesized small accumulations of myofilaments (→) in the cytoplasm prior to fusing. (X19,400).

Figure 10B: A myoblast with dense heterochromatin in the nucleus, is in the early process of fusing to an adjacent myoblast. Note the interdigitation of plasma membranes (↔) which occurs just prior to fusion into a myotube. (X19,400).

Figure 10C: An early myotube during fusing which will eventually reestablish myofibre continuity. Arrows (↔) indicate the complex interconnections between the limiting membranes of adjacent muscle precursors cells. (X19,400).

Figure 10D: A regenerated myotube demonstrates a characteristic central or eccentric nucleus internal in the myofibre with highly organized myofibrils. There appear to be collections of gold particles over radial accumulations of nuclear filaments in the top right quadrant of the nucleus, suggesting bFGF on nuclear (possibly DNA) binding sites. (X21,200).

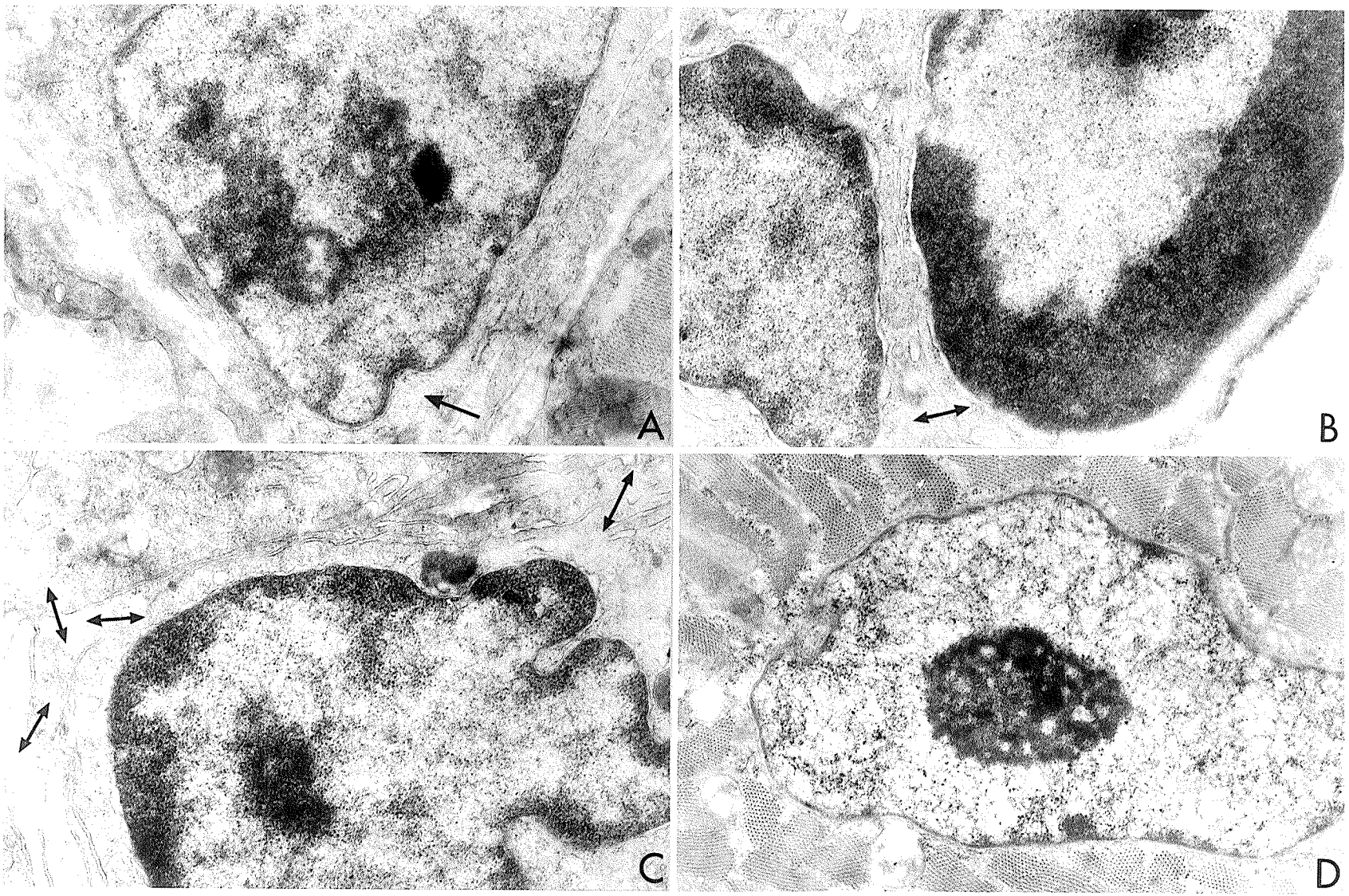
A
B
C
D

Figure 11: This plate shows representative micrographs of mononuclear infiltrative non-muscle cells attracted to an area of recent degeneration in the mdx DIA.

Figure 11A: A mast cell is releasing histamine granules. (x25,000)

Figure 11B: A polymorphonuclear lymphocyte contains a bilobed nucleus. (x15,000)

Figure 11C: A macrophage containing dense lysosomes. Two myoblasts (m) are adjacent to the macrophage. (x20,000)

Figure 11D: A lymphocyte showing a very dense heterochromatic nucleus which occupies almost all of the cell. (X20,000)

Gold labels for bFGF were generally evident in descending order, on the macrophage, mast cell, and PMN (not shown here) suggesting their potential role in accumulating, synthesizing, or transporting bFGF at/to the site of injury.

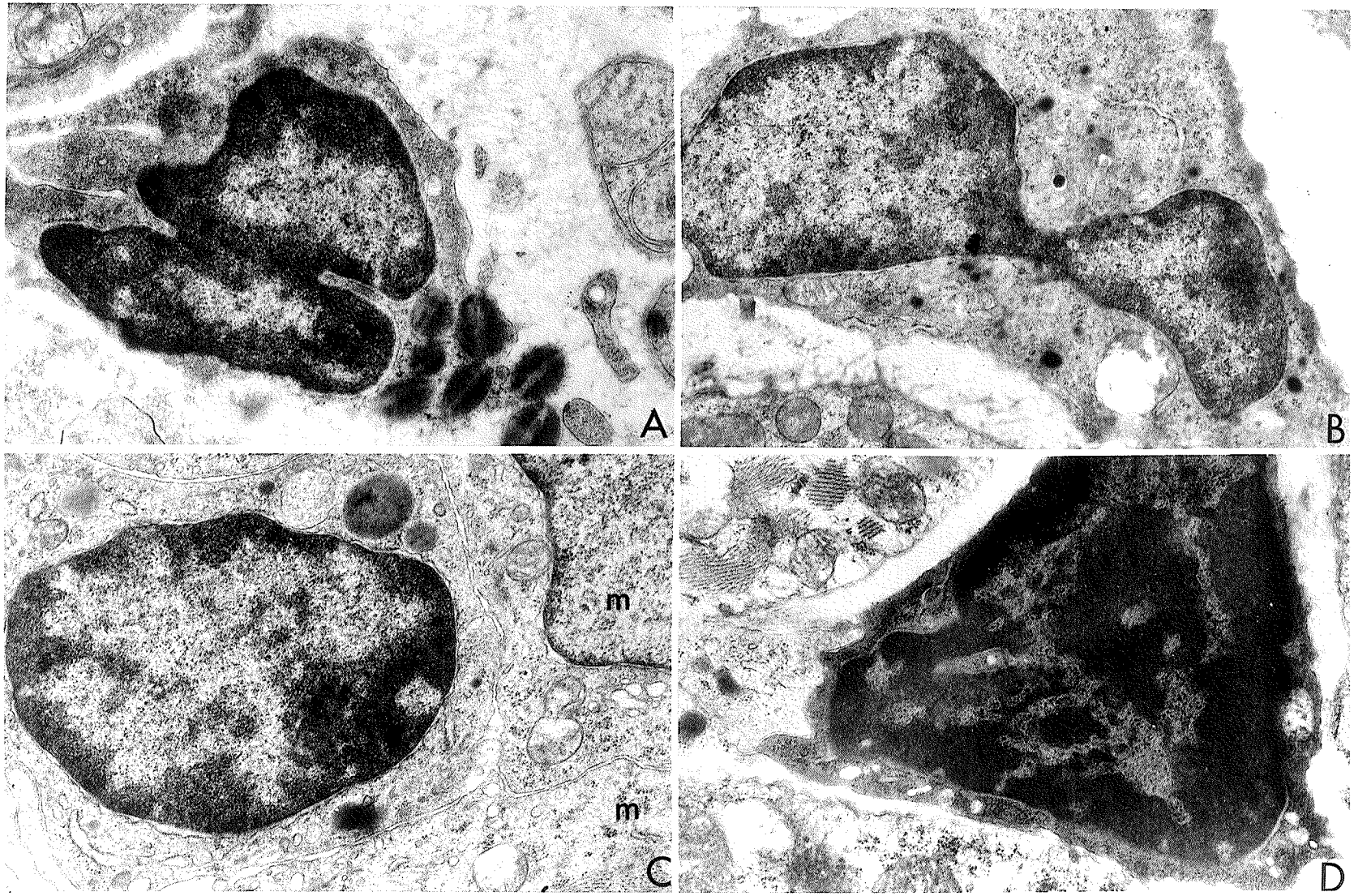
A
B
m
m
C
D

Figure 12: Micrographs of nerve cross-sections and neuromuscular junctions in mdx SOL muscle.

Figure 12A: A few gold particles are visible over myelin sheaths (**my**) and nerve axons (**a**) adjacent to Schwann cell (**swn**) which appear normal in this section. (X25,000)

Figure 12B: This section of mdx SOL was processed without a primary antibody to bFGF, and has no gold particles on the myelin sheath (**my**), axon (**a**) or Schwann cell (**swn**) in a region of active dystrophy. The absence of gold label demonstrates the minimal influence of non-specific conditions which might spuriously label bFGF and many other epitopes with gold particles. (X20,000)

Figure 12C: A low magnification of mdx SOL shows a myofibre undergoing degeneration (darker cell in centre of micrograph) which has maintained a very long, circumferential synaptic connection with a nerve at the neuromuscular junction (→). Double etching of tissue sections has made the tissue prone to tearing and caused corrosion of the grid, which deposited pieces of the grid bar (**g**) on tissue sections. (X10,300)

Figure 12D: A regenerated mdx SOL myofibre with a neuromuscular junction which demonstrates truncated folds and shallow, irregular, and widely-spaced secondary synaptic clefts. These junctiions are histologically aberrant although they are functional. (X25,000)

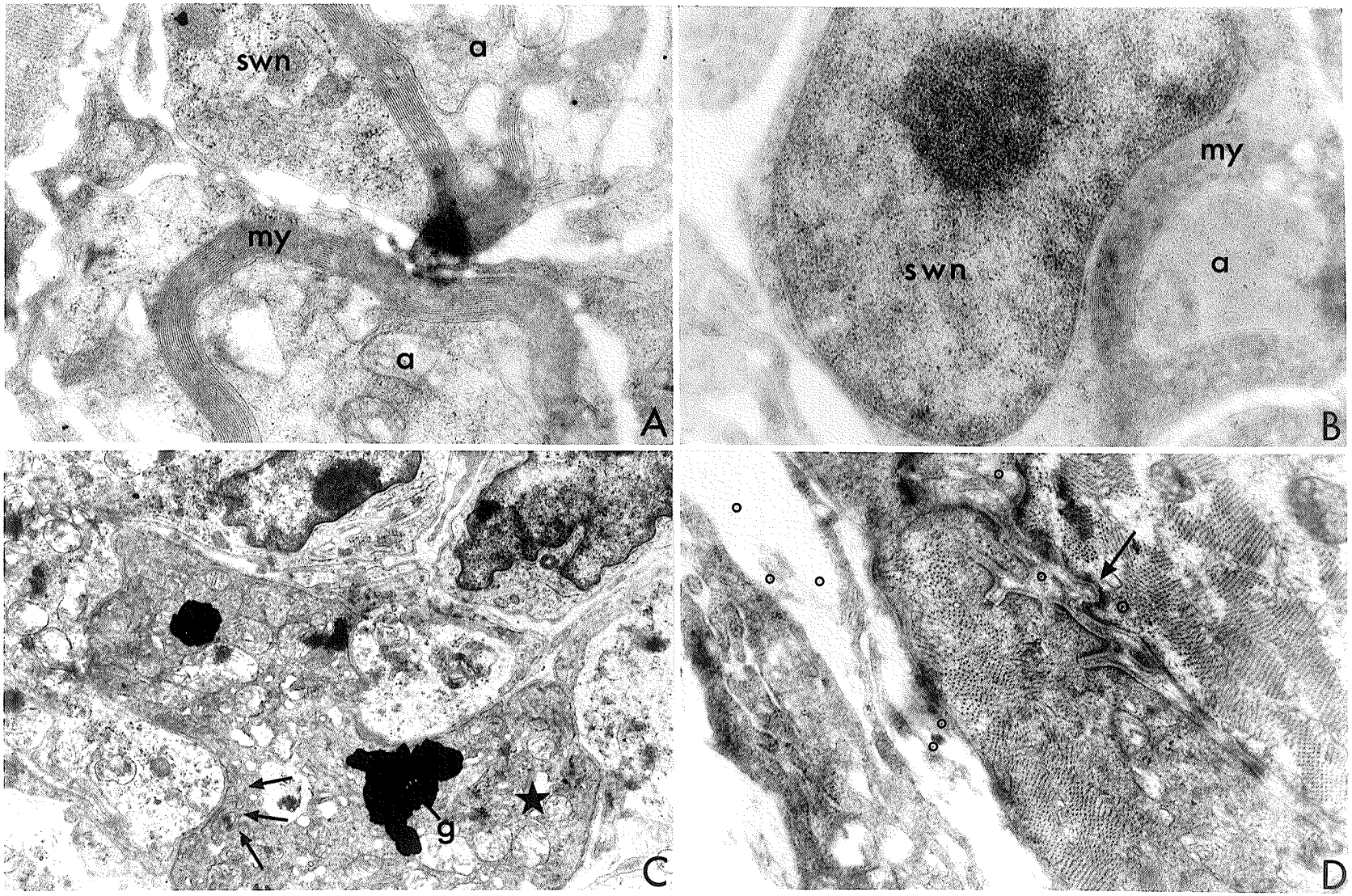
swn
a
my
a
A
my
swn
a
B
g
C
D

Table 1: Schematic representation of the immunogold labelling process.

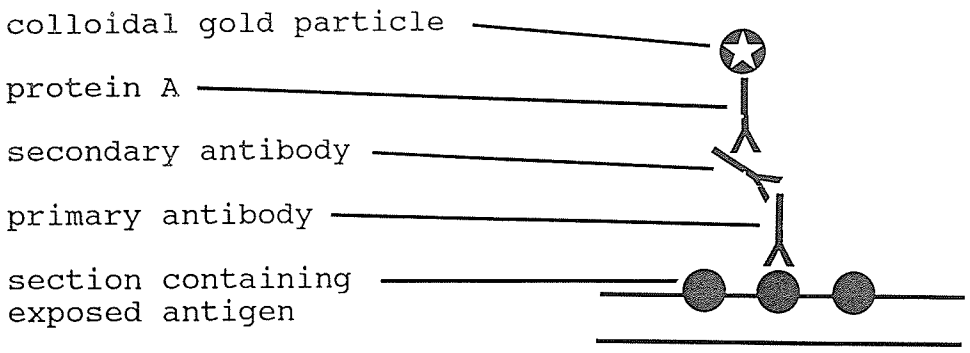

Table 2: Lab worksheet of the final immunogold protocol, which was used with each experiment to record methods followed, and list observations which might affect the outcome of labelling experiments.

IMMUNOGOLD PROTOCOL:

Date:_____ Purpose of run:_____

#1:_____ #2:_____ #3:_____

#4:_____ #5:_____ #6:_____

#7:_____ #8:_____ #9:_____

#10:_____ #11:_____ #12:_____

#13:_____ #14:_____ #15:_____

#16:_____ #17:_____ #18:_____

1) ETCHING:

)____ Float grids section side down on ddH20...5 mins.
)____ " " saturated aqueous NaMp (.1gm/mlPBS)...60 mins
)____ Wash in dd H2O, float section side down...5 mins.
)____ Wash in PBS...5 mins, then 10 sec. gentle stream rinse

2) IMMUNOGOLD LABELLING:

)____ Protein block nonspecific binding: OA sol'n...5 mins.
)____ Block for background staining: 0.15M glycine....30 mins
)____ Primary Antibody at _____ dilution (in OAT)...2 hours
)____ Wash grids in OA sol'n 3 x 5 mins... 1 2 3.
)____ Secondary antibody at 1:100 dilution (in OAT)...2 hours.
)____ Wash in OA sol'n 3 x 5 mins... 1 2 3.
)____ Gold Labelling using Protein__ __ with _ ___nm.gold.
Diluted 1:100 in OAT.... 1 hour.

)____
)____ Wash in PBS...5 mins, then 10 sec. gentle stream rinse
))___ Wash in dd H2O: 10 sec. gentle stream rinse, dip 10 X in 5 successive beakers ddH2O.
1)___ Blot dry and leave overnight.

3) CONTRAST STAINING:

)____ Uranyl Acetate, centrifuged & filtered...2 hours.
)____ Wash grids ddH20 ...5 mins
)____ Wash grids in dd H2): 10 sec. gentle stream rinse, dip 10 X in 5 successive beakers ddH20.
)____ Blot dry and leave overnight.

)____ Lead Citrate (fresh), centrifuged & filtered...3 mins. (1/2 pellet NaOh,0.375 mg.PbCit, 12.5 ml ddH20)
)____ Wash grids 0.1M NaOh.....5 mins.
)____ Wash grids ddH20.....5 mins.
)____ Wash in ddH20: 10 sec. gentle stream rinse, dip 10 X in 5 successive beakers ddH20.
)____ Blot dry.

.5gm Ovalbumin, .5gm skim milk powder, 50 ml PBS
: 10 ml OA, .3 gm NaCl. 5 microltr. Tween-20 (0.05%)

Table 3: This table summarizes the variables assessed by separate staining experiments during the development phase of the final protocol.

VARIABLES TESTED	CONCLUSIONS
Fixation:	
Perfusion vs. immersion	cytoskeletal integrity maintained with immersion
3% vs. 1.5% glutaraldehyde	1.5% gave reasonable fixation, 3% decreased bFGF detection
Embedding:	
Araldite vs. Epon	contrast and post-etching stability under the TEM beam was better with Epon
Grid Preparation:	
Cleaning: ethanol vs. glacial acetic acid + ethanol + ddH_2O	acetic acid regime resulted in very clean grids; water rinsing must be thorough or grids etch and corrode considerably
Grids with sections heated overnight vs. processed without prior heating	tissue adherence to grid improved marginally with overnight heating
Etching:	
Sodium metaperiodate freshly prepared vs. stock solution grids.	stock solution turned acidic, resulting in corroded grids
Etch with sodium ethoxide and sodium metaperiodate vs. only with sodium metaperiodate	double etching resulted in very fragile sections, prone to tearing without significantly improving antigen accessibility

<u>Blocking and Rinsing:</u>	
Protein block with 1% ovalbumin in 0.01M PBS vs. with 1% ovalbumin + skim milk powder in PBS	less non-specific background staining with the addition of skim milk powder
OA and OAT solutions mixed fresh vs. refridgerated stock	fresh solutions were more consistent when processing and reduced contamination on grids
0.15M glycine added after primary block with OAT solution	background staining much less with glycine block, allowed use of lower dilution of primary antibody
OA and OAT solutions centrifuged & Buchner filtered vs. as above plus millipore filtered	millipore filtration decreased contamination and retained blocking of nonspecific staining
Rinsing with 0.01M PBS and ddH_2O vs. rinsing with OA solution	improved specificity with OA solution
Rinsing by floating grids on drops vs. dipping in solutions vs. jet-stream rinsing vs. slow spin on droplets using magnetic stir plate	slow spinning technique resulted in cleanest grids with low background, although sections easily tear if spun after grid sinks into droplet. Needs close monitoring. Rapid serial dipping yielded good results.
<u>Primary Antibody:</u>	
Diluted with 1% ovalbumin in 0.01M PBS vs. diluted with OAT solution	improved specificity with OAT
Dilutions: 1:20, 1:40, 1:80, 1:100, 1:160, 1:200, 1:250, 1:300, 1:400, 1:500, 1:600, 1:800, and 1:1000.	lower dilutions resulted in high background staining. Without glycine, 1:400 clearly labelled muscle sections with low background; with glycine block, 1:100 maintained low background and improved signal
Omission of primary antibody	only sections exposed to primary antibody were labelled
Incubation with primary antibody vs. incubation with primary antibody plus excess bFGF	characteristic staining patterns were absent following presorbtion; antibody staining is specific
<u>Secondary Antibody:</u>	
Goat anti-rabbit secondary antibody vs. no secondary antibody	use of secondary antibody amplified labelling; results easier to visualize by EM

Protein A-colloidal gold:	
20nm vs. 10nm particles	improved labelling with 10nm gold particles: small clusters of particles seen over the same sites as in grids labelled with 20nm particles. 20nm particles easier to locate

Table 4: This table summarizes factors that influence bFGF localization.

Variable	Comments
Tissue processing	fixation, embedding, specimen preparation & sectioning protocols all influence outcome
Immunogold labelling	etching, blocking, labelling, tagging, and washing protocols all affect tissue integrity and signal clarity
Contrast staining	uranyl acetate may mask tag, lead particles may mimic gold, contrast staining for enhanced morphometric analysis makes gold visualization difficult, but allows morphological study
TEM viewing	cellular organelles, inclusions (eg. nuclear heterochromatin) may mask gold particles. Optimal viewing conditions (high illumination and magnification) may distort sections or result in regions not scanned. Focus must be acute for accurate counts. Areas adjacent to grid bars or with tissue tears may trap unbound gold and must be avoided
Micrograph viewing	contrast printing for enhanced morphometric analysis detracts from gold visualization

Table 5A: Labelling index (LI) data for colloidal gold-labelled anti-bFGF immunostaining of muscle and non-muscle cells in control and mdx diaphragm muscle.

cell type	aspect[a]	control LI (n)	mdx LI (n)
myoblast┼ϕ^i	nucleus cytoplasm	4.17 ± 1.20 (4) 3.12 ± 0.75	1.46 ± 0.34* (23) 1.77 ± 0.36*
fusing myoblast┼	nucleus cytoplasm	-- --	0.74 ± 0.11 (19) 0.51 ± 0.09
satellite cell┼	nucleus cytoplasm	1.42 ± 0.70 (3) 0.94 ± 0.16	1.09 ± 0.21* (4) 1.34 ± 0.14*
regenerated muscle┼	nucleus--CN	--	1.06 ± 0.26 (15)
muscle[i]	nucleus-PN sarcoplasm▲ →→ecm	1.28 ± 0.65 (7) 2.40 ± 0.47 (66) 0.70 ± 0.24	0.47 ± 0.23 (3) 0.92 ± 0.12* (59) 1.20 ± 0.73
fibroblastϕ^i	nucleus cytoplasm	1.87 ± 0.49 (18) 1.39 ± 0.27	1.25 ± 0.25 (15) 1.06 ± 0.29
endothelialϕ^i	nucleus cytoplasm	4.73 ± 1.52 (14) 3.63 ± 1.23	1.39 ± 0.34* (12) 1.26 ± 0.33*
extracellular matrix┼	endomysium + external▲ lamina	3.65 ± 0.37 (64)	2.60 ± 0.35* (78)

*:indicates significant difference from control by ANOVA or Duncan's tests (mean ± SE)
┼:indicates significant difference from the other myoblast populations
ϕ:indicates significant difference between myoblast cell types and non-muscle cells
a:there was no significant difference between the nuclear and cytoplasmic compartments
i:indicates significant interaction between cell type and strain (control or mdx)
→→ecm:indicates the cytoplasm compartment between peripheral nucleus and external lamina
▲:indicates significant difference between these two parameters for both control and mdx

Table 5B: Labelling index (LI) data for colloidal gold-labelled anti-bFGF immunostaining of muscle and non-muscle cells in control and mdx soleus muscle.

cell type	aspect[a]	control LI (n)	mdx LI (n)
myoblast┼ϕ^i	nucleus cytoplasm	1.65 ± 0.91 (4) 1.50 ± 0.49	2.22 ± 1.42 (12) 1.45 ± 0.41
fusing myoblast┼	nucleus cytoplasm	-- --	1.24 ± 0.65 (4) 0.51 ± 0.09
satellite cell┼	nucleus cytoplasm	3.42 ± 1.0 (3) 0.98 ± 0.40	5.68 (1) 1.34 ± 0.14 (3)
regenerated muscle┼	nucleus--CN	--	3.70 ± 1.57 (3)
muscle[i]	nucleus-PN sarcoplasm▲ ↠ecm	0.77 ± 0.15 (12) 0.85 ± 0.17 0.73 ± 0.28 (6)	3.43 ± 0.82* (6) 1.60 ± 0.71 4.48 ± 1.36*
fibroblastϕ^i	nucleus cytoplasm	0.94 ± 0.66 (3) 1.31 ± 0.84	1.30 ± 0.11 (5) 2.12 ± 0.80 (14)
endothelialϕ^i	nucleus cytoplasm	1.01 ± 0.62 (6) 0.75 ± 0.46	4.63 ± 2.23* (5) 3.42 ± 1.58
extracellular matrix┼	endomysium + external lamina▲	1.61 ± 0.47 (12)	2.84 ± 2.88 (2)

*:indicates significant difference from control by ANOVA or Duncan's tests (mean ± SE)
┼:indicates significant difference from the other myoblast populations
ϕ:indicates significant difference between myoblast cell types and non-muscle cells
a:there was no significant difference between the nuclear and cytoplasmic compartments
i:indicates significant interaction between cell type and strain (control or mdx)
↠ecm:indicates cytoplasm compartment between peripheral nucleus and external lamina
▲:indicates significant difference between these two parameters for both control and mdx

Table 6A: Comparison between control and mdx strains of the gold-labelled bFGF indices (LI) from diaphragm muscle. Myonuclei labelled for bFGF include migrating myoblasts (M), fusing myoblasts (FM), central myonuclei (CN), satellite cells (SC), and peripheral nuclei (PN). Other cell types and compartments which labelled for bFGF include endothelial cells (E), fibroblasts (F), the sarcoplasm (S), and the extracellular matrix (ECM). Significant differences between control and mdx strains are indicated by an asterisk (*).

Table 6B: Comparison between control and mdx strains of the gold-labelled bFGF indices (LI) from soleus muscle. Cell types and compartments labelled for bFGF as noted in Figure 6A above.

Diaphragm bFGF Nuclear Index

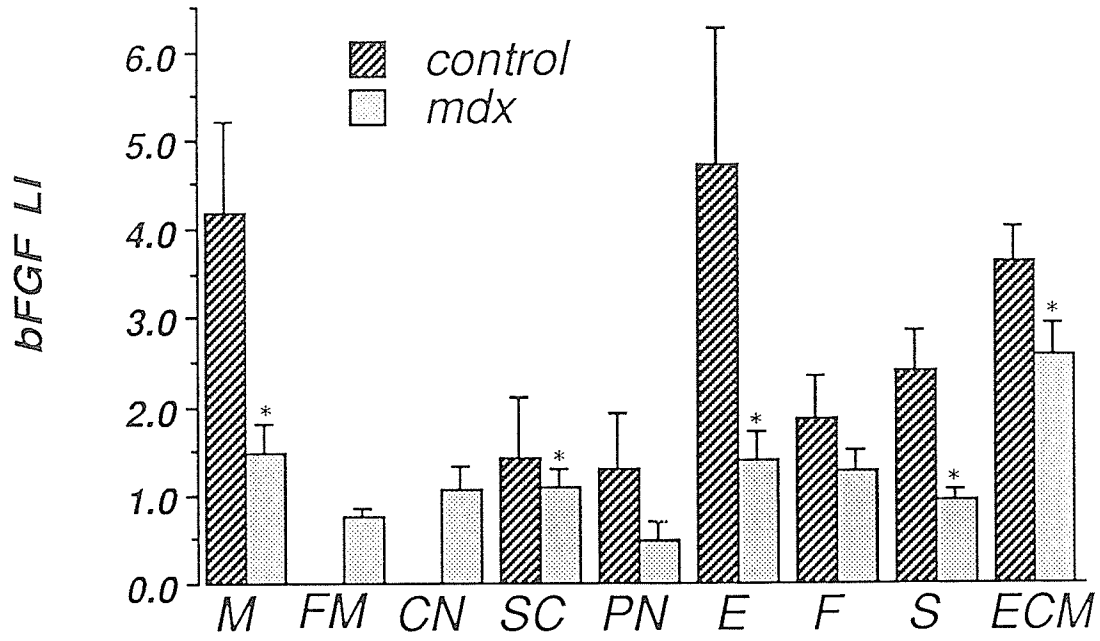

Soleus bFGF Nuclear Index

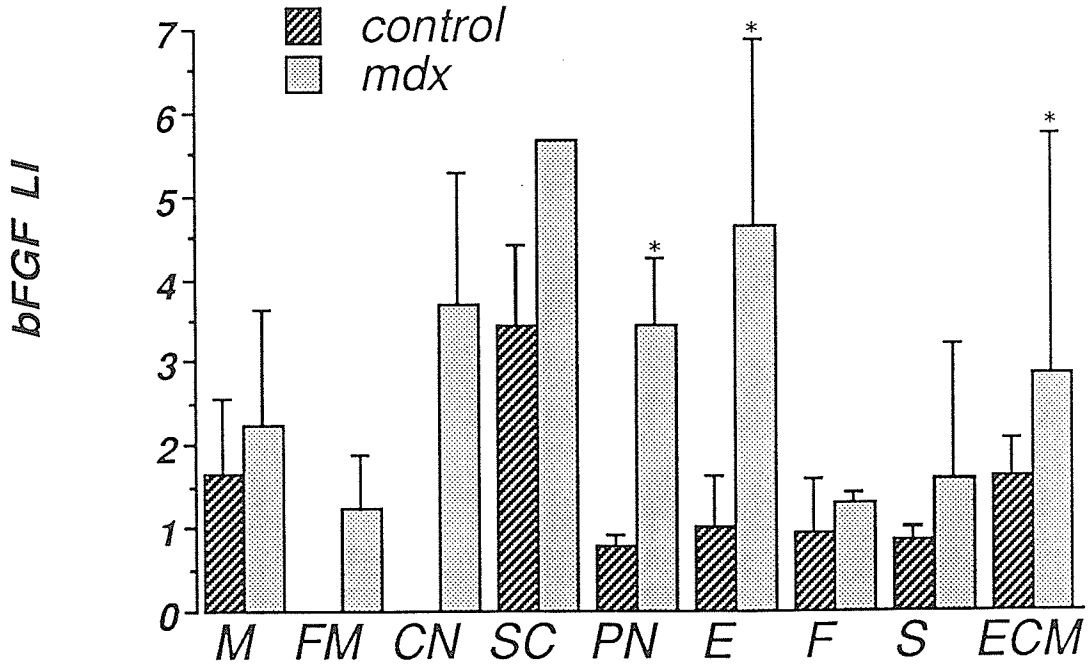

Table 6C: Comparison between mdx diaphragm and mdx soleus muscles of the gold-labelled bFGF indices. Cell types and compartments labelled are as noted Figure 6A.

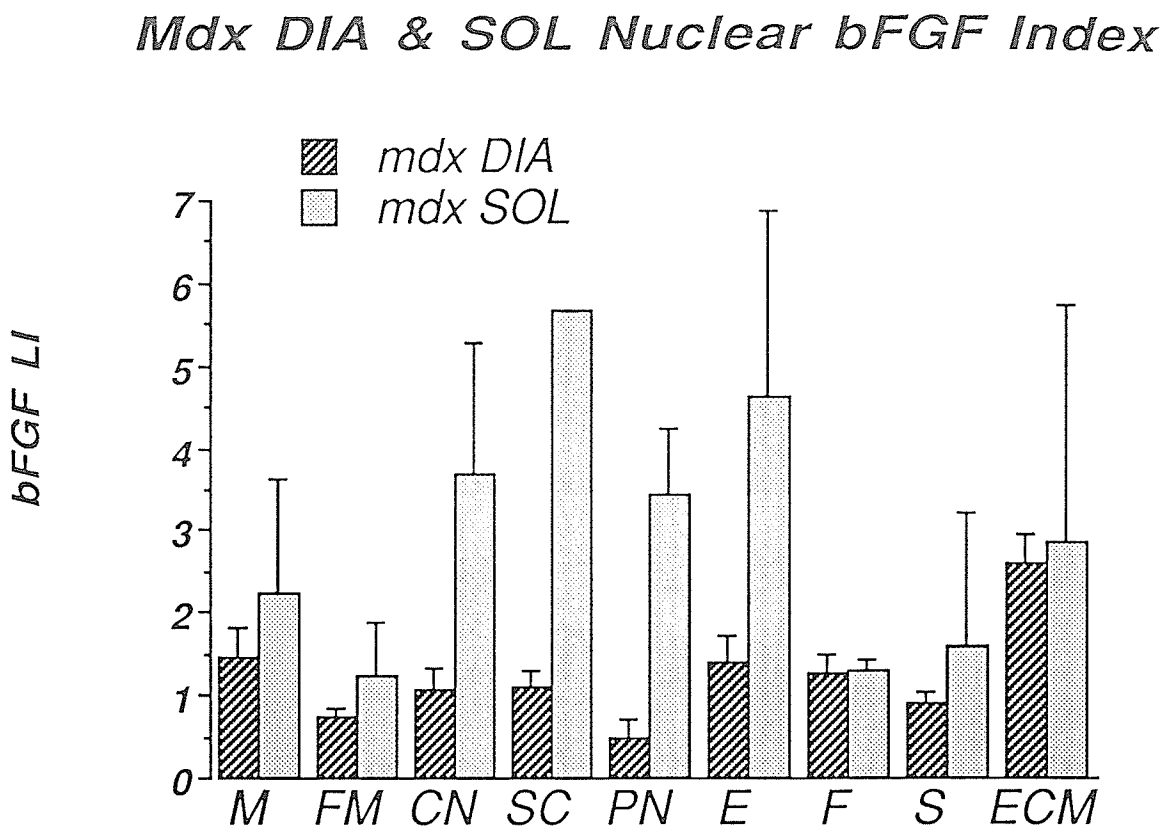
Mdx DIA & SOL Nuclear bFGF Index
mdx DIA
mdx SOL
bFGF LI
0
1
2
3
4
5
6
7
M
FM
CN
SC
PN
E
F
S
ECM

12.0 **BIBLIOGRAPHY:**

Abbas AK, Lichtman AH, Prober JS.: Cellular and Molecular Immunology, W.B.Saunders Co., Philadelphia, Chapter 1, pg. 1-12, 1991a.

Abbas AK, Lichtman AH, Prober JS.: Cellular and Molecular Immunology, W.B.Saunders Co., Philadelphia, Chapter 3, pg. 38-43, 64-67, 1991b.

Allen RE, Boxhorn LK: Regulation of skeletal muscle satellite cell proliferation and differentiation by transforming growth factor-beta, insulin-like growth factor-I, and fibroblast growth factor. J. Cell. Physiolo. 138: 311-15, 1989.

Alterio J, Courtois Y, Robelin J, Dechet D, Martelly I.: Acidic and basic fibroblast growth factor mRNAs are expressed by skeletal muscle satellite cells. Biochem. Biophys. Res. Commun., 166: 1205-1212, 1990.

Anderson JE, Ovalle W, Bressler B: Electron microscopic and autoradiographic characterization of hindlimb muscle regeneration in the mdx mouse. The Anatomical Record, 219: 243-257, 1987.

Anderson JE, Bressler B, Ovalle W: Functional regeneration in the hindlimb skeletal muscle of the MDX mouse. Journal of Muscle Research and Cell Motility, 9: 488-516, 1988.

Anderson JE, Kao L, Bressler B, Gruenstein E: Analysis of dystrophin in fast and slow twitch skeletal muscles from mdx and dy^{2J} mice at different ages. Muscle & Nerve, 13:6-11, 1990.

Anderson JE: Myotube phospholipid synthesis and sarcolemmal ATPase activity in dystrophic (mdx) mouse muscle. Biochem. Cell. Biol., 69:835-841, 1991.

Anderson JE, Liu L, Kardami E: Distinctive patterns of basic fibroblast growth factor (bFGF) distribution in degenerating and regenerating area of dystrophic (mdx)striated muscles. Developmental Biology, 147:96-109, 1991.

Anderson JE, Kakulas BA, Jacobsen PF, Johnson RD, Kornegay JN, Grounds MD: Comparison of basic fibroblast growth factor in X-linked dystrophin-deficient myopathies of human, dog, and mouse. Growth Factors, (9), in press, 1993.

Arahata, K, Beggs AH, Honda H, Ito S, Ishiura S, Tsukahara T, Ishiguro T, Eguchi C, Orimo S, Arikawa E, Kaido M, Nonaka I, Sugita H, Kunkel LM.: Preservation of the C-terminus of dystrophin molecule in the skeletal muscle from Becker muscular dystrophy. J. of Neurol. Sci, 101: 148-156, 1991.

Baird A, Bohlen P: Fibroblast Growth Factors in:Sporn M, Roberts A.: Peptide Growth Factors and Their Receptors. Springer-Verlag, New York. 369-418, 1991.

Baird A, Walicke P: Fibroblast Growth Factors. British Medical Bulletin, 45, (2): 438-452, 1989.

Beilharz MW, Lareu RR, Garrett KL, Grounds MD, Fletcher S.: Quantitation of muscle precursor cell activity in skeletal muscle by northern analysis of MyoD and myogenin expression: application to dystrophic (mdx) mouse muscle. Molecular and Cell Neurosciences, 3: 326-331, 1992.

Bischoff R.: A satellite cell mitogen from crushed adult muscle. Dev. Biol., 115: 140-147, 1986.

Bischoff R: Cell cycle commitment of rat muscle satellite cells. J. Cell. Bio., 111: 201-207, 1990.

Blau HM, Webster C, Pavlath GK: Defective myoblasts identified in Duchenne muscular dystrophy. Proc. Natl. Acad. Sci., 80: 4856-4860, 1983.

Bober E, Lyons GA, Braus T, Cossu G, Buckingham M, Arnold HH: The muscle regulatory gene, Myf-6, has a biphasic pattern of expression during early mouse development. Journal of Cell Biology, 113: 1255-1265, 1991.

Boettiger D, Weinstein G, Menko S: Triggering terminal myogenic differentiation. in Kedes L, Stockdale F, (eds): Cellular and Molecular Biology of Muscle Development, Alan Liss, Inc., New York, 1989.

Bozzola JJ, Russell LD.: Electron Microscopy- Principles and techniques for biologists. Jones and Bartless Pub., Boston, 235-251, 1991.

Bulfield G, Siller W, Wight P, Moore K: X chromosome-linked muscular dystrophy (mdx) in the mouse. Proc Natl Acad Science, 81: 1189-1192, 1984.

Campbell K, Kahl S: Association of dystrophin and an integral membrane glycoprotein. Nature, 338: 259-262, 1989.

Carpenter S: Regeneration of skeletal muscle fibers after necrosis. in Griggs RC, Karpati G, (eds): Myoblast transfer therapy: Advances in Experimental Medicine and Biology, Plenum Pub. Co., New York, 280: 13-17, 1990.

Cordon-Cardo C. et al.: Expression of BFGF in normal human tissues. Labratory Investigation, 63(6):832-840, 1991.

Carnwath J, Shotton D: Muscular dystrophy in the mdx mouse: histopathology of the soleus and extensor digitorum longus muscles. Journal of Neurological Sciences, 80:39-54, 1987.

Carpenter S, Karpati G: Pathology of Skeletal Muscle. Churchill Livingstone Pub., New York, 1-754, 1984.

Carpenter J, Hoffman E, Romanul F, Kunkel L, Rosales R, Ma S, Dasbach J, Raae J, Moore F, McAfee M, & Pearce L: Feline muscular dystrophy with dystrophin deficiency. American Journal of Pathology, 135:909-919, 1989.

Chamberlain J. et al: Analysis of Duchenne muscular dystrophy gene mutations in mice and humans. in Kedes L, Stockdale F, (eds.): Cellular and Molecular Biology of Muscle Development, Alan Liss, Inc., New York, 1989.

Clegg C, Linkhart T, Olwin B, Hayschka S: Growth factor control of skeletal muscle differenation: commitment to terminal differentiation occurs in G1 phase and is repressed by fibroblast growth factos. J. Cell Biol. 105: 949-56, 1987.

Cooper BJ: Animal models of Duchene and Becker muscular dystrophy. Br. Med. Bull., 45: 703-718, 1989.

Cooper B, Winand N, Stedman H, Valentine B, Hoffman E, Kunkel L, Scott M, Fishbeck F, Kornegay J, Avery R, Williams J, Schmickel R, Sylvester J: The homologue of the Duchenne locus is defective in X-linked muscular dystrophy of dogs. Nature, 334: 145-156, 1988.

Coulton G, Curtin N, Morgan J, Partridge T: The mdx mouse skeletal muscle myopathy: I. A Histochemical, morphometric and biochemical investigation. Neuropathology and Applied Neurobiology, 14: 53-70, 1988.

Coulton G., Curtin N., Morgan J., & Partridge T.: The mdx mouse skeletal muscle myopathy: II. Contractile properties. Neuropathology and Applied Neurobiology, 14: 299-314, 1988a.

Cox R, Buckingham M: Actin and myosin genes are transcriptionally regulated during mouse skeletal muscle development. Developmental Biology, 149: 228-234, 1992.

Cullen M, Jaros E: Ultrastructure of the skeletal muscle in the X chromosome-linked dystrophic (mdx) mouse. Acta Neuropathologica, 77: 69-81, 1988.

Cullen M, Walsh J, Nicholson L,Harris J: Ultrastructural localization of dystrophin in human muscle using gold immunolabelling. Proc. R Soc London B, 240: 197-210, 1990.

Czech MP, Clairmont KB, Yagloff KA, Corvera S.: Properties and regulation of receptors for growth. in Sporn AH, Roberts AB (eds): Peptide growth factors and their receptors I, Springer-Verlag, USA, 37-39, 1991.

D'Amore P: Modes of FGF release in vivo and in vitro. Cancer and Metastasis Reviews, 9: 227-238, 1990.

Dangain J, Vrbova G: Muscle development in mdx mutant mice. Muscle and Nerve, 7: 700-704, 1984.

DiMario J, Buffinger N, Yamada S, Strohman R: Fibroblast growth factor in the extracellular matrix of dystrophic (mdx) mouse muscle. Science, 244: 688-690, 1989.

DiMario J, Strohman R: Satellite cells from dystrophic (mdx) mouse muscle are stimulated by fibroblast growth factor in vitro. Differentiation, 39: 42-49, 1988.

DiMario J, Uzman A, Strohman R: Fiber regeneration is not persistent in dystrophic (MDX) mouse skeletal muscle. Developmental Biology, 148: 314-321, 1991.

Dupont-Versteegden E, McCarter R.: Differential expression of muscular dystrophy in diaphragm versus hindlimb muscles of mdx mice. Muscle & Nerve, 15: 1105-1110, 1992.

Emery A: Clinical and molecular studies in Duchenne Muscular Dystrophy. in Bartsicas C: Genetics of Neuromusuclar Disorders. Alan Liss, Inc, New York, 1989.

Ervasti J, Ohlendieck K, Kahl S, Gaver M, Campbell K: Deficiency of a glycoprotein component of the dystrophin complex in dystrophic mice. Nature, 345: 315-319, 1990.

Flaumenhaft R, Moscatelli D, Rifkin DB: Journal Cell Biology, 111: 1651-1664, 1990.

Florini J, Ewton D, Magri K: Hormones, Growth Factors, and Myogenic Differentiation. Annu. Rev. Physiol. 53: 201-16, 1991.

Florini J, Magri K: Effects of growth factors on myogenic differentiation. American Journal of Physiology, 256: 701-711, 1989.

Fox JC, Swain JL.: Auto and transactivation of FGF expression: potential mehcanisk for regulation of myogenic differentation. In Vitro Cell. Dev. Biol., 29A: 228-230, 1993.

Ganong WF: Review of Medical Physiology, Lange Medical Books, San Francisco, 50-60, 1989.

Gospodarowicz D, Weseman F, Moran J: Presence in the brain of a mitogenic agent distinct from fibroblast gworth factor that promotes the proliferation of myoblast in low density cultures. Nature 256: 216, 1975.

Gospodarowicz D, Weesman F, Moran J, Linstrom J: Effect of fibroblast growth factors on the division and fusion of bovine myoblast. J. Cell Biol. 70: 395-, 1976.

Gospodarowicz D, Neufled G, Schweigerer L: Review- Fibroblast Growth Factor. Molecular and Cellular Endocrinology, 46: 187-204, 1986.

Gospodarowicz D, Ferrara N, Schweigerer L, Neufeld G: Structural Characterization and Biological Functions of Fibroblast Growth Factor. Endocrine Reviews, 8 (2):95-114, 1987a.

Gospodarowicz D, Neufled G, Schweigerer L: Fibroblast grwoth factor: Structural and biological properties. Journal of cellular physiology supplement 5:15-26, 1987b.

Grounds MD.: Towards understanding skeletal muscle regeneration. Pathol. Res. Pract, 118: 1-22, 1991.

Grounds M, McGeachie J: Skeletal muscle regeneration after crush injury in dystrophic mdx mice: an autoradiographic study. Muscle and Nerve,15: 580-586,1992.

Grounds MD, Robertson TA, Mitchell CA, Papadimitriou JM.: Necrosis and regeneration in dystrophic and normal skeletal muscle. ???J's # 3967.

Grounds MD, Yablonka-Reuveni Z.: Molecular and cell biology of skeletal muscle regeneration. In Partridge TA ed.: Molecular and Cell Biology of Muscle Regeneration. Chapman Hall, in press.

Gutheridge M, Wilson M, Cowling J, Bertolini J, Hearn MTW.,: The role of basic fibroblast growth factor in skeletal muscle regneration. Growth Factors, 6: 53-63, 1992.

Haws C, Lansman J: Developmental regulation of mechanosensitive calcium channels in skeletal muscle from normal and mdx mice. Proc. R. Soc. London. B, 245: 173-177, 1991.

Heeley DH, Anderson JE.: Tropomyosin phosphorylation in regenerating mdx muscle. Submitted to Muscle & Nerve 1993.

Herrera G: Ultrastructural immunolabelling:the next logical step. Ultrastructural Path., 15: iii-v, 1991.

Hoffman E: The animal models of Duchenne muscular dystrophy: Windows on the pathophysiological consequences of dystrophin deficiency. in Morrow J, Mooseker M (eds): Ordering the Membrane- Cytoskeleton Trilayer, Academic Press, New York, 1991.

Hoffman E, Bertelson C, Kunkel L: Alterations of dystrophin quality and quantity; the genetic and biochemical basis of Duchenne and Becker muscular dystrophy. in Kedes L, Stockdale F (eds): Cellular and Molecular Biology of Muscle Development, Alan Liss, Inc., New York, 1989.

Hoffman E, Brown R, Kunkel L: Dystrophin: the protein product of the Duchenne muscular dystrophy locus. Cell, 51: 919-928, 1987.

Hoffman E, Kunkel L: Dystrophin abnormalities in Duchenne/ Becker muscular dystrophy. Neuron, 2: 1019-1029, 1989.

Hoffman E, Morgan J, Watkins S, Partridge T: Somatic reversion/ suppression of the mouse mdx phenotype in vivo. Journal of the Neurological Sciences, 99: 9-25, 1990.

Hu X, Ray P, Murphy E, Thompson M, Worton R: Duplicational mutation at the Duchenne muscular dystrophy locus: its frequency, distribution, origin and phenotype/ genotype correlation. American Journal of Human Genetics, 46: 682-695, 1990.

Huard J, Bouchard JP, Roy R, Labrecque C, Dansereau G, Lemieux B, Tremblay JP: Myoblast transplantation produced dystrophin-positive muscle fibers in a 16-year-old patient with Duchenne muscular dystrophy. Clinical Science, 81: 287-288, 1991.

Huard J, Labrecque C, Dansereau G, Robitaille L, Tremblay JP: A light and electron microscopic study of dystrophin localization at the mouse neuromuscular junction. Synapse, 10: 83-93, 1992.

Hudecki M, Pollina C: Mdx mouse as therapeudic model system: development and implementation of phenotypic monitoring. in Griggs RC, Karpati G (eds): Myoblast Transfer Therapy: Advances in Experimental Medicine and Biology. Plenum Pub. Co., New York, 280: 251-266, 1990.

Hutter OF, Burton FL, Bovells DL: Mechanical properties of normal and mdx mouse sarcolemma: bearing on function of dystrophin. Journal of Muscle Research and Cell Motility, 12: 585-589, 1991.

Johnson A, Bettica A.: On-grid immunogld labelling of glial intermediate filaments in epoxy-embedded tissue. The Amer. J. of Anat., 185: 335-341, 1989.

Jospeh-Silverstein J, Consigli SA, Lyser KM, Pault V: Basic fibroblast growth factor in the chick embryo: immunolocalization to striated muscle cells and their precursors. J. Cell Biol. 108:2459-2466, 1989.

Kardami E.: Stimulation and inhibition of cardiac myocyte proliferation in vitro. Journal of Mol. Cell. Biochem, 92: 124-134, 1990.

Kardami E, Fandrich RR.: Basic fibroblast growth factor in atria and ventricles of the vertebrate heart. J. Cell. Biol., 109: 1865-1875, 1989.

Kardami E, Murphy LJ, Liu L, Padua RR, Fandrich RF.: Chracterization of two preparation fof antibodies to basic fibroblast growth factor which exhibit distinct patterns of immunolocalization. Growth Factors, 4: 69-80, 1990.

Kardami E, Spector D, Strohman RC.: Selected muscle and nerve extracts contain an activity which stimulates myoblast proliferation and which is distinct from transferrin. Dev. Bio., 112: 353-358, 1985.

Karpati, G.: Principles of skeletal muscle histochemistry in neuromuscular disease. Handbook of CLinical Neurology, 1-61, 1979.

Karpati G, Carpenter S, Prescott S: Small-caliber skeletal muscle fibers do not suffer necrosis in mdx mouse dystrophy. Muscle & Nerve, 11: 795-803, 1988.

Karpati G: Implantation of nondystrophic allogenic myoblasts into dystrophic muscles of MDX mice produces "mosiac" fibers of normal microscopic phenotype. in Kedes L, Stockdale F (eds): Cellular and Molecular Biology of Muscle Development, Alan Liss, Inc., New York, 1989.

Karpati G, Pouliot Y, Zubrzycka-Gaarn E, Carpenter S, Ray P, Worton RG, Holland P: Dystrophin is expressed in mdx skeletal muscle fibers after normal myoblast implantation. Am. J. of Pathology, 135: 27-32, 1989.

Karpati G: Immunological aspects of histoincompatable myoblast transfer in non-tolerant hosts. in Griggs RC, Karpati G (eds):Myoblast Transfer Therapy, Advances in Experimental Medicine and Biology. Plenum Pub. Co, New York, 280: 31-34, 1990.

Karpati G.: The principles and practice of myoblast transfer. Griggs RC, Karpati G (eds): Myoblast Transfer Therapy:Advances in Experimental Medicine and Biology. Plenum Pub. Co, New York, 280: 69-74, 1990.

Karpati G, Zubrzycka-Gaarn E, Carpenter S, Bulman D, Ray P, Worton R: Age-related conversion of dystrophin- negative to -positive fiber segments of skeletal but not cardiac muscle fibers in heterozygote mdx mice. Journal of Neuropathology and Experimental Neurology, 49 (2): 96-105, 1990.

Kaufman S: Immunochemical analysis of the myoblast membrane and lineage. in Griggs RC, Karpati G (eds): Myoblast Transfer Therapy:Advances in Experimental Medicine and Biology. Plenum Pub. Co, New York, 280: 47-56, 1990.

Kaufman S, Foster R: Prenatal differentiation in myogenic lineage. in Kedes L, Stockdale F (eds):Cellular and Molecular Biology of Muscle Development, Alan Liss, Inc., New York, 1989.

Kelly A, Shrager J, Narusawa M, Panettieri R, Maguire H, Sladkey J, Sweeney L, Stedman H: Progressive muscle degeneration in the mdx mouse diaphragm. Abstract fro EMBOS, 1992.

Kessler DA, Langer RS, Pless NA, Folkman J: Mast cells and tumor angiogenesis. Int. J. Cancer 18:703-796, 1976.

Kornegay JN, Tuler SM, Miller DM, Llevesque DC: Muscular dystrophy in a litter of golden retriever dogs. Muscle & Nerve, 11: 1056-1064, 1988.

Korenyi-Both A: Muscle Pathology in Nueormuscular Disease. Charles C. Thomas Pub., Illinois, 3-29,220-235, 1983.

Lathrop B, Olson E, Glaser L: Control by fibroblast growth factor of differentiation in the BC3H1 muscle cell line. J. Cell Biol 100:1540, 1985.

Lathrop B, Olson E, Glaser L: Control of myogenic differentiation by fibroblast growth factor is mediated by position in the G1 phase of the cell cycle. J. Cell Biol 101:2194, 1985a.

Law, P: Palusible structural/ functional/ behavioral/ biochemical transformation following myoblast transfer therapy. in Griggs RC, Karpati G (eds): Myoblast Transfer Therapy:Advances in Experimental Medicine and Biology. Plenum Pub. Co, New York, 280: 241-250, 1990.

Linkart TA, Clegg CH, Hauschka SD: Control of mouse myoblast commitment to terminal differentiation by mitogens. J. Supramol Struct 14:483-6, 1980.

Linkart TA, Clegg CH, Hauschka SD: Myogenic differentiation in permanent clonal myoblast cell lines: regulation by macromolecular growth factors in the culture medium. Dev. Biol 86:19-24, 1981.

Logan A: Intracrine regulation at the nucleus- a furthur mechanism of growth factor activity. Journal of Endocrinology, 125: 339-343, 1990.

Lyons P, Slater C: Structure and function of the neuromuscular junction in young adult mdx mice. Journal of Neurocytology, 20: 969-981, 1991.

Marshall P, Williams P, Goldspink G: Accumulation of collagen and altered fiber-type ratios as indicators of abnormal muscle gene expression in the mdx dystrophic mouse. Muscle & Nerve, 12: 528-537, 1989.

Mauro A: Satellite cells of skeletal muscle fibers. J Biophys Biochem Cytol, 9: 493-495, 1961.

McArdle A, Edwards R, Jackson M: Effects of contractile activity on muscle damage in the dystrophin-deficient mdx mouse. Clinical Science, 80: 367-371, 1991.

McGeachie J, Grounds M, Partridge T, Morgan J: Replication of myogenic cells with age and myogenesis after experimental injury in mdx mouse muscle; quantative autoradiographic studies. in Kakulas BA, McChowell J (eds): Models for Duchenne Muscular Dystrophy and Genetic Manipulation . Raven Press, New York, in press.

McNeil PL, Muthukrishnan L, Warder E, D'Amore PA: Growth factors are released by mechanically wounded endothelial cells. J. Cell Biol. 109: 811-22, 1989.

Mendell J: Immunosuppressive therapy in Duchenne muscular dystrophy: considerations for myoblast transfer studies. in Griggs RC, Karpati G (eds): Myoblast Transfer Therapy:Advances in Experimental Medicine and Biology. Plenum Pub. Co, New York, 280: 287-295, 1990.

Menke A, Jockush H: Decresed osmotic stability of dystrophin less muscle cells from the mdx mouse. Nature, 349: 69-71, 1991.

Miyatake M: Dystrophin: localization and presumed function. Muscle and Nerve, 14: 113-119, 1990.

Mignatti P, Rifkin D: Release of basic fibroblast growth factor, an angiogenic factor devoid of secretory sequence: a trivial phenomenon or a novel secretion mechanism? Journal of Cellular Biochemistry, 47:201-207, 1991.

Miike A: Immunohistochemical dystrophin reaction in synaptic regions. Brain Dev., 344-346, 1989

Miller JR.: Family response to Duchenne muscular dystrophy. in Charas LI, Lovelace RE, Leach CF, Kutscher AH, Goldberg RJ, Roye DP (eds): Muscular Dystrophy and other neuromuscular diseases: psychosocial issues. Haworth Press, New York, pg 31-42, 1991.

Monaco A, Bertelson C, Ljechti-Gallati S, Moser H, Kunkel L: An explanation for the phenotypic differences between patients bearing partial deletions of the DMD locus. Genomics, 2: 90-95, 1988.

Morgan JE, Coulton GR, Partridge TA: Mdx muscle grafts retain the mdx phenotype in normal hosts. Muscle & Nerve, 12: 401-409, 1989.

Moscatelli D: High and low affinity binding sites for basic fibroblast growth factor on cultured cells: absence of a role for low affinity binding in the stimulation of plasminogen activator production by bovine capillary endothelial cells. J. Cell Physio 131: 123-130, 1987.

Moscatelli D, Quatro N: Transformation of NIH 3T3 cells with basic fibroblast growth factor or the hst/K-fgf oncogene causes downregulation of the fibroblast growth factor receptor: reversal of morphological transformation and restoration of receptor number of suramin. J. Cell Biol 109: 2519-27, 1989.

Moss FP, LeBlond CP: Satellite cells as the source of nuclei in muscles of growing rats. Anat. Rec.,178: 211-228.
Mullins DE, Rifkin DB: Induction of proteases and protease inhibitors by growth factors. in Sporn MB, Roberts AB (eds): Peptide Growth Factors and their receptors II, Springer-Verlag, USA, 481-, 1991.

Nagel A, Lehmann-Horn F, Engel A: Neuromuscular transmission in the mdx mouse. Muscle & Nerve, 13: 742-749, 1990.

Neufeld G, Gospodarowicz D: The identification and partial characterization of fibroblast growth receptor of baby hamster kidney cells. J. Biol Chem. 260: 13860, 1985.

Ohlendieck K, Campbell K: Dystrophin-associated proteins are greatly reduced in skeletal muscle from mdx mice. Journal of Cell Biology, 115 (6): 1685- 1694, 1991.

Olwin BB, Hauschka SD: Identification of the fibroblast growth factor receptor of Swiss 3T3 cells and mouse skeletal myoblast. Biochemistry 25:3488, 1986.

Olwin BB, Hayschka SD: Cell surface fibroblast growth factor and epidermal growth factor receptors are permanently lost during skeletal muscle terminal differentiation in culture. J. Cell Biol 107: 761-769, 1988.

Ontell M: Muscle satellite cells: a validated technique for light microscopic identification and a quantative study of changes in their population following denervation. Anatomical Record, 178: 211-228, 1978.

Ornitz D, Yayon A, Flanagan J, Svahn C, Levi E, Leder P: Heparin is required for cell-free binding of basic fibroblast growth factor to a soluble receptor and for mitogenesis in whole cells. Molecular and Cellular Biology, Vol 12: pg 240-247, 1992.

Papadimitriou JM, Robertson TA, Mitchell CA, Grounds MD: The process of new plasmalemma formation in focally injured skeletal mumscle fibers. Journal of Structural Biology, 103: 124-134, 1990.

Partridge TA: Animal models of muscular dystrophy: what can they teach us? Neuropathology and Applied Neurobiology, 17: 353-363, 1991.

Partridge TA, Morgan JE, Coulton GR, Hoffman EP, Kunkel LM.: Conversion of mdx myofibres from dystrophin-negative to -positive by injection of normal myoblasts. Nature, 337: 176-179, 1989.

Petrof BJ, Shrager JB, Stedman HH, Sweeney HL, & Kelly AM. Effects of Dystrophin Deficiency on mdx muscle fibers. Proceedings of EMBO Workshop on Molecular Biology and Pathology of Skeletal and Caardiac Myogenesis (Abstract), 1992.

Petrof BJ, Shrager JB, Stedman HH, Kelly AM, Sweeney HL: Dystrophin protects the sarcolemma from stresses developed during muscle contraction. Proc. Natl. Acad. Sci., 90: 3170-3174, 1993.

Petrof BJ, Stedman HH, Shrager JB, Eby J, Sweeney HL, Kelly AM: Adaptive alterations in myosin heavy chain expression and contractile function in dystrophic (mdx) mouse diaphragm. in press.

Powell P, Klagsbrun M: Threeforms of rat basic fibroblast growth factor are made from a single mRNA and localize to the nucleus. Journal of cellular physiology, 148: 202-210, 1991.

Ragot T, Vincent N, Chafey P, Vigne E, Gilgenkrantz H, Couton D, Cartaud J, Briand P, Kaplan JC, Perricaudet M, Kahn A: Efficient adeno-virus-mediated transfer of a human minidystrophin gene to skeletal muscle of mdx mice. Nature, 361: 647-650, 1993.

Renko M, Morimoto T, Rifkin D: Nuclear and cutoplasmic localization of different basic fibroblast growth factor species. Journal of Cellular Physiology: 108-114, 1990.

Rifkin D, Moscatelli D: Recent Developments in the Cell Biology of Basic fibroblast growth factor. J. of Cell Biology, 109: 1-6, 1989.

Robertson M.: More to muscle than MyoD. Nature, 344: 378, 1990.

Robertson TA, Grounds MD, Mitchell CA, Papadimitrious JM: Fusion between myogenic cells in vivo: an ultrastructural study in regenerating murine skeletal muscle. Journal of Structural Biiology, 105: 170-182, 1990.

Rojas C, Hoffman E: Recent advances in dystrophin research. Current Opinion in Neurobiology, 1: 420-429, 1991.

Rowland LP, Layzer RB.: X-linked muscular dystrophies. in Vinkert,PJ, Bruyn GW (eds): Handbook of Clinical Neurology. North Holland Pub., USA, 28:349-413, 1979.

Sacco P, Jones D, Dick J, Vrbova G: Contractile properties and susceptibility to exercise- induced damage of normal and mdx mouse tibialis anterior muscle. Clinical Science, 82: 227-236, 1992.

Schultz E, Albright DJ, Jaryszak DL, David Tl.: Survival of satellite cells in whole muscle transplants. Anatomical Record, 222: pg. 12-17, 1988.

Schweigerer, L: Basic fibroblast growth factor: Properties and clinical implications. in A. Habernicht (ed.): Growth factors, differentiation factors, and cytokines. Springer-Verlag, New York. pg. 42-55, 1990.

Shimizu T, Matsumura K, Sunada Y, Mannen T.: Dense immunostaining on both neuromuscular and myotendon junctions with an antidystrophin monoclonal antibody. Biomedical Research, 10: 405-409, 1989.

Shomrat R, Driks N, Legum C, Shiloh Y: Use of dystrophin genomic and cDNA probes for solving difficulties in carrier detection and prenatal diagnosis of Duchenne muscular dystrophy. American Journal of Medical Genetics, 42: 281-287, 1992.

Sicinski P, Geng Y, Ryder-Cook A, Barnard E, Darlison M, Barnard P: The molecular basis of muscular dystrophy in the mdx mouse: a point mutation. Science, 244: 1578-1580, 1989.

Slack JMW, Darlington BF, Heath HK, Godsave SF. Heparin binding growth factors as agents of mesoderm induction in early xenopus embryo. Nature 326: 297, 1987.

Snow MH.: Satellite cell distribution within the soleus muscle of adult mouse. The Anatomical Record, 201: 463-468, 1981.

Sporn MR, Roberts AB.: The multifunctional nature of peptide growth factors in MB Sporn & AB Roberts eds. Peptide Growth Factors and Their Receptors I, Springer-Verlag, USA, 3-15, 1991.

Stedman H, Sweeney H, Shrager J, Maguire H, Panettieri R, Petrof B, Narusawa M, Leferovich J, Sladky J, Kelly A: The mdx mouse diaphragm reproduces the degenerative changes of Duchenne msuscular dystrophy. Nature. 352: 536-538, 1991.

Stirling JW.: Immuno- and affinity probes for electron microscopy: a review of labeling and preparation techniques. Journal of Histochemistry and Cytochemistry, 38: 145-157, 1990.

Stockdale, F: Myogenic Cell Lineages: Commitment and modulation during differentiation of avian muscle. in Kedes L, Stockdale F (eds): Cellular and Molecular Biology of Muscle Development, Alan Liss, Inc., New York, 1989.

Stockdale F: Myoblasts, satellite cells, and myoblast transfer. in Griggs RC, Karpati G (eds): Myoblast Transfer Therapy:Advances in Experimental Medicine and Biology, Plenum Pub. Co, New York, 280: 7-12, 1990.

Stratford-Perricaudet LD, Makeh I, Perricaudet M, Briand P: Widespread long-term gene transfer to mouse skeletal muscles and heart. J. CLin. Invest., 90: 626-630, 1992.

Swash M, Schwartz M: Biopsy Pathology of Muscle. Chapman and Hall Ltd, London, 34-47, 1984.

Tanabe Y, Esaki K, Nomura T: Skeletal muscle pathology in X chromosome-linked muscular dystrophy (mdx) mouse. Acta Neuropathol, 69: 91-95, 1986.

Tapscot SJ, Davis RL, Lasser AB: MyoD: A regulatory gene of skeletal myogenesis. in Griggs RC, Karpati G(eds): Myoblast Transfer Therapy:Advances in Experimental Medicine and Biology, Plenum Pub. Co, New York, 280: 3-6, 1990.

Tessler S, Neufeld G: Basic fibroblast growth factor accumulates in the nuclei of various bFGF-producing cell types. Journal of Cellular Physiology, 145: 310-317, 1990.

Torres L, Duchen L: The mutant mdx: inherited myopathy in the mouse. Brain, 110: 269-299, 1987.

Vaidya TB, Rhodes SJ, Taparowsky EJ.: Fibroblast growth factor and transforming growth factor beta repress transcription of the myogenic regulatory gene MyoD1. Mol. Cell. Biol., 9: 3576-3579, 1989.

Valentine BA, Cooper BJ, Cummings J, deLahunta A: Canine X-linked muscular dystrophy: morphologic lesions. Journalof the Neurological Sciences, 97: 1-23, 1990.

Valentine BA, Cooper BJ: Canine X-linked muscular dystrophy: selective involvement of muscles in neonatal dogs. Neuromuscular Disorders, 1: 31-38, 1991.

van Essen AJ, and 27 others: Parental origin and germline mosiacism of deletions and duplications of the dystrophin gene: a European study. Human Genetics, 88: 249-257, 1992.

Vlodavsky I, Bar-Shavit R, Ishai-Michaeli R, Bashkin P, Fuks Z: Extracellular sequestration and release of fibroblast growth factor: a regulatory mechanism? TIBS 16: 268-271, 1991.

Wakayama Y, Shibuya S: Gold-labelled dystrophin molecule in muscle plasmalemma of mdx control mice as seen by electron microscopy of deep etching replica. Acta Neuropathologica, 82: 178-184, 1991.

Walsh F: N-CAM is a target cell surface antigen for the purification of muscle cells for myoblast transfer therapy. in Griggs RC, Karpati G(eds): Myoblast Transfer Therapy:Advances in Experimental Medicine and Biology, Plenum Pub. Co, New York, 280: 1-46, 1990.

Webster C, Silberstein L, Hays AP, Blau HM: Fast muscle fibers are preferentially affected in Duchenne muscular dystorphy. Cell, 52: 503-513, 1988.

Weller B, Karpati G, Carpenter S.: Dystrophin-deficient mdx muscles fibers are preferentially vulnerable to necrosis induced by experimental lengthening contractions. J. of Neuro. Sci, 100: 9-13, 1990.

Westerman R, Grothe C, Unsicker K: Basic fibroblast growth factor (bFGF), a multifunctional growth factor for neuroectodermal cells. Journal Celllular Science Suppl. 13: 97-117, 1990.

Woo S, Buckwalter J (eds.): Injury and Repair of Musculoskeletal Soft Tissues. American Academy of Orthopedic

Yaffe, D: Tissue- and stage- specificity of expression of the Duchenne muscular dystrophy gene. in L. Kedes and F. Stockdale (eds.): Cellular and Molecular Biology of Muscle Development, Alan Liss, Inc., New York, 1989.

Yamada S, Buffinger N, DiMario J, Strohman R: Fibroblast growth factor is stored in the fiber extracellular matrix and plays a role in regulating muscle hypertrophy. Med. Sci. Sports Exerc. 21: S173-80, 1989.

Yang J, Seelig M, Rayner S, Bredesen DE: Increasing the proliferative capacity of muscular dystrophy myoblasts. Muscle & Nerve, 15: 941-948, 1992.

Yayon A, Klagsbrun M: Autocrine regulation of cell growth and transformation by basic fibroblast growth factor. Cancer and Metastasis Reviews: 9: 191-202, 1990.

Zacharias JM, Anderson JE: Muscle regeneration after imposed injury is better in younger than older mdx mice. J. Neurol. Sci. 9: 190-196, 1991.

Zubrzycka-Gaarn, E: Localization of the Duchenne muscular dystrophy protein to the sarcolemma of human skeletal muscle. in Kedes L, Stockdale F (eds): Cellular and Molecular Biology of Muscle Development, Alan Liss, Inc., New York, 1989.

Zubrzycka-Gaarn EE, Hutter OF, Karpati G., Klamut HJ, Bulman DE, Hodges RS, Worton RG, Ray P.: Dystrophin is tightly associated with the sarcolemma of mammalian skeletal muscle fibers. Exp. Cell. Res., 192: 278-288, 1991.